Mass Spectrometric Analysis of Biological Molecules

by

Christopher Ronald Taormina

BS, University of Pittsburgh, 2000

Submitted to the Graduate Faculty of

Arts and Science in partial fulfillment

of the requirements for the degree of

Doctor of Philosophy

University of Pittsburgh

2007

UNIVERSITY OF PITTSBURGH

Faculty of Arts and Science

This dissertation was presented

by

Christopher Ronald Taormina

It was defended on

August 1, 2007

and approved by

Michael A. Trakselis, Assistant Professor, Department of Chemsitry

Sunil K. Saxena, Assistant Professor, Department of Chemistry

David N. Finegold, Professor, Department of Human Genetics

Dissertation Advisor: Joseph J. Grabowski, Associate Professor, Department of Chemistry

Mass Spectrometric Analysis of Biological Molecules

Christopher Ronald Taormina, PhD

University of Pittsburgh, 2007

The investigation of biological molecules through electrospray ionization mass spectrometry has expanded over the past 20 years. With a nanospray source allowing small volumes to be analyzed, perturbation of the sampled system is kept to a minimum. Two studies take advantage of the lack of perturbation to quantitate molecules within biological fluids. The first focuses on the concentration of glucose in tears.

A quantitative method is developed to determine the concentration of glucose in human tears. Aqueous solutions of known glucose concentrations and induced tears are used to validate the method. Non-diabetic and diabetic subjects' tears are sampled. After overnight fasting, non-diabetic tear glucose concentration is shown to be 28 ± 14 μM. Tear glucose concentrations from samples taken before and after a meal are compared to the subjects' blood glucose concentrations.

The second study that dealt with small biological fluid volumes sought to quantitate neuropeptides within a rat's cerebrospinal fluid. A tapered fused silica capillary is used to obtain cerebrospinal fluid in order to minimize damage to the brain. It was demonstrated that the matrix in the collected biological fluid caused the limit-of-quantitation of the method to be above the neuropeptide concentration within the sample.

Protein-RNA complexes are also explored through ESI-MS. The observation of proteins and RNA is demonstrated. Further experiments are performed to determine how many monomers of neuroblastoma apoptosis-related protein bind to RNA during replication.

In addition to these biological inquiries, a few silyl containing compounds are examined. Different ionization techniques and collision-induced-dissociation are used to characterize hexamethyldisiloxane, tert-butoxy trimethylsilane, and 2-trimethylsiloxy-propene to determine if they can differentiate volatile organic compounds. Collision-induced-dissocitaion of the silyl ions with argon, acetone-d_6, and propanal as the collision gas provided structural identification and possible isomer discrimination. Results show that the ion originating from the loss of a methyl group from hexamethyldisiloxane can provide an avenue to distinguish between acetone and propanal.

TABLE OF CONTENTS

LIST OF TABLES

LIST OF FIGURES

PREFACE

I am deeply indebted to my advisor Dr. Joseph J. Grabowski for his time, patience, support, and understanding through my graduate years. He has advanced my knowledge not only in chemistry but also in life in general more ways than he will ever acknowledge. I have grown to look up to him ~~much~~ more than I ever thought I would. I wish to thank my other committee members, Dr. Michael Trakselis, Dr. Sunil Saxena, and Dr. David Finegold for helping me along the way. I also wish to acknowledge Dr. Adrian Michael, Dr. Sandford Asher, Dr. Stephen Weber, and Dr. Paula Grabowski for their guidance through the menagerie of projects that I have gone through. Thank you to Dr. Kasi Somayajula and Dr. John Williams for sharing their knowledge about mass spectrometry. Also I am indebted to Kevin Kuchta, Rick Schaeffer who is dearly missed, and the rest of the Extrel crew for allowing me to work with them. I thank my group members here and gone especially Mingxiang Lin, Kevin Davies, and Abdil Ozdimir for their help and support. My fellow graduate students Zeeshan Ahmed and Justin Baca deserve my thanks for keeping me sane through the years. I wish to acknowledge all of the undergrads that have graced our group, especially Jim O'Connor, Chris Riese, Angela Minnici, Brett Burkholder, and Brian Craig for the work that we shared. Thanks goes to the electronic and machine shops for which I would have accomplished nothing without them. My friends also require thanks, even though they harassed me about graduating for years on end, for taking me

away from chemistry every so often. Mike Pschirer and Nick High especially deserve thanks for being there when I needed anything. Lastly, I would like to thank my family for encouraging and supporting me throughout my whole life. My mom and dad have been proud of me even for the smallest thing and though it is annoying I love them all the more for it. Special thanks to my wife Trisha for waiting this long for me to graduate. I hope I can give back a percentage of the patience that she showed me during the rest of our lives together. There is no way I know to show how much I love her. All in all, everyone listed here has shared a least a little piece of their lives with me and enriched my life by doing so. I appreciate it and give all my sincerest thanks.

LIST OF ABBREVIATIONS

ESI	electrospray ionization
EI	electron ionization
APCI	atmospheric-pressure chemical ionization
Q1	first quadrupole and multipole in the SWISS-484
O	octopole collision cell and second multipole in the SWISS-484
Q3	second quadrupole and third multipole in the SWISS-484
CID	collision induced dissociation; synonymous with CAD, collision activated dissociation
amu	atomic mass unit (1/12 of carbon)
MS	mass spectrometry
MS/MS	tandem mass spectrometry; synonymous with MS^2
m/z	mass over charge
SRM	selected reaction monitoring
SIM	selected ion monitoring
MIM	multiple ion monitoring
LC	liquid chromatography
ID	inner diameter
OD	outer diameter

cm	centimeter
mm	millimeter
μm	micrometer
mM	millimolar
μM	micromolar
nM	nanomolar
L/s	liters per second
μL/min	microliters per minute
nL/min	nanoliters per minute
MW	molecular weight
SD	standard deviation
CPU	computer processing unit
MagTran	Magic Transformer (v1.0)
mV	millivolts
aCSF	artificial cerebral spinal fluid
LEnk	leucine-enkephalin
MEnk	methionine-enkephalin
PEG	polyethylene glycol
CA	carbonic anhydrase II
BSA	bovine serum albumin
PTB	polypyrimidine tract binding protein
NAPOR	neuroblastoma apoptosis-related protein

1.0 INTRODUCTION

The quadrupole-octopole-quadrupole (triple multipole) mass spectrometer with a custom-built electrospray ionization (ESI) source in the Grabowski group allows specific problems related to the quantification and characterization of biological molecules to be solved. The mass spectrometer, known as the SWISS-484, consists of, in succession, an ionization source, a quadrupole (Q1) used as a mass analyzer, an octopole (O) used for collision-induced-dissociation reactions, a second quadrupole (Q3) used as a mass analyzer, a conversion dynode, and an electron multiplier as the detector. The triple multipole has unique capabilities for the verification of structure, especially in mixtures, and for quantification at lower detection limits.[1,2] The ionization source consists of a nanospray emitter, based on Wilm and Mann's design,[3] and atmosphere-to-vacuum ion transfer optics. The implementation of the nanospray source is a crucial aspect to the SWISS-484 for efficient quantification of biological molecules.

The nanospray source uses a lower flow rate of the sample than traditional electrospray, to both decrease the volume of sample needed and increase the sensitivity of the method.[4] Data in the literature suggests that nanospray sources are compatible with low nanomolar concentrations of biological samples (ex., 2 pM leucine-enkephalin[5] and 130 nM carbonic anhydrase[6]). If these advantages are general, they will allow biological specimens to be examined without the need for unrealistic collection volumes.

Analysis of small volumes initiated the discussion with the Asher group about glucose monitoring for *Diabetes Mellitus*. Close monitoring of blood glucose is important in order to prevent complications from Diabetes.[7] There has been significant research to produce a non-invasive method to monitor blood glucose.[8-11] One of the methods has examined tear fluid glucose as a surrogate for blood glucose. Over the past 70 years there has been significant disagreement in the glucose concentration in tear fluid. It has been stated that the discrepancy in reported glucose concentrations is due to the differing degree of irritation of the eye when sampling.[12-14] To obtain reliable tear fluid data, irritation of the eye must be kept to a minimum; hence only one or two microliters of fluid can be sampled. In collaboration with the Asher group, the determination of tear glucose concentration commenced with the use of isotopic dilution mass spectrometry. Tear fluid of non-diabetic and diabetic subjects was analyzed to establish a population trend of tear glucose concentration. Also, associated blood glucose and tear glucose concentrations were obtained to determine a blood-tear glucose relationship.

Another project dealt with the detection of peptides in the interstitial fluid of the brain. Neuropeptides have been associated with many neurological disorders such as schizophrenia, depression, and chronic pain.[15-17] The concentrations of the peptides within the interstitial fluid of the brain are needed to understand the relationship that the peptides have in signal transmission in regards to psychological functions and disorders. Opioid peptides are a subset of neuropeptides which are known to modulate the pain response in the nervous system.[16,17] The understanding of the quantitative release of these peptides into the interstitial fluid will be valuable in on-going research to improve the treatment of pain. Previous research has been performed on these peptides with the use of dialysis probes.[5,18] However, the insertion of dialysis probes has been shown to damage cells that end up surrounding the probe.[19] The

damaged cells have the potential to change the composition of the adjacent interstitial fluid through the exposure of the cell's interior. The use of tapered fused-silica capillaries, which are less disruptive than dialysis probes, obtains interstitial fluid surrounding undamaged tissue. With this unique collection technique (in collaboration with Professor Michael's group) and subsequent tandem mass spectrometry (MS/MS) experiments, the identification and quantification of selected peptides in the fluid was attempted.

The last project dealing with biology is to characterize proteins that regulate RNA splicing. Gene expression which regulates cell development and function is dependent on the splicing event; however, the splicing mechanisms are not fully understood.[20] Proteins which have been identified to have a role in the splicing mechanisms are the polypyrimidine-tract-binding proteins (PTB) and neuroblastoma apoptosis-related protein (NAPOR).[20,21] With the use of ESI-MS, the proteins' amino acid sequence can be identified through a combination of digestion and collision-induced-dissociation (CID). Also, the protein-RNA complex can be explored with the "soft ionizaton" of electrospray ionization which allows non-covalent binding to be transferred to the gas phase.

The one project that does not partake specifically in biological fluids deals with the characterization of silicon containing compounds. A method is sought to identify and quantify in real-time volatile organic compounds in a complex mixture. The use of hydronium ion in chemical reaction mass spectrometry has been demonstrated to this end.[22] One limitation to the hydronium ion is that it clusters with water which greatly complicates analysis. The replacement of the hydrogen atoms with trimethylsilyl groups on the hydronium ion is one way to eliminate the clustering reactions since the trimethylsilyl cation has similar reactivity as a proton[23] but does not cluster. In this study three molecules (hexamethyldisiloxane, tert-butoxy trimethylsilane, and

2-trimethylsiloxy-propene) are ionized by way of electron ionization (EI), ESI, and atmospheric-pressure chemical ionization (APCI). The resulting ions are subjected to CID with argon, acetone-d_6, or propanal as the collision gas to identify structure and to determine if any can differentiate isomeric volatile organic compounds.

2.0 THEORY AND INSTRUMENTATION

Improvement of instrumentation, specifically the SWISS-484, can not be successful without fundamental information concerning electrospray ionization, quadrupoles, and collision-iduced-dissociation. For the SWISS-484 to be applicable in biological fluid quantitation the electrospray ionization source needed to be able to perform in the nanospray regime. A nanospray source can increase the signal-to-noise ratio and provide longer analysis times on small volumes. Additional knowledge about quadrupoles and collision-induced-dissociation allows the combination of source design, multipole analyzers, and fragmentation experiments to form a triple-multipole mass spectrometer.

2.1 ELECTROSPRAY IONIZATION

Electrospray ionization (ESI) is a widely used but not completely understood technique. The ions detected are indisputably ions sprayed from the solution, however the mechanics of ion transfer to the gas phase from solution has not been unequivocally established.[24] Theories have been published about the ion transfer method, but none have been demonstrated to be flawless. The spray process begins with an electrophoretic mechanism to form droplets from a solution contained within a capillary biased to several thousand volts.[24] These droplets are charged due to the electrophoretic spray process and are thus attracted to the counter electrode. The steps by

which charged, single molecules are formed from these droplets are where questions remain. Solvent evaporation, ion emission, and coulombic fission, seem to be the factors, weighted in an unknown way, that are necessary to describe the process. Of particular note, the molecules can retain the multiple charges they possessed in solution leading to *m/z* values that other ionization methods can not produce.[25] The charges can be from the addition of a proton or sodium (or other metal) ion or the removal of a proton, to produce positive or negative ions respectively.

2.1.1 Spray Process

The most simplistic view of an electrospray source contains a capillary with a few kilovolts applied to it and a counter electrode. The solution that is within the capillary will experience the applied field to the capillary, causing the ions to propagate in accordance to the field lines established between the capillary and the counter electrode. In the case of positive ion ESI, a positive voltage is applied to the capillary. The positive ions will gather at the tip of the capillary, the farthest point from the applied voltage, forming a Taylor cone extending out of the capillary.[26] Once the combined charges of the positive ions can no longer be held together by surface tension, droplets are emitted from the cone. The droplets, with their abundance of positive charge, will be attracted by the counter electrode (Figure 2.1). This flow of charge produces a current from the capillary to the counter electrode which is proportional to the solution flow rate (V_f) and the conductivity of the solution (K), equation 1.[24] To determine the

$$I \propto (V_f * K)^n \qquad n < 0.5 \tag{1}$$

required voltage to begin spraying, the electric field around the tip, produced by the voltage on

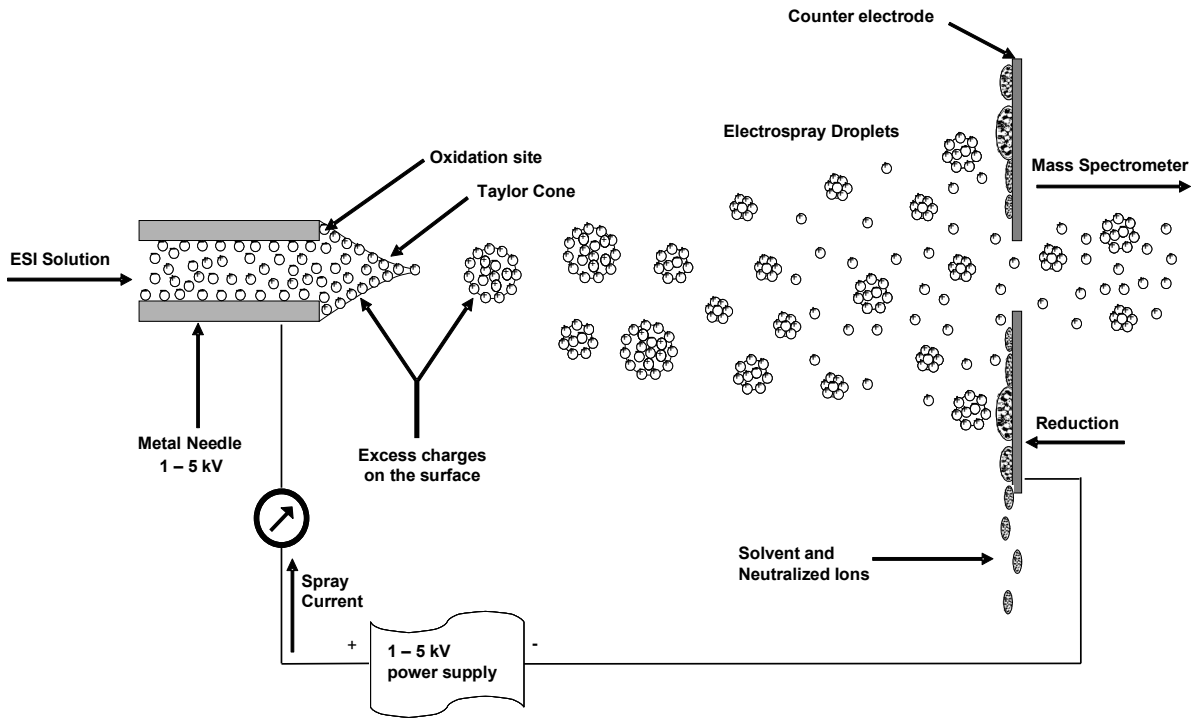

Figure 2.1: Simple electrospray ionization setup

the capillary, needs to be known.[24] In equation 2, E_c is the electric field in the air around the tip,

$$E_c = 2V_c / r_c \ln(4d / r_c) \tag{2}$$

V_c is the applied voltage, r_c is the capillary radius, and d is the distance from the tip to the counter electrode. Smith[24] derived equation 3 which describes the electric field needed for the

$$E_{on} \approx \sqrt{2\gamma \cos\theta / \varepsilon_o r_c} \tag{3}$$

onset of spraying, where γ is the surface tension, θ is the half angle of the Taylor cone, and ε_o is the permittivity of vacuum. To determine the voltage to initiate spray, equation 4 is produced by

$$V_{on} \approx \ln(4d / r_c)\sqrt{r_c \gamma \cos\theta / 2\varepsilon_o} \tag{4}$$

the substitution of E_{on} from equation 3 into equation 2 as E_c, wherein V_{on} is the required voltage to initiate spray and the rest of the parameters are as described above for equations 2 and 3.

Table 2.1: Onset voltages for 100% water with different nebulizers

d (cm)	0.3	0.5	0.5	1.0	1.0
r_c (μm)	5.0	5.0	7.5	10.0	12.5
V_{on} (kV)	0.9	0.96	1.12	1.36	1.48
γ = 0.073 N/m			θ = 49.3		

Once the droplets are formed, they rapidly break apart to form charged single molecules. As long as the droplet has a radius greater than 10 nanometers coulombic fission dominates the decrease in droplet size.[26] As the solvent in the droplet evaporates (i.e., the solvent density decreases) the electrostatic repulsion increases until the Rayleigh stability limit (equation 5) is

$$q_{Ry} = 8\pi\sqrt{\varepsilon_o \gamma R^3} \tag{5}$$

nearly reached. In equation 5 R is the radius of the droplet and q_{Ry} is the charge at which point the radius of the droplet creates a repulsion force of the surface charges equal to the surface tension of the droplet. The repulsion force or coulombic fission is reported to create a slightly smaller (but still large) droplet with "a cloud of small droplets".[24] Afterward, the large droplet again undergoes evaporation until the Rayleigh stability limit is reached and the process is repeated (Figure 2.2). The 'evaporation then coulombic fission' cycle repeats until the droplets are less than 10 nm in radius.

Two different hypotheses exist to describe the final step in ion formation (i.e. once the 10 nm radius threshold is reached). The first is the 'charge residue method' introduced by Dole and co-workers.[27] The method mimics coulombic fission throughout the transition from the spray to a single molecule. With further support from Schmelzeisen-Redeker et al.[28] the method appears to be valid until the droplet reaches a radius of 1 nm. In contrast, 'ion evaporation theory'[29,30] introduced by Iribaine and Thomson states that once a small enough size of droplet is reached

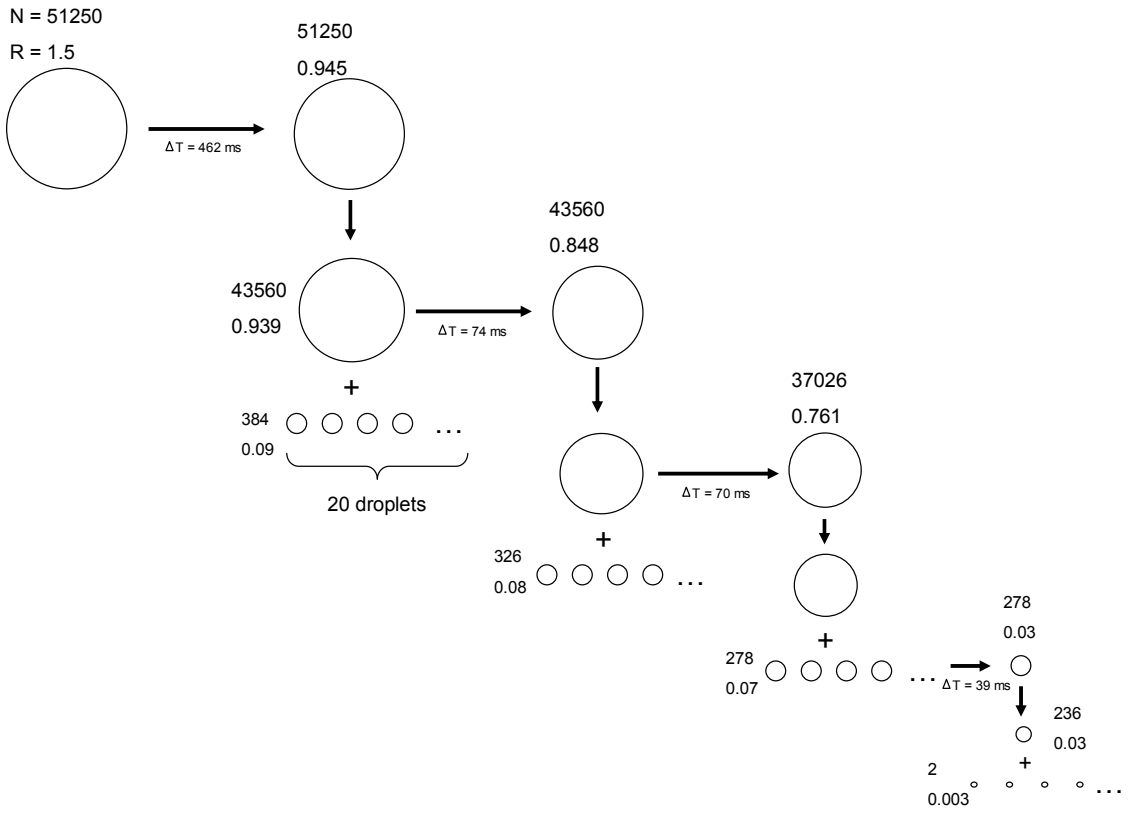

Figure 2.2: Rayleigh stability limit pathway where N is the number of elementary charges on the droplet and R is the radius of the droplet in micrometers.[26]

(sub 10 nm radius) an ion can then be directly emitted with a solvation shell (Figure 2.3).[31] This expulsion of a single ion with its solvent shell is called ion emission or ion evaporation. The solvent shell then evaporates to leave the charged single molecule. Unlike the charge residue method, ion evaporation appears to be valid from the 10 nm to molecular radius.[24] However both methods have flaws in predictions based upon subtle aspects and both have been criticized for failing to take into consideration all of the factors in the case of a microscopic droplet.[24] At the current level of ESI theory development, neither ion evaporation nor the charge residue method have been established as a better model for ion production.

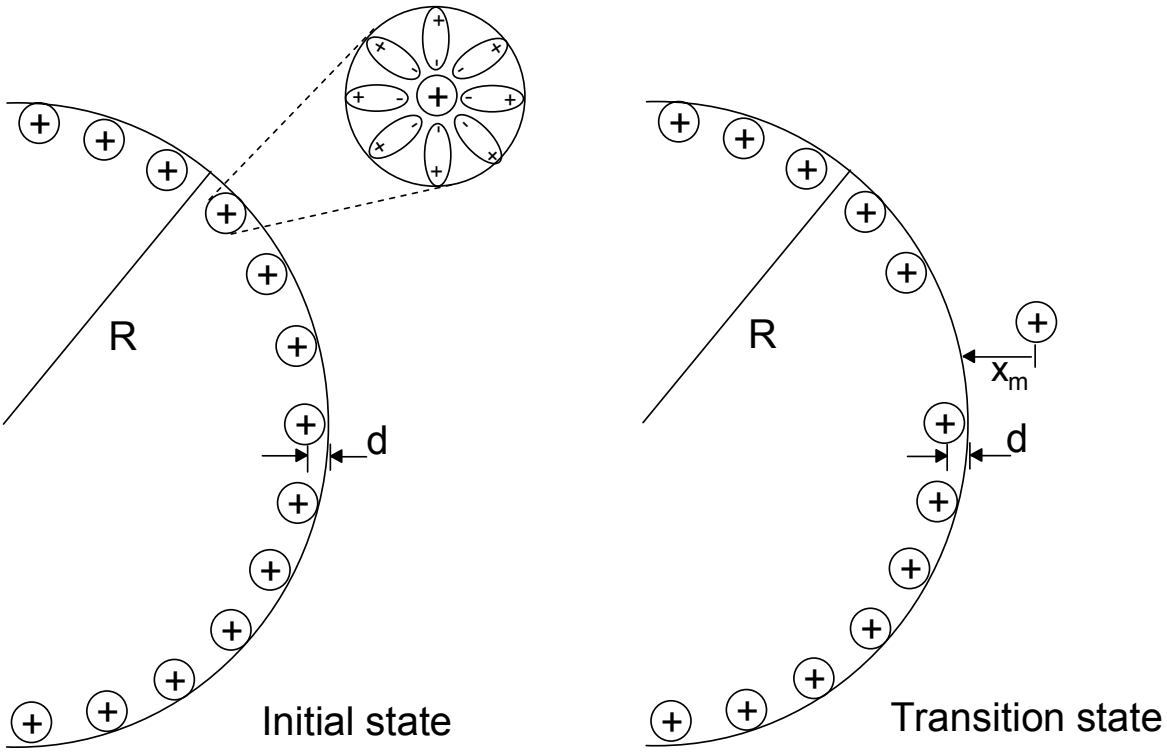

Figure 2.3: Ion evaporation pathway[26] where d is the radius of an ion plus its solvent shell and x_m is the distance the ion and solvent shell has moved outside the droplet.

2.1.2 Nanospray Properties

Upon consideration of the different techniques being used today for analytical mass spectrometry, nanospray is arguably the most convenient for biological research.[32] The major difference involved in the change from macrospray to nanospray is the flow rate that is applied to the sample. For traditional macrospray a sample flow rate above 1 μL/min is typical.[6] Nanospray is usually defined by a flow rate of 10-50 nL/min while microspray has a flow rate in-

between macrospray and nanospray. The two benefits of the low flow rate are the extended period of time that given volumes of material can be analyzed and the need for a drying gas is eliminated.[33] The extended period of time for analysis allows for multiple experiments to be performed, which can be especially valuable in the case of a triple multipole instrument like the SWISS-484. Also, more averaging is possible the longer the sample can be analyzed, resulting in a better signal-to-noise ratio. Because of the small amount of fluid flowing through the capillary, the need for assisting the desolvation of the analyte is greatly decreased,[33] this is because the less fluid being sprayed over a given time produces smaller radius droplets.[24] These droplets take less time to transform to a single ion state and fewer analytes are lost to incomplete desolvation, as compared to the higher flow rate techniques, eliminating the need for nebullizing or drying gas. These factors allow the capillary to be placed on a direct line and closer to the orifice to the mass spectrometer. The one major drawback to the use of the nanospray is that smaller capillaries are required for the low flow rates. With the capillary orifice, around 10 μm in diameter, clogging becomes a regular occurrence. Even though the samples can be, in principle, sprayed for longer times, the ion current must be monitored for the onset of tip blockage. At this occurrence, the tip either must be opened by increasing the voltage on the tip or breaking off the end for a clear path or the tip must be replaced.

2.1.3 Ionization Output

The ions produced by the sprays are often unique to the electrospray technique.[6] Since the ions are formed by evaporation and emission from the solvent, the molecules are usually intact and rarely are fragmented prior to analysis. Because of the general lack of fragmentation, electrospray ionization is considered to be a “soft ionization” method.[34] Along with the lack of

fragmentation, non-covalent complexes can remain intact through the spray process.[35] This provides the unique possibility of solution phase complexes being characterized as gas phase ions.

Since the ions are produced from the substances in solution, the type and intensity of ions created will depend on the pH and salt content of the solution. Large molecules, such as those greater than 2000 Daltons, are likely to be able to accommodate several-to-many charges, converting the high molecular weight molecule into an "envelope" of lower *m/z* values (where *m* is mass and *z* is charge). A change in pH may result in an increase or decrease in the number of charges borne by the molecule. With an increased concentration of salt, the likelihood of the corresponding cation addition instead of a proton is amplified (e.q., MNa^+ vs MH^+).

2.2 QUADRUPOLES

The experiments performed on the SWISS-484 utilize the capabilities of the three multipoles. Each could act as a mass analyzer on its own or be combined together to perform MS/MS experiments. The first and third multipole (Q1 and Q3) are quadrupoles which act as mass analyzers. These two independently can be set to pass all ions, to allow a window of *m/z*(s) to pass through, or to scan from one *m/z* to another. The particular *m/z* passed is contingent on the rf and dc voltages that are applied to the quadrupoles.[36] The middle multipole is an octopole and acts as an ion guide between the two mass analyzers. Collision gas can be introduced into the octopole (which is shrouded) to induce dissociation of the ions.[1] Since the octopole guides all ions through its region, any ion that is produced or left unchanged from the collisions will make it to the octopole exit which is also the entrance to Q3.

All three multipoles use the principles of electric fields to enable them to perform as mass analyzers. The identical rods (four for a quadrupole and eight for an octopole) are all aligned at a set radius of $1.148r_o$ centimeters, where r_o is the radius of each rod.[36] The electric connections in a quadrupole are arranged as shown in Figure 2.4. The basis of the selection process of the quadrupoles hinges on the stability of the path of an ion of a particular *m/z* value.[36] With both voltages causing the ion to deflect according to the fields produced, both voltage values combined will determine which ions will have a stable path and make it through the quadrupole. The starting point in understanding which ions will have the stable pathway begins with equation 6, wherein *F* is the force on the ion, *m* is the mass of the ion, and *a* is the acceleration in the *x*

$$F = ma = m\frac{d^2x}{dt^2} \tag{6}$$

direction. In dealing with electric fields or potentials equation 6 can be rewritten as equation 7 wherein *P* is the potential. In a three dimensional electric field the potential will follow equation 8 wherein r_o is the radius of the circle of poles, λ, σ, and γ are weighting parameters for the three

$$m\frac{d^2x}{dt^2} = -e\frac{dP}{dx} \tag{7}$$

$$P = \frac{P_o}{r_o^2}(\lambda x + \sigma y + \gamma z) \tag{8}$$

dimensions, and P_o is the applied electric potential as in equation 9 where *U* is the dc potential, *V*

$$P_o = U - V\cos\Omega t \tag{9}$$

the rf potential, and Ω the angular frequency.[37] Taking the derivative of equation 8 in respect to either the x or y axis and the substitution of equation 9 into equation 8 provides equation 10.

$$\frac{dP}{dx} = \frac{2\lambda x}{r_o^2}(U - V\cos\Omega t) \tag{10}$$

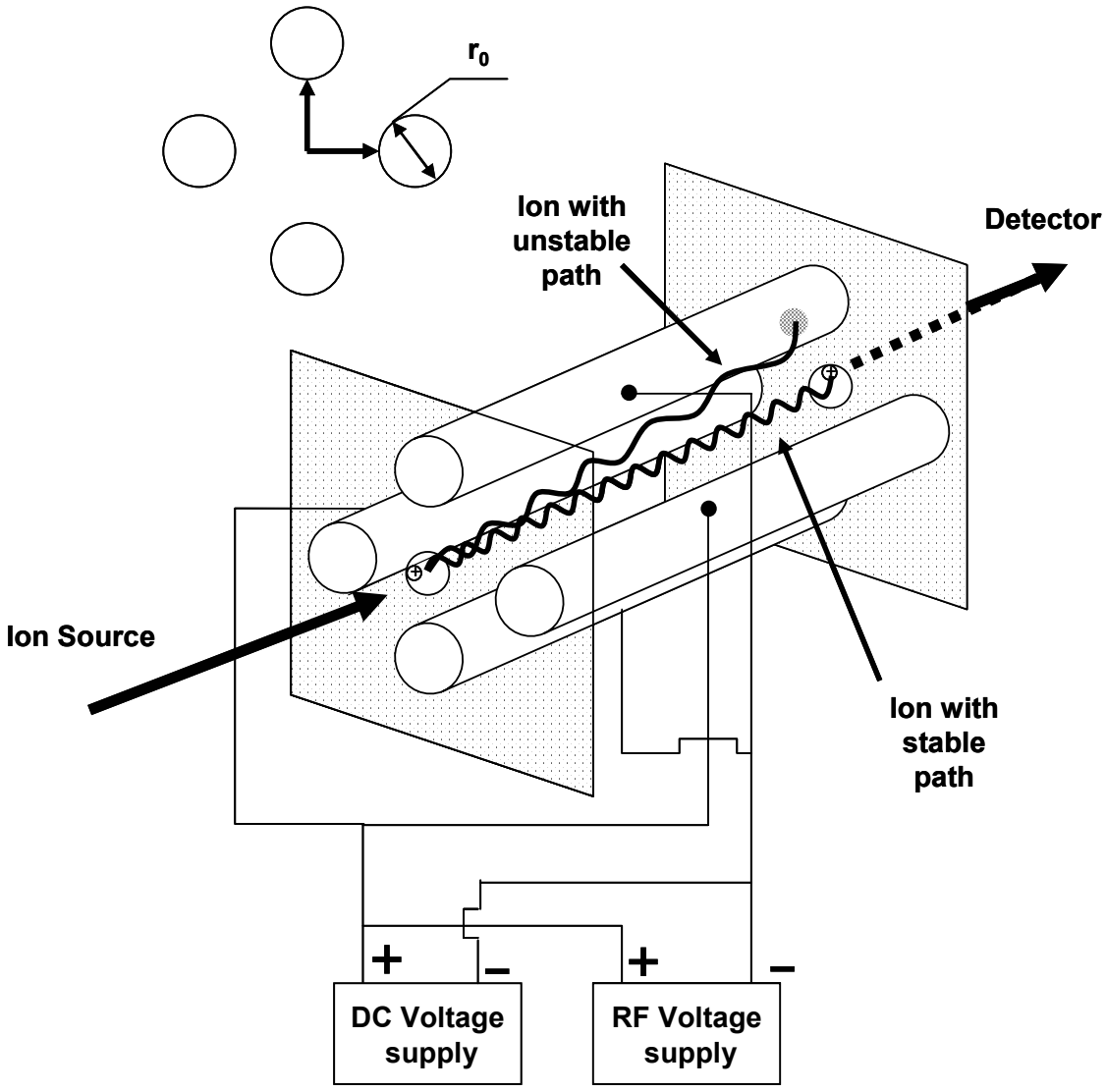

Figure 2.4: Quadrupole configuration

Furthermore, substituting equation 7 into 10 produces equation 11. With the purpose of

$$m\frac{d^2x}{dt^2} = \frac{-2e\lambda x}{r_o^{\,2}}(U - V\cos\Omega t) \tag{11}$$

simplification one sets to equation 12. Hence equation 13 is equation 11 rewritten with the

$$\zeta = \Omega t / 2 \tag{12}$$

$$\frac{m\Omega^2}{4}\frac{d^2x}{d\zeta^2} = \frac{-2e\lambda x}{r_o^{\,2}}(U - V\cos 2\zeta) \tag{13}$$

substitution of . So for each axis the ion would have this force upon it. However in the case of a linear multipole the *z* direction is unfocused so its weighting parameter is zero. Equation 8 will have one less variable as in equation 14. Taking into effect the Laplace conservation law, which states equation 15, the weighting parameter must then add up to zero for a linear

$$P = \frac{Po}{r_o^{\,2}}(\lambda x - \sigma y) \tag{14}$$

$$\nabla P = 0 \tag{15}$$

multipole.[38] With γ equaling zero for the *z* direction and $(q - x)$ equaling zero, equation 16 is

$$\sigma = -\lambda \tag{16}$$

produced. First rearranging equation 13 to the differential of equation 17, it can be simplified with the use of the Mathieu parameters,[36] equations 18 and 19, to provide equation 20 which

$$\frac{d^2x}{d\zeta^2} = \frac{-8e\lambda xU}{r_o^{\,2}m\Omega^2} + \frac{8e\lambda xV\cos 2\zeta}{r_o^{\,2}m\Omega^2} \tag{17}$$

$$a = \frac{8e\lambda U}{r_o^{\,2}m\Omega^2} \tag{18}$$

$$q = \frac{4e\lambda V}{r_o^{2}m\Omega^2} \tag{19}$$

$$\frac{d^2x}{d\zeta^2} = -(a - 2q\cos 2\zeta)x \tag{20}$$

takes into effect only the *x* direction. To obtain the y axis, the use of equation 16 provides the substitution of equations 21 and 22 as the Mathieu parameters. Finally the ion motion is governed in the x axis as determined in equation 23. Using the Mathieu parameters as axis,

$$ax = -ay \tag{21}$$

$$qx = -qy \tag{22}$$

$$\frac{d^2x}{d\zeta^2} + (a - 2q\cos 2\zeta)x = 0 \tag{23}$$

stability diagrams can be produced as in Figure 2.5. The shaded areas describe an ion with a stable pathway. Taking into effect both axis will produce the stability diagram of Figure 2.6.[36] An ion will be allowed to pass through a multipole where the x and y stable pathways cross. There are three distinct regions of stability, however the region closest to the origin is the only one that has been extensively studied and used.[37] When scanning a range of *m/z*, one can use a fixed ratio for *a/q* (Figure 2.7a). This ratio can be rearranged to be *2U/V* (equation 24).

$$\frac{a}{q} = \frac{8e\lambda U}{r_o^2 m\Omega^2} * \frac{r_o^2 m\Omega^2}{4e\lambda V} = \frac{2U}{V} \tag{24}$$

Manipulating the rf and dc voltages on the poles will guide the stability region to the desired ion.

Another feature of multipoles that can be easily understood from Figure 2.7b is the resolution of the scan line. Changing the value of *a/q* or the slope of the scan line will increase or decrease the resolution. If the scan line is tangent to the top of the stability region then the resolution will be very high but the intensity will be low. A smaller slope of the scan line will produce poorer resolution but higher intensity due to the wider range of ions in the stable region. Thus the resolution can be changed according to the type of spectrum that is desired.

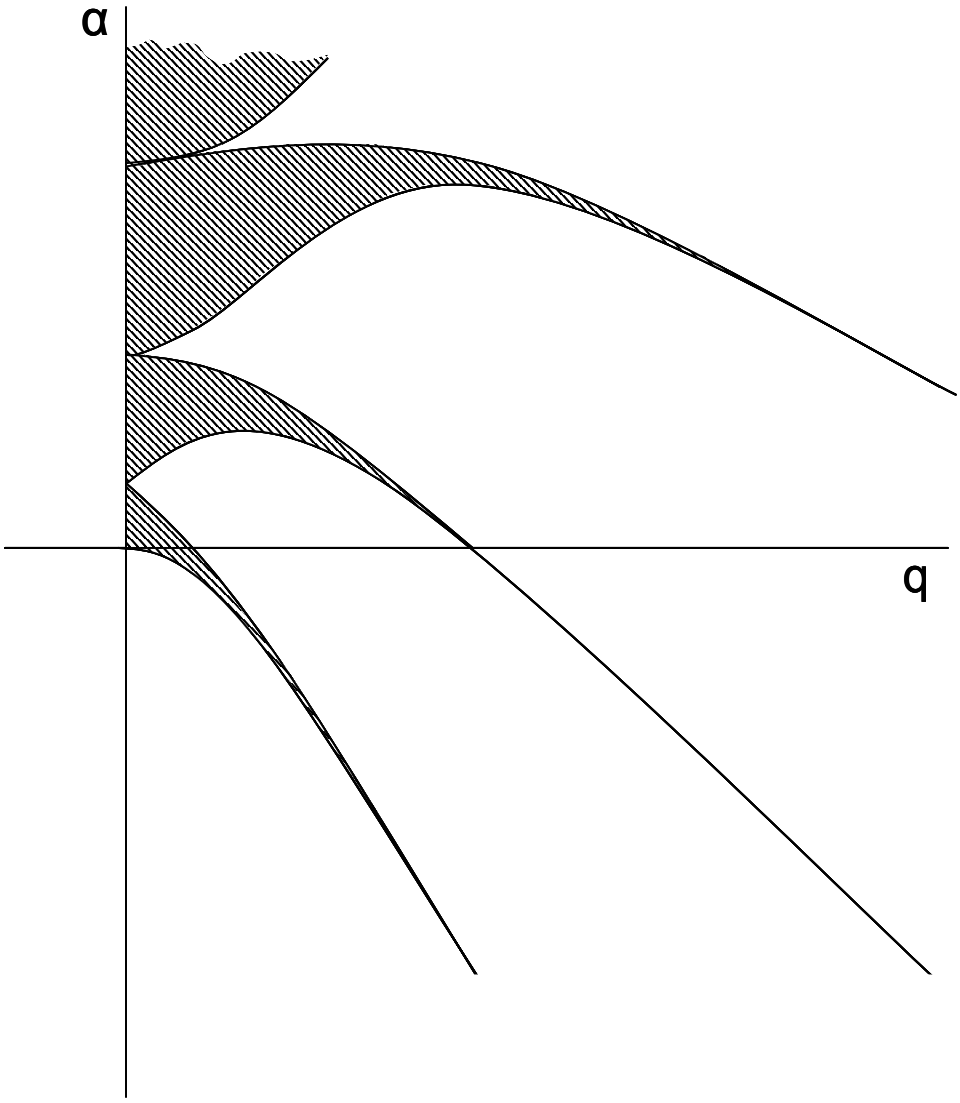

Figure 2.5: Quadrupole stability plot - 1 dimension[32]

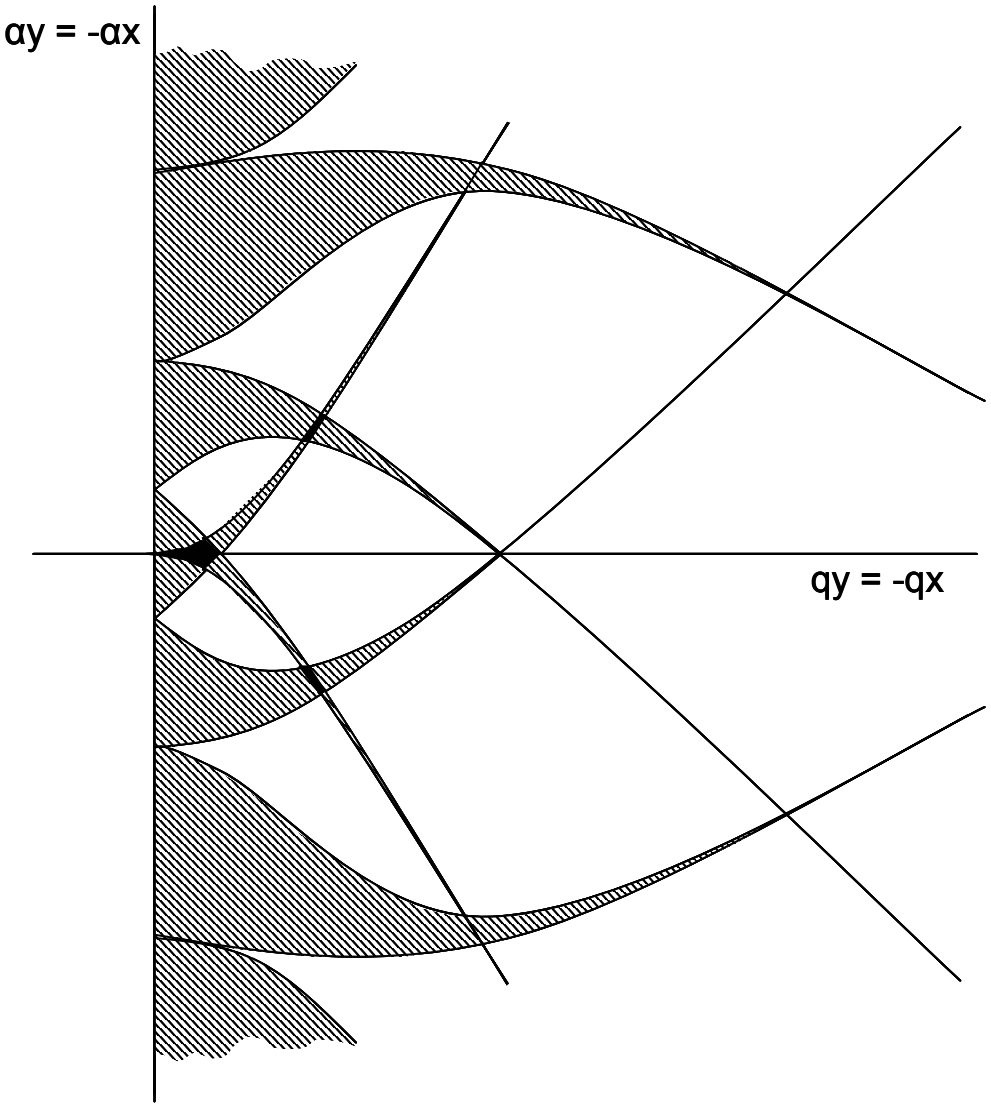

Figure 2.6: Quadrupole stability plot - 2 dimensions[32]

(a)

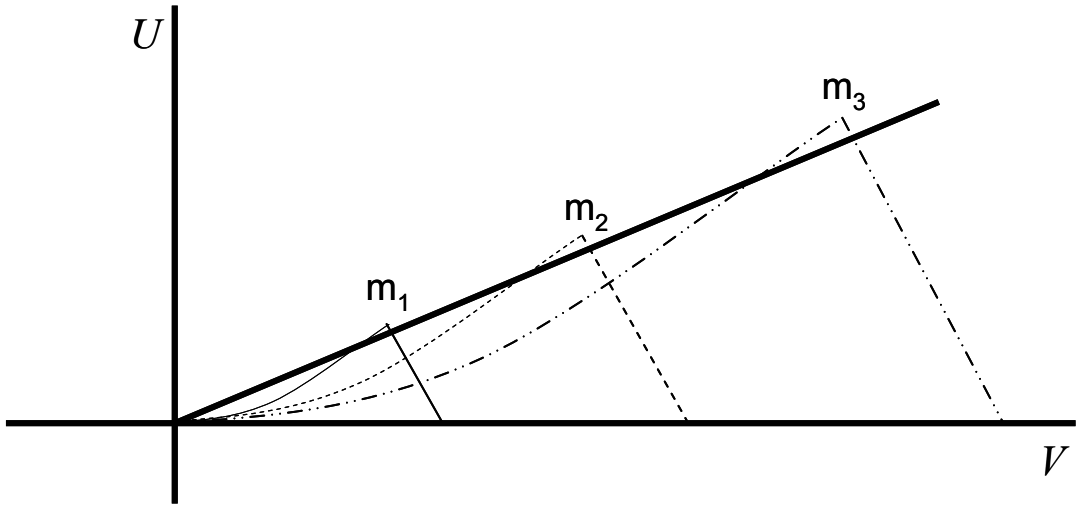

(b)

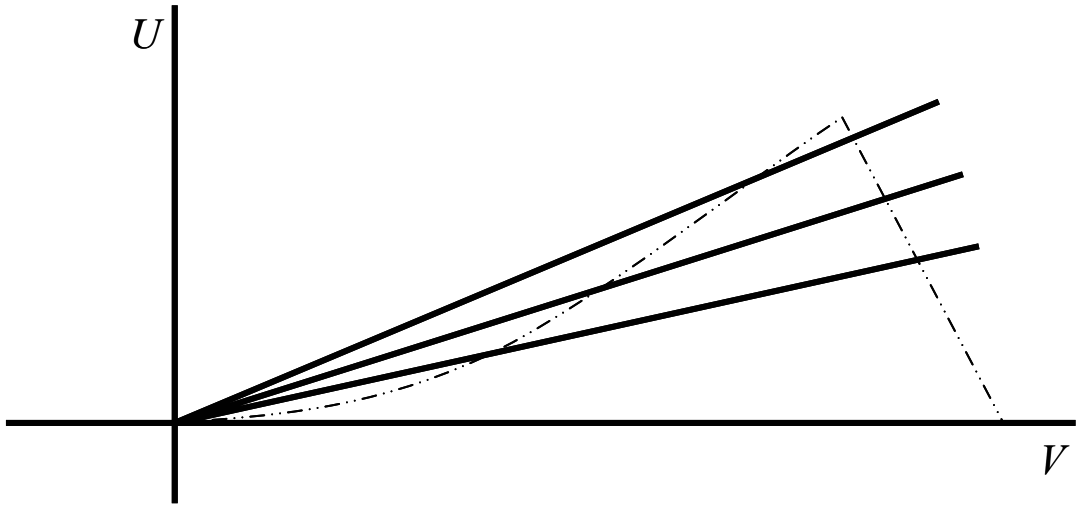

Figure 2.7: Quadrupole (a) scan line and (b) resolution

2.3 COLLISION INDUCED DISSOCIATION

The triple multipole configuration can perform CID experiments by having the first multipole set to pass selected *m/z*, the second multipole acting as a collision cell, and the third multipole scanning for the fragment ions. In these experiments a dissociation reaction occurs in the octopole (also known as the collision cell). In a typical CID experiment, Q1 selects a single ion, the precursor ion, to pass through to the octopole. Collision gas (i.e., argon) is placed inside the octopole to obtain a higher pressure (~$5x10^{-5}$ Torr) than within the quadrupoles. The higher pressure in the collision cell provides the opportunity for the ions to collide with neutral species. At $5x10^{-5}$ Torr a pentapeptide would have a mean free path of about 21 cm. The collision between an ion and the collision gas can provide enough energy for fragmentation of the ion to occur.[1] Q3 can then either be configured to scan all of the product ions, or monitor a single known fragment ion from the precursor ion. The former method can be used to identify the structural composition of the ion entering the collision cell.[1] The latter method is known as selected reaction monitoring (SRM) and maximizes the identification of the selected ion presence in solution. Whereas the scanning procedure provides qualitative information, SRM is typically used for increased sensitivity for quantitative experiments.[39]

To clarify the function of each multipole in a given experiment, a set of three rectangles will be utilized. Four different graphics within the rectangles will signify if the multipole is functioning as an ion guide, scanning a range of *m/z*, functioning as a collision cell, or monitoring a single ion (Figure 2.8). With the use of the graphic for the octopole functioning as a collision cell, the type of collision gas will be stated on the spectrum. The graphic of the quadrupole monitoring a single ion will contain the m/z selected and the window width being passed in atomic mass units (amu). Figure 2.9 shows a typical CID experiment set of rectangles.

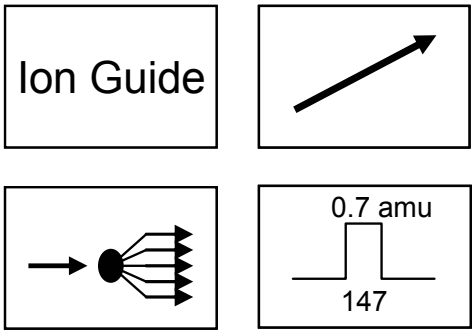

Figure 2.8: The multipole function clarification graphics: (upper-left) ion guide, (upper-right) scanning, (lower-left) collision cell, and (lower-right) single ion monitoring.

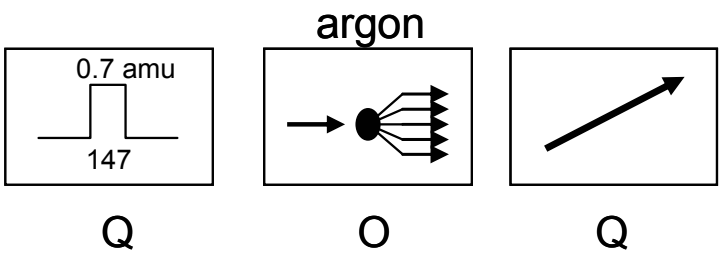

Figure 2.9: Typcial CID experiment graphic where the first quadrupole is monitoring a single ion (*m/z* 147) with a width of 0.7 amu, the octopole is functioning as a collision cell with argon as the collision gas, and the last quadrupole is scanning a range of *m/z*.

2.4 SWISS-484

The SWISS-484 consists of three main sections, the ionization interface, the multipoles, and the detector. The ionization interface encompasses the electrospray mechanism and the transfer optics from atmospheric pressures to the vacuum chambers containing the multipoles. The electrospray apparatus, Figure 2.10, has a syringe pump to provide a constant flow of solution. A connecting capillary carries the flow from the pump to the nebullizing capillary from which the spray occurs. The connecting capillary is connected to the nebullizer capillary by a PEEK connector. The nebullizer capillary is a 5 cm long, 360 μm OD, 25 μm ID fused silica capillary that has a pulled tip providing a smaller orifice. The capillary is normally gold coated to provide the electrical connection to the high voltage required for electrospray ionization. The tips we have used most often were purchased from New Objective, Inc. The setup is connected to a Plexiglas mount (for electrical isolation) via a stainless steel bulkhead.

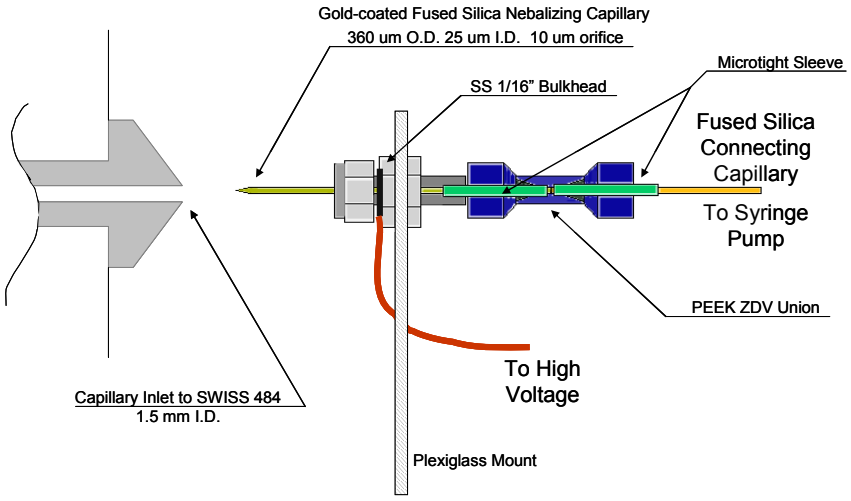

Figure 2.10: SWISS-484 electrspray setup

The capillary inlet to the SWISS-484 is a 12 cm long stainless steel capillary with a 1.5 mm ID. The capillary is thermally isolated for heating, typically to 200^{o}C, and the temperature is monitored via a thermocouple. This capillary inlet begins the transfer of ions to the first quadrupole as summarized in Figure 2.11. The skimmer_1 chamber is located directly after the capillary inlet and is terminated by skimmer_1 which contains a 1.0 mm ID orifice. Following skimmer_1 is the skimmer_2 chamber which is terminated by skimmer_2 which contains a 0.75 mm ID orifice. Each skimmer chamber is evacuated by its own dedicated Pfeifer Balzers BZ 43 model mechanical pump with a pumping speed of 4.44 L/s. After skimmer_2 is the source chamber which is evacuated by an Edwards Diffstak Model 160 oil-diffusion pump (700 L/s) backed by an Edwards E2M-18 mechanical pump (6.94 L/s). An einzel lens is placed between skimmer_2 and the entrance to Q1. The einzel lens consists of three lenses each with a 1 cm ID, a 4.6 cm OD, a 1.6 mm thickness, and spaced 1.5 cm apart.

The other two sections of the SWISS-484 are the multipole chamber and the detector. They are evacuated by a Leybold-Heraeus 360 CSV Turbo pump with a pumping speed of 360 L/s, backed by a Pfeifer Balzers BZ 43 mechanical pump with a 4.44 L/s pumping speed. The multipoles are arranged in the following order (Figure 2.12): entrance lens, Q1 quadrupole, lens 1_2, collision cell octopole, lens 2_3, Q3 quadrupole, and exit lens. The four lenses each have a 1 cm ID orifice and the multipoles are positioned equidistant between the adjacent lenses. Following the exit lens is the conversion dynode which is biased ±5000 V depending on the ions to be detected (negative or positive). The dynode is followed by the electron multiplier. Normal settings for the multiplier are 1800 V with a preamp gain of 1x10^{9}.

Figure 2.11: SWISS-484 electrospray source

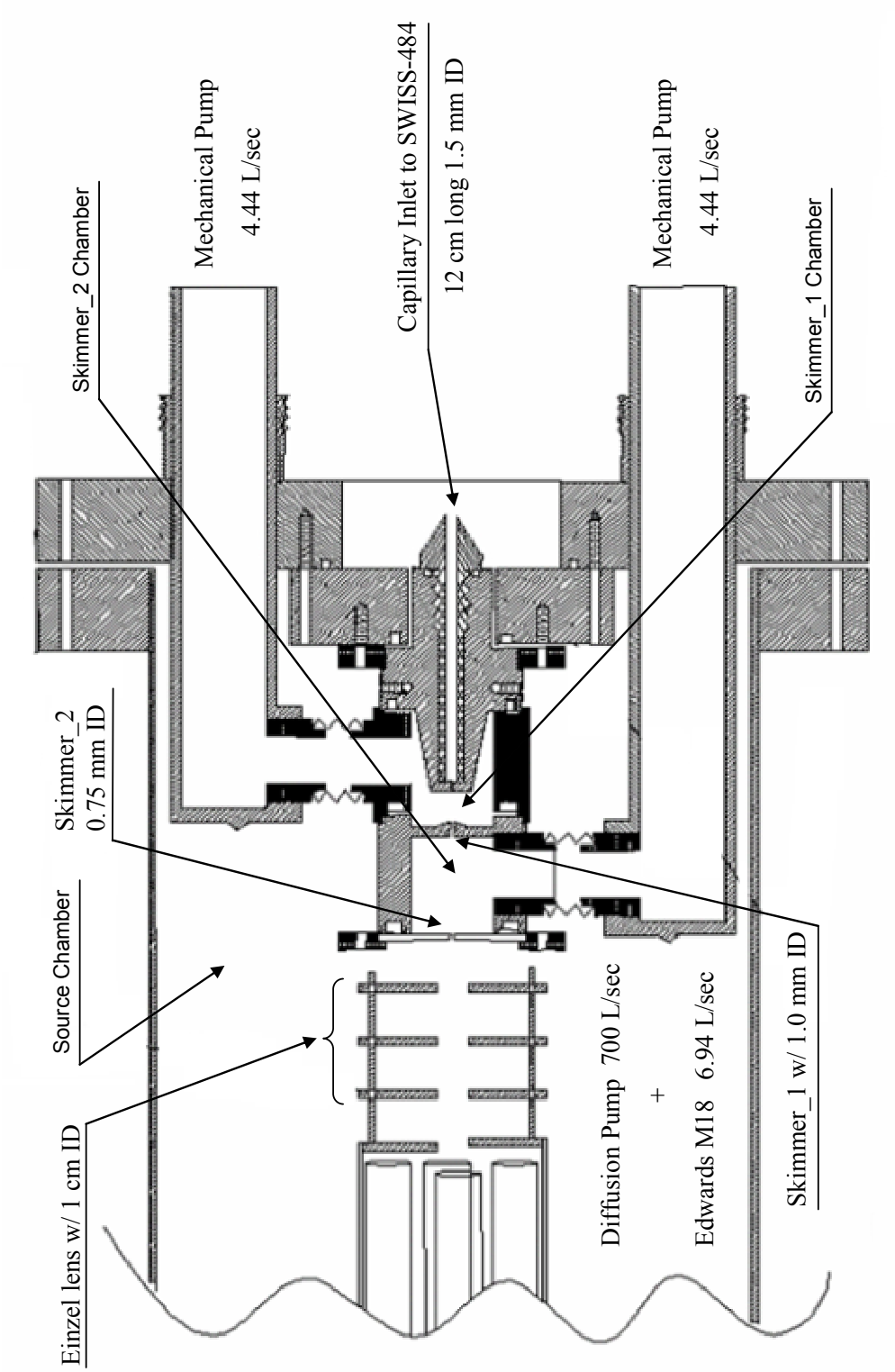

Figure 2.12: SWISS-484 Design

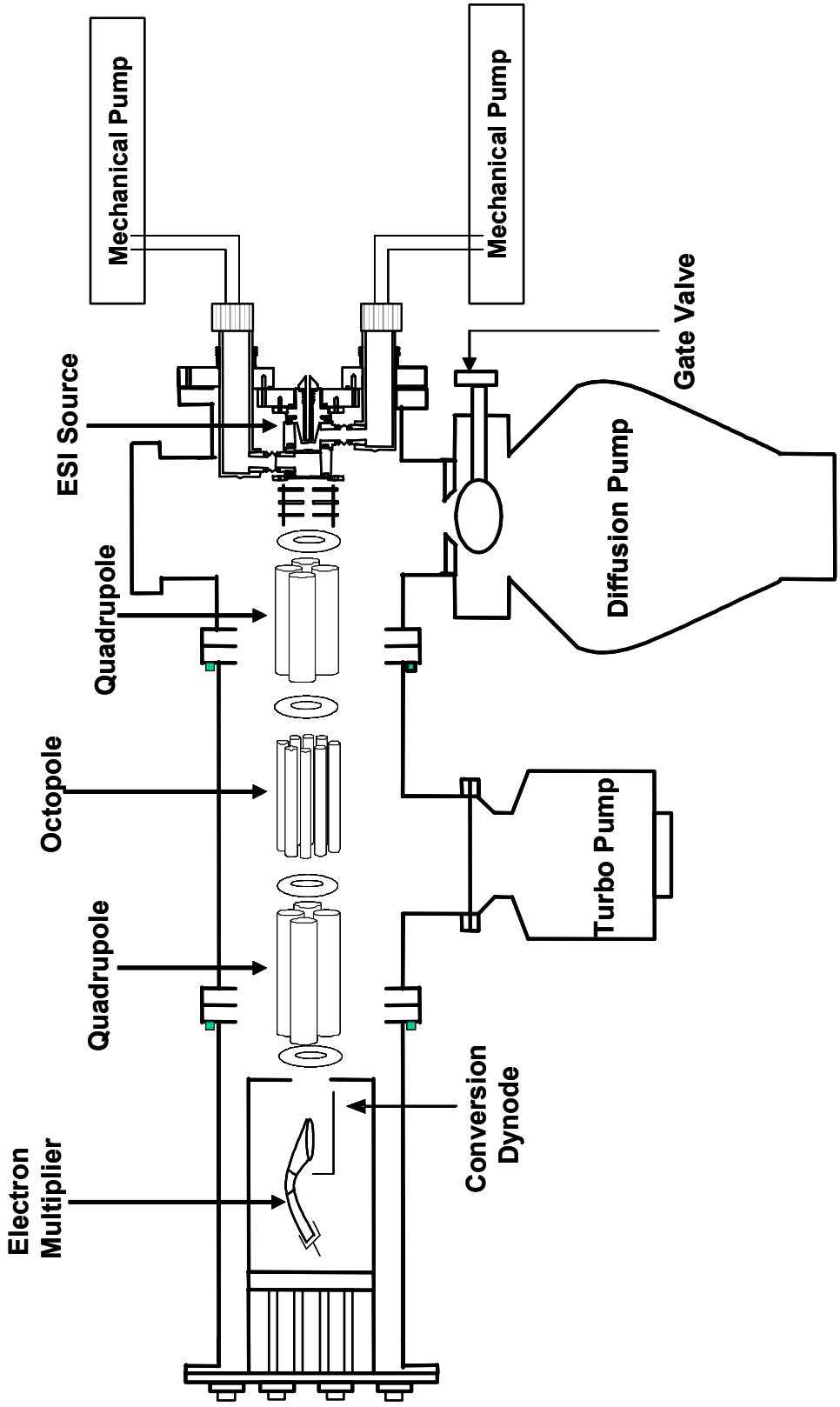

The instrument controller is a Merlin Automation system version 1.0.15 from Extrel CMS with a CPU containing a 2.60 GHz processor and 1.0 GB of RAM. The system was calibrated with three different compounds ($Me_4N^+Cl^-$, polyethylene glycol (PEG), and myoglobin).

The program Magic Transformer (MagTran) was used to deconvolute multiply charged ESI spectra. MagTran was obtained from Zhongqi Zhang and uses a algorithm designed by Zhang and Alan G. Marshall.[40] Deconvolution is needed for the high number of peaks in the analyte's charge "envelopes". Raw data files were transferred to a text file of two columns, *m/z* and abundance (mV) by the Merlin Automation Data System and imported into MagTran. On occasion analytes which contain only a few peaks are assigned by hand, based on the known molecular weights of the compounds in the solution.

$Me_4N^+Cl^-$ was used to calibrate sub 200 *m/z* values. A 23 μM solution in 50% methanol, 50% water was used with a flow rate of 50 nL/min. The New Objective tip with a 10 μm orifice had 2.0 kV applied to it. The single ion ($(CH_3)_4N^+$, *m/z* 74) and the aggregate ($((CH_3)_4N^+)_2Cl^-$, *m/z* 183) were observed (Figure 2.13).

Polyethylene glycol (PEG) with an average weight of 400 was used as a reference for the peptides, *m/z* range of 200 to 1000. A 10 μM solution in 50% methanol and 50% water was used with a flow rate of 100 nL/min and with 2.0 kV applied to a tip with a 10 μm orifice. The sodiated polymers, $HO(CH_2CH_2O)_nH(Na^+)$, with between 5 and 15 repeat units were observed (Figure 2.14).

Horse heart myoglobin (molecular weight is 16951.4 amu) was used as a reference for the proteins; the majority of which contain signals above *m/z* 1000. A 4.5 μM solution in 25% methanol and 75% water containing 1% acetic acid was used with a flow rate of 300 nL/min and

with 2.0 kV applied to a tip with a 15 μm orifice. The "envelope" of the addition of 10 to 20 protons to the molecule is observed (Figure 2.13). MagTran provided a molecular weight of 16973.3 amu which has a 0.13% difference compared to the known value of 16951.4 amu for horse heart myoglobin.

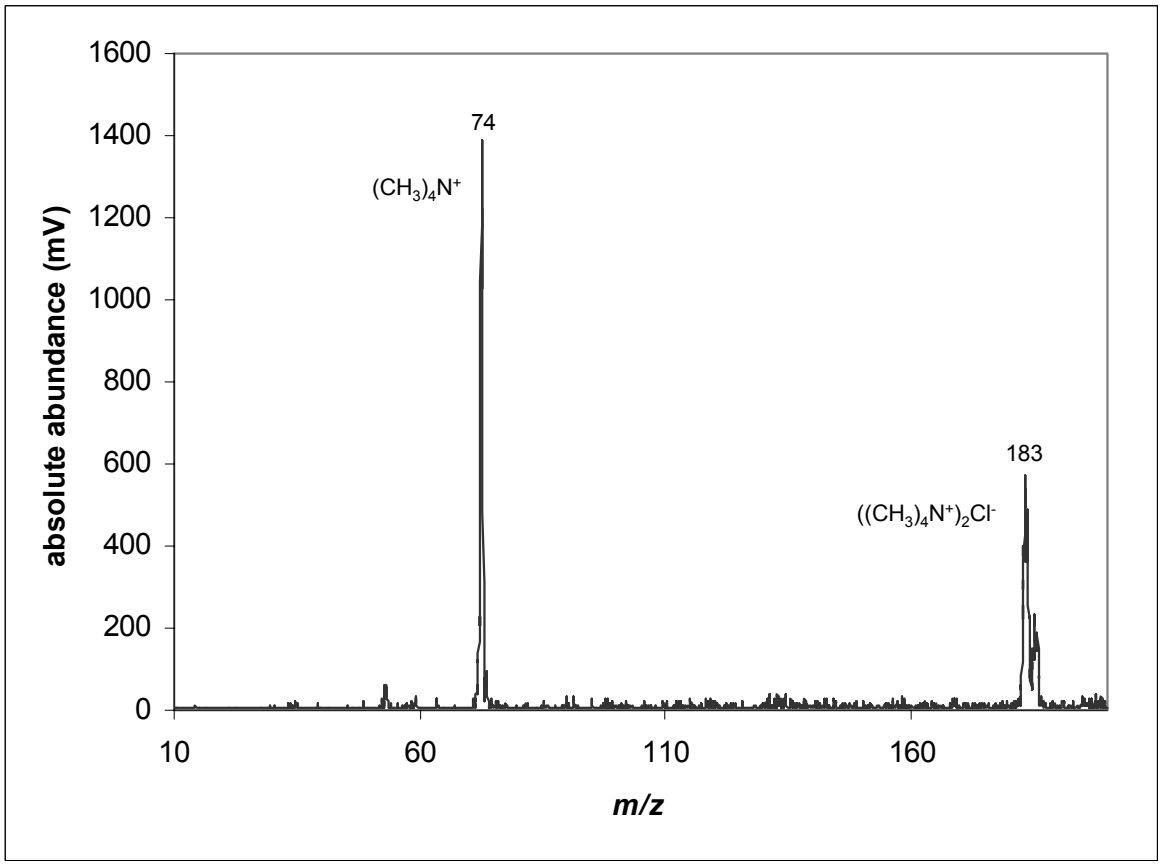

Figure 2.13: Spectrum of tetramethylamine (23 μM in 50:50 methanol:water)

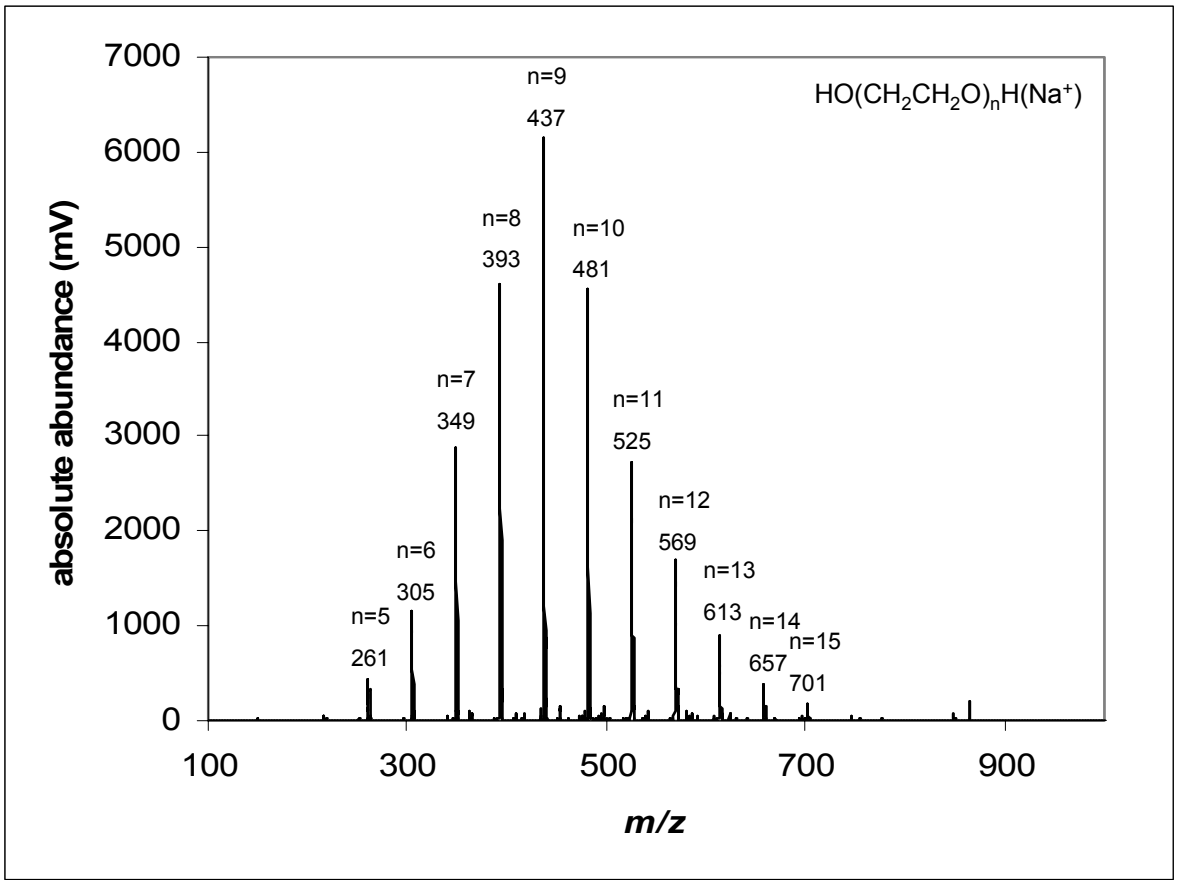

Figure 2.14: Spectrum of polyethylene glycol 400 (10 µM in 50:50 methanol:water with addition of NaCl to promote sodiation)

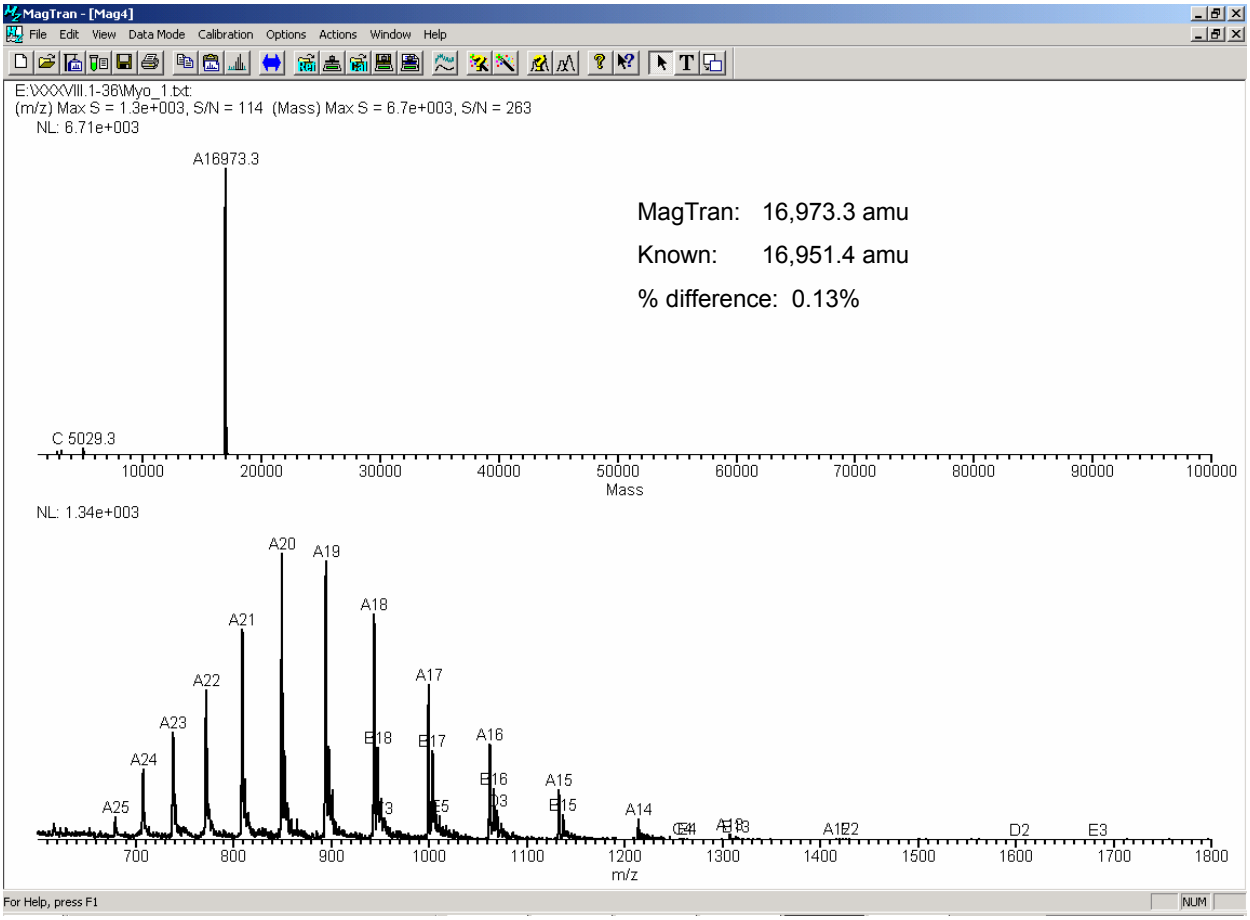

Figure 2.15: Spectrum of myoglobin shown in Magic Transformer (4.5 µM in 75:25 methanol:water with 1% acetic acid). The lower spectrum is the raw data with letters (A, B, C, …) signifying an "envelope" and numbers (15, 16, 17, …) signifying the number of protons on the structure. The upper spectrum is the deconvoluted output showing the molecular weight and abundance of each "envelope".

3.0 GLUCOSE

The elevation of blood glucose due to poor insulin production and/or poor insulin action defines *Diabetes Mellitus*.[41] Glucose monitoring is important in order to prevent complications resulting from the high blood glucose concentrations.[7] The prevalent method to monitor glucose relies on a finger stick and a glucose oxidase based meter. To alleviate the pinprick there has been significant research to produce a non-invasive method to monitor blood glucose.[8-11] Some of the research has examined tear fluid glucose as an indicator for blood glucose; however, there has not been a definitive answer to the concentration of glucose present in tears.[42] Section 3.1 provides details about the tear glucose discrepancy over the past 70 years and is taken from Baca et al. (Chapter 5)[43]. A few studies make a significant observation that irritation of the eye causes higher glucose concentrations in tears.[12-14] This observation makes the method of sampling tear fluid critical dependent on the type of tears desired. To obtain tear glucose concentrations of common/non-stimulated tears, less than 2 μL of fluid can be sampled due to the low volume of tear fluid (~7 μL) on the eye. Electrospray ionization mass spectrometry (ESI-MS) can easily analyze microliter sized samples. A method is developed utilizing 1 μL capillaries and ESI-MS to determine tear glucose concentrations. With this method a correlation then could be determined between blood and tear glucose.

3.1 LITERATURE REVIEW

Daum and Hill [12] reviewed the experimental data available in 1982, and noted that reported values of tear glucose in normal individuals range between 0 and 3.6 mM (65 mg/dL), with the median values ranging between 110 and 280 μM (1.98 and 5.04 mg/dL). More recently, capillary electrophoresis and laser-induced fluorescence measurements of tear glucose concentration in a single subject found a glucose concentration of 138 μM (2.49 mg/dL).[44] A study by this group on six non-diabetic adults found glucose concentrations ranging between 128 and 166 μM (2.31 and 2.99 mg/dL) with an average of 139 μM (2.50 mg/dL).[45]

A recent study by Lane et al.[46] compared tear glucose values in 48 diabetic and 73 non-diabetic subjects. They found average tear glucose concentrations of 160 μM (2.9 mg/dL) for non-diabetic subjects and 350 μM (6.3 mg/dL) for diabetic subjects. These average concentrations include measurements of tear samples taken before and after a carbohydrate load. The reported range of tear glucose concentrations was exceptionally high, ranging from below the limit of detection to 5.7 mM (103 mg/dL) for non-diabetic subjects and from below the limit of detection to 9.1 mM (164 mg/dL) for diabetic subjects.

Van Haeringen and Glasius specifically addressed the dependence of tear fluid glucose on the method of collection.[13] They used a glucose dehydrogenase method to analyze chemically stimulated tears collected with a capillary and non-chemically stimulated tears collected by contact with filter paper. They found higher glucose concentrations in the tears collected by filter paper. Van Heringen and Glasius concluded that the increased tear glucose concentration found in tears collected by filter paper is due to the mechanical stimulation of the corneal and conjunctival epithelium, and noted similar findings in previous experiments on

rabbits.[14] Daum and Hill found increased tear glucose concentrations in subjects immediately after swimming.[12] This increase was ascribed to mechanical or osmotic stress.

While previous studies generally report increased tear glucose concentrations with increased blood glucose concentrations, many used very irritating collection methods, and some required large (stimulated) tear volumes for glucose measurements. These results are not clearly germane for understanding basal tear glucose concentrations. Lane et al. see a clear increase in average tear glucose concentration with increased average blood glucose concentration for diabetic subjects undergoing a glucose tolerance test.[46] Unfortunately, they do not present data from individual subjects, but only population averages at various time points.

Recently, two groups studied contact lens-based glucose sensors using glucose-dependent, boronic acid fluorophores.[10,47] In a clinical trial including four subjects, these glucose sensing contact lenses showed clear correlations between the fluorescence intensity and blood glucose concentrations upon feeding. However, these studies did not correlate fluorescence intensity with absolute glucose concentrations.[11] Initial clinical testing of a holographic glucose sensor in a contact lens also indicated a correlation of tear and blood glucose by demonstrating that the diffracted wavelength of light tracked the blood glucose concentration.[47] This study also measured only relative glucose concentrations and did not correlate peak wavelength shift with absolute tear glucose concentrations.

A recent study of five critically ill patients found a mean tear fluid glucose concentration of 7.25 ± 5.47 μM (0.13 ± 0.10 mg/dL), and found no statistically significant correlation between tear and capillary blood glucose concentrations (R^2=0.052, p=0.12).[48] However, as these patients were critically ill, the relevance of the results to normal and healthy diabetic subjects is questionable (Luis A. Colon, Personal Communication, 8/7/06).

3.2 EXPERIMENTAL

Two ESI-MS instruments were used for the experiments, the SWISS-484 (described in Chapter 2 section 2.4) and the HP LCMS 1000. Glucose, $^{13}C_6$-glucose, acetonitrile, acetic acid, and salts (NaCl, KCl, and $Pb(NO_3)_2$) were purchased from Sigma Chemical Company (St. Louis, MO). They were dissolved in water, with acid or salts already added, and then acetonitrile. For experiments on the SWISS-484, solutions were sprayed from a New Objective capillary tip with an orifice of 10 μm with 2.0 kV applied to the spray tip and with a flow rate of 100 nL/min set on the syringe pump. Data were collected for five minutes and all scans were averaged to provide the spectra. Experiments performed on the HP LCMS were conducted as described in Chapter 4 section 4.3.

3.3 INITIAL RESULTS

To maximize the sensitivity, lower the detection limit, and have conclusive evidence of glucose, MS^2 experiments were determined to be the best avenue to obtain quantitative data. Experiments were initiated on the SWISS-484 due to its tandem mass spectrometry capabilities. Known solutions of glucose were characterized on first the SWISS-484 and then later on the HP LCMS.

3.3.1 SWISS-484

Solutions ranging from 20 mM to 100 μM of glucose in 50% water and 50% acetonitrile were analyzed. In each spectrum only the sodiated peaks were observed (Figure 3.1). To determine if

different adducts of glucose could be observed, acetic acid or salts (KCl and $Pb(NO_3)_2$) were added to the solution. The addition of acetic acid to the above described solutions, to promote protonation, did not provide protonated glucose and sodiated glucose was still abundant. With potassium chloride (2 mM) in a solution of 50 µM glucose, potassium-glucose adduct ion along with sodiated glucose along with each cationized glucose dimer were observed. The intensities of the potassium-glucose adduct peaks were 20% of the sodiated peaks in the corresponding solutions (2 mM NaCl and 50 µM glucose) spectrum. With the addition of lead nitrate (9 µM) to a 40 µM glucose solution, (glucose-H^+)Pb^{2+} was observed but half as intense as sodiated glucose. With the sodiated ion the most intense of all ions, *m/z* 203 was used for quantitative analysis.

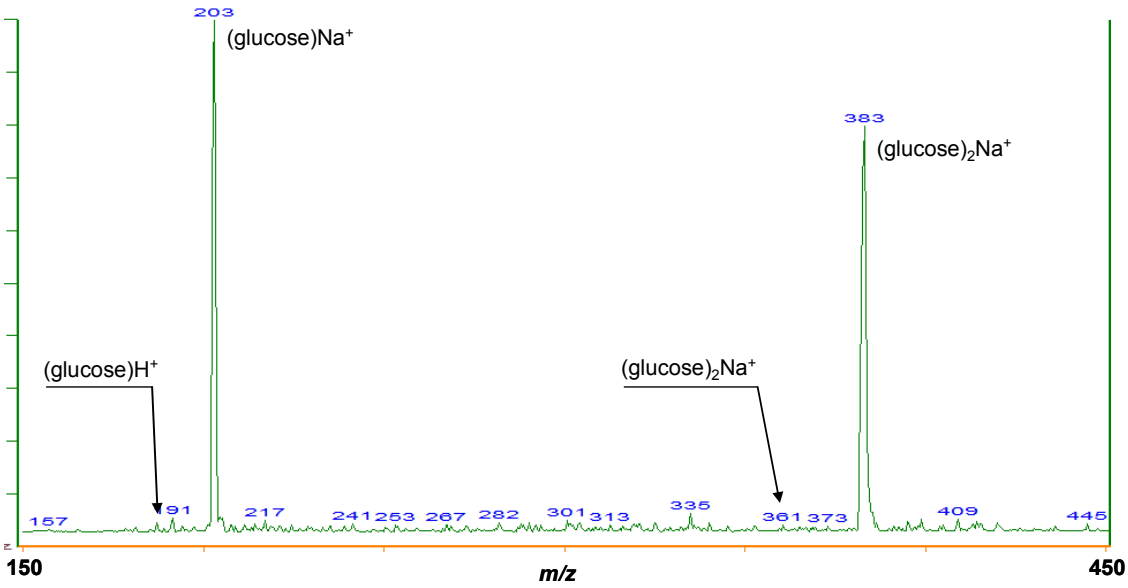

Figure 3.1: Spectrum of glucose (20 mM) solution taken with the SWISS-484

To make sure that glucose and not other hexoses were being measured MS^2 data was found in the literature demonstrating hexose differentiation. Most hexoses fragment into identical product ions not allowing the identification through unique fragment ions to be

possible. Salpin et al.[49] showed that CID of Pb^{2+} cationized hexoses produced signature abundance ratios that can be used to differentiate hexose isomers. As described above, the SWISS-484's sensitivity to lead cationized glucose is less than to that of sodiated glucose. Add this reduced sensitivity to the fact that the SWISS-484 at present has a detection limit for glucose just below one micromolar, fragmentation studies would not be helpful.

Without the ability at present to use the MS^2 method, proof that glucose is the only hexose in tears and verification of glucose quantitation by single quadrupole MS was needed. Out of all of the hexoses, glucose is the only sugar typically found above the 1 millimolar in blood. Any hexose transfer from the blood will reflect this concentration dominance. To our knowledge, glucose is the only hexose found in tears above micromolar concentrations.[50-52] To facilitate quantitation of glucose, an isotopic dilution method was utilized. In the method a known amount of a glucose isotope is added to the sample. In the spectra of the sample the intensity ratio of the natural glucose ion to the glucose isotope ion is representative to the corresponding concentration ratio. The unknown concentration of the natural glucose can then be calculated from the known concentration of the isotope and the intensity ratio. Using an isotope of glucose prevents the need to worry about ionization discrepancies that would occur if one used a different molecule.[2,53] Since the isotope has an identical structure as natural glucose, any effect occurring in the method would influence glucose and the isotope in the same way. For the initial part of this study $^{13}C_6$-glucose was employed as the standard since the addition of 6 daltons to the mass was away from any interference in the spectrum for the SWISS-484.

3.3.2 HP LCMS

With the decision to not pursue the MS^2 data, a triple multipole instrument was no longer a necessity. Experiments were now performed on the HP LCMS which is a single quadrupole mass spectrometer. The use of the HP LCMS instead of the SWISS-484 had a couple advantages. The LCMS system has an autosampler and the ability to perform flow-injection analysis. The autosampler provides high throughput of samples which was needed due to the many tear samples that would be collected. The flow-injection analysis allows sample spectra to be compared to background spectra which are contained at different time points of a single experiment. Also, multiple injections can be performed in a row in one continuous experiment. Any fluctuations occurring to the background over the course of the injections can be easily seen in the total ion chromatogram. This advantage became apparent when the intensity of sodiated $^{13}C_6$-glucose was studied. During multiple injections (typically 15) in a single run, which lasted over 30 minutes, the background at *m/z* 209 fluctuated greatly. This could normally be cancelled out with flow-injection analysis but the change in slope of the fluctuations was too high to obtain an accurate glucose measurement. Ideally the background would be stable and any increase in intensity would be a result from the analyte. With fluctuations in the background signal, the subtracted background no longer is equal over time in the analyte peak. One way to solve this is to extrapolate the background before the analyte peak to the background after the analyte peak. However, if the fluctuations are too great then one has to question the validity of the extrapolation. To solve this problem, the signal of *m/z* 205 was monitored and found to have a stable background and the isotope used for quantitation was changed to glucose-d_2. Another advantage in using the HP LCMS was that the only observed ion for glucose was the sodiated

monomer unlike the SWISS-484 where the dimer also was observed. Having the analyte at one *m/z* allows the possibility to increase the signal-to-noise.

As the development of the method progressed, it came apparent that the detection limit needed to be lowered to determine tear glucose concentrations. A C_{18} column was added online prior to the mass spectrometer to separate glucose from the other constituents within tears. By using the C_{18} column, compared to no column, the signal-to-noise ratio for glucose was increased (Figure 3.2) and the limit-of-quantitation was lower by a factor of ten. The analysis difference can also be seen in the meal studies described and shown in Appendix A. The complete final method is described in Chapter 4.

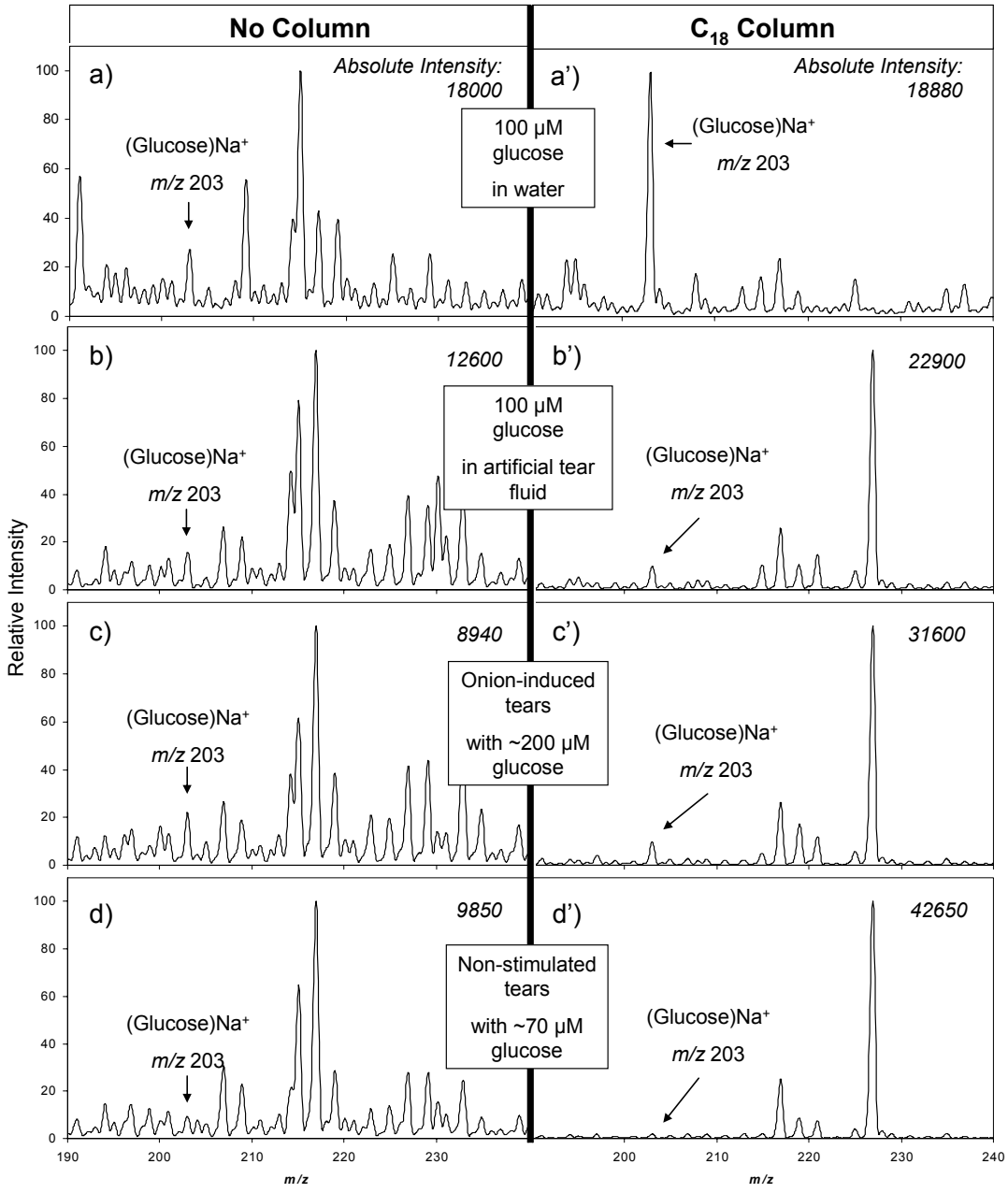

Figure 3.2: ESI-MS spectra (*m/z* 190 – 240) of glucose in different matrixes: a) 100 µM glucose in water, b) 100 µM glucose in artificial tear fluid, c) onion-induced tears (estimated to be ~200 µM glucose based on other experiments), and d) non-stimulated tears (estimated to be ~70 µM glucose based on other experiments). All samples were injected directly to the mass spectrometer for panels a, b, c, and d; no separation column was used. The same samples were analyzed with the addition of a C_{18} column (a', b', c', and d'). Insert in d' is a close-up of m/z 200 – 209 of d'.

4.0 ANALYSIS OF TEAR GLUCOSE CONCENTRATION WITH ELECTROSPRAY IONIZATION MASS SPECTROMETRY

This work was published as:

Christopher R. Taormina, Justin T. Baca, David N. Finegold, Sandford A. Asher, and Joseph J. Grabowski. *Journal of the American Society for Mass Spectrometry*. **2007**, 18, 332.[42]

4.1 ABSTRACT

We have developed a mass spectrometry-based method which allows one to accurately determine the glucose concentration of tear fluid. We used a 1 μL micro-capillary to collect tear fluid from the tear meniscus with minimal irritation of the eye. We analyzed the 1 μL volume of collected tear fluid with liquid-chromatography electrospray ionization mass spectrometry with the use of D-glucose-6,6-d_2 as an internal standard. Repeated measurements and a recovery experiment on pooled, onion-induced tears showed that the analysis of the glucose in tears was precise (4% relative standard deviation) and provided 100% recovery. We found the tear glucose concentration of one fasting non-diabetic subject to be 13 to 51 μM while the onion-induced tear glucose concentration of a different non-diabetic subject to be 211 to 256 μM.

4.2 INTRODUCTION

In the United States, 9.6% of the population over 20 years of age and 20.9% of the population over 60 years of age have *Diabetes Mellitus*[41]. The Diabetes Control and Complications Trial has shown that close monitoring and tight control of blood glucose concentration is critical in preventing the complications of Diabetes[7]. Current self-monitoring methods rely on invasive finger sticks to directly measure blood glucose levels to provide the critical information required to achieve glycemic control. A number of non-invasive approaches to monitoring blood glucose concentrations are being pursued; however, none have been successfully developed to the point where they have gained widespread clinical acceptance[54]. There has been significant recent activity in exploring non-invasive monitoring by using tear fluid glucose as an indicator for blood glucose[9,11,55]. Such an approach will be effective only if the glucose concentrations in tear fluid are a reliable surrogate for blood glucose concentrations.

A survey of the literature over the last 70 years on tear glucose determinations indicates significant disagreement in measured tear glucose concentrations and on the relationship of tear fluid glucose to blood glucose concentrations. Daum and Hill[12] noted in their 1982 review of the human tear glucose literature that reported values of tear glucose in normal individuals range between 0 and 3600 μM with the median values between 110 and 280 μM. More recently, a study of six non-diabetic adults found glucose concentrations in tear fluid ranging between 128 and 166 μM with an average of 139 μM[45].

The differences in tear glucose concentrations between these reports are likely due to the use of different tear fluid collection methods. Van Haeringen and Glasius specifically addressed the dependence of tear fluid glucose on the method of collection[13]. They used a glucose dehydrogenase method to analyze chemically stimulated tears collected with a capillary and

mechanically stimulated tear fluid collected by filter paper. Van Haeringen and Glasius found higher glucose concentrations in the tear fluid collected by the filter paper and concluded that the increase is due to the mechanical stimulation of the corneal and conjunctival epithelium[13]. Other studies reported similar findings in experiments on rabbits[14] and in subjects that were tested immediately after swimming[12]. Therefore, it is apparent that to determine a physiologically-relevant, baseline tear glucose concentration, tear fluid must be acquired with minimal tear stimulation and eye irritation.

Several previous studies used mass spectrometry to analyze tears for constituents other than glucose. Fung et al.[50] characterized the protein profile in the human tear fluid with MALDI-ToF and electrospray ionization mass spectrometry. Ham et al.[51] identified the lipid profile in tear fluid and reported on their variations between normal and dry eyes. There have been many reports of glucose measurement by mass spectrometry on bodily fluids other than tears. The majority of these studies use gas chromatography and an electron ionization source[56-59]. With gas chromatography, glucose typically needs to be derivatized to make it more volatile. Other studies used liquid chromatography to bypass the volatility issue[60,61]. Sodium[62], lithium[63,64], cesium[60], and chloride[65] ions have been used with electrospray ionization to form the cationic adduct of glucose from aqueous solutions.

We discuss here a new, robust method of determining physiological tear glucose concentrations by using electrospray ionization mass spectrometry (ESI-MS). This method enables reliable studies of tear glucose concentrations in tear fluid. We use a tear fluid sampling method that is minimally irritating to the eye to collect 1 μL tear samples. We validate the ESI-MS method by using glucose standard solutions, artificial tear fluid, and large volumes of stimulated tears. We determine tear glucose concentration in a non-diabetic, fasting adult.

4.3 EXPERIMENTAL

All tear samples were collected and transferred with 1 μL "Microcaps" micro-capillaries (Drummond Scientific Company, Broomall, USA). The tear film meniscus on the bottom eyelid was visualized using a slit lamp ophthalmic microscope (American Optics, Burlington, Canada). The micro capillary was gently touched to this tear fluid meniscus and the tear fluid was drawn in by capillary action. During half the collections, there was inadequate tear fluid to immediately fill the capillary with one touch. In these cases, the subject was asked to blink in order to redistribute the tear fluid and the capillary was again touched to the meniscus. This process was repeated until the capillary was completely filled. A few samples required as many as five repetitions of this process. Care was taken throughout tear fluid collection to avoid stimulation of reflex tearing. The aqueous glucose standards were collected and transferred with the same process as a tear sample; the capillary was touched to the solution surface and was filled by capillary action. For studies involving larger volumes of stimulated tears, the subject chopped onions until tearing was induced. These tears were collected by capillary action with glass Pasteur pipettes (2 mL) and pooled for each subject in order to analyze a homogeneous sample.

Immediately after collection, the tear sample was transferred to a glass vial (Agilent, Palo Alto, USA) with a glass insert (Restek, Bellafonte, USA) containing 10 μL of acetonitrile (Mallinckrodt Baker, Inc., Phillipsburg, USA) and 10 μL of an aqueous stock solution of isotopically labeled glucose (D-glucose-6,6-d_2, 99% labeled, Cambridge Isotope Laboratories, Andover, USA) used as an internal standard. A typical value for the concentration of the D-glucose-6,6-d_2 stock solution was 27.5 μM, corrected for the 99% labeling (leading to a D-glucose-6,6-d_2 concentration of 13.1 μM in the sample injected into the mass spectrometer). The

vials were then shaken and centrifuged for five minutes to ensure mixing and that the liquid was collected at the bottom of the vial. The samples were refrigerated at 5^{o}C until analyzed.

Glucose concentrations were measured using ESI-MS. Samples were analyzed by flow injection analysis on a HP 1000 LC-MS (Agilent, Palo Alto, USA). Initial studies used an autosampler connected directly to the mass spectrometer. However, our optimized method used a 2 μm filter and a Nova-Pak C_{18} 3.9 x 150 mm column (Waters, Milford, USA) placed in-between the autosampler and the mass spectrometer. In both methods, the mobile phase consisted of acetonitrile and water with 0.1% formic acid (Mallinckrodt Baker, Inc., Phillipsburg, USA) with a constant flow rate of 0.2 mL/min. The ratio of water to acetonitrile was 1:1 in the absence of the column and 17:3 with the column. The ion chromatograms of sodiated glucose isotopes (*m/z* 203 for natural glucose and *m/z* 205 for D-glucose-6,6-d_2) were selected from the total ion chromatogram using the ChemStation software (Rev. A.06.03 [509]). These selected ion chromatograms were integrated to provide peak areas for the two glucose signals. During integration, the software option "baseline hold" was used. The peak areas of *m/z* 203 and 205 were used to determine the glucose-to-D-glucose-6,6-d_2 ratio. When calculating the peak area ratio, we took into account the 1.3% *m*+2 natural isotopic contribution of Na^+(glucose), *m/z* 203, to *m/z* of 205; 1.3% of the observed glucose peak area of *m/z* 203 was subtracted from the observed *m/*z 205 peak area to determine the area due solely to the internal standard. Each sample was injected three times at 6.5 μL per injection and the average glucose concentration recorded. All human samples were collected through protocols approved by the University of Pittsburgh Institutional Review Board.

4.4 RESULTS AND DISCUSSION

The cationization of glucose with H^+, Na^+, K^+, or Pb^{2+} was examined. An initial survey comparing negative ion to positive ion ESI suggested greater promise with positive ion methods. With the exception of sodium, millimolar concentrations of the acid or salt were needed to observe the glucose cation adducts as the base peak. The sodium-glucose adduct was present in all of the spectra and in the majority of them was the most abundant ion. Since sodiated glucose dominated even without the addition of sodium and since tear fluid contains ~160 mM of sodium[52], our glucose analysis is based on the sodiated glucose ion. Further experiments were conducted to ascertain the solvent composition (water, acetonitrile, and methanol) that provided the maximum signal for sodiated glucose. Based on the results of these experiments, a 1:1 ratio of water to acetonitrile for the sample solvent was selected. For the experiments without the use of the Nova-Pak C_{18} column, the 1:1 solvent ratio was also used for the mobile phase with the addition of 0.1% formic acid to the aqueous phase to produce more stable baseline ion currents. In our initial work, $^{13}C_6$-glucose was used as an internal standard but an unidentified peak at *m/z* 209 (which would interfere with the detection of sodiated $^{13}C_6$-glucose) was observed in the absence of the internal standard. Therefore, D-glucose-6,6-d_2 was a superior alternative since no signal was observed at *m/z* 205 in the absence of the internal standard.

With the optimal solvents and internal standard established, the effect of the biological matrix on the glucose signal was examined. The sodiated-glucose signal intensity observed for both artificial and real tear fluid was low compared to the background signal in our initial studies in which samples were directly infused into the mass spectrometer. Addition of a C_{18} column separated proteins, such as lysozyme, globulin, and albumin, and excess salts from the elution time of glucose. This in-line purification increased both the sensitivity and signal-to-noise ratio

for sodiated-glucose. Analysis of the blank (a protein-free glucose-free artificial tear solution [9]) showed an average glucose concentration of 0.98 ± 0.56 μM. With the use of the column the statistical limit of detection was lowered to 3 μM. These improvements occurred in the presence of the column with the mobile phase optimized at a solvent ratio of 17:3 of water with 0.1% formic acid to acetonitrile which maximized the glucose signal and minimized overlapping peaks.

The precision of the micro-capillaries was measured by gravimetric means. Five individual capillaries were weighed, filled with water at 20°C, and weighed again. The average value for the water contained in the capillaries was 1.008 ± 0.013 mg (1.011 ± 0.013 μL at 20°C). Therefore, in all of our analysis of tears we assume a collection volume of 1.00 μL.

To test the linearity of the method, aqueous solutions with known glucose concentrations (0 – 200 μM) were prepared and analyzed. The linear regression of measured versus added glucose gave an equation of $y = 0.99\ x - 0.78$ ($R^2 = 0.98$). The increase in the relative sodiated glucose signal *m/z* 203 can be easily seen when the mass spectra are normalized to the sodiated D-glucose-6,6-d_2 signal *m/z* 205 (Figure 4.1).

The mass spectral measurement over time of the glucose concentration in the 1:1 ratio of water-to-acetonitrile was examined. A 200 μM glucose aqueous solution was prepared and sampled multiple times. These vials were stored in a refrigerator and tested immediately, a few hours later, three days later, and one week later. The average value for all of the samples was 201 ± 15 μM with no increasing or decreasing trend over storage time (data not shown).

The reproducibility of the method was determined with the use of a pooled sample of onion-induced tears. Six samples were collected from the pool and analyzed. The average glucose concentration was 211 ± 8 μM in this stimulated tear sample (data not shown).

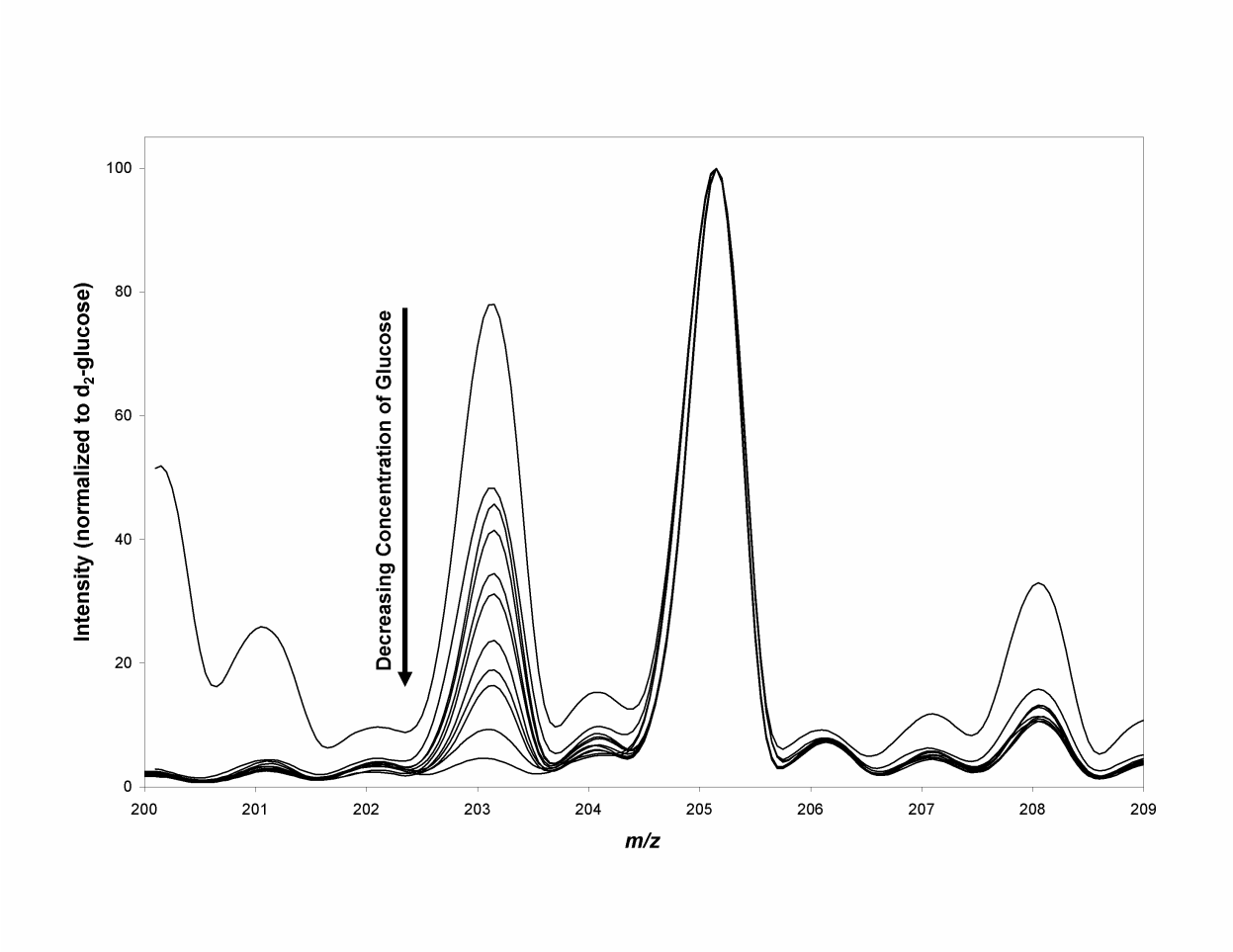

Figure 4.1: Eleven spectra of aqueous solutions of known glucose concentrations (0 – 200 µM) with intensities normalized to the internal standard D-glucose-6,6-d_2 signal intensity at *m/z* 205. The linear regression of the experimental glucose concentration verses the known glucose concentration provided the best fit equation of $y = 0.99\ x - 0.78$ ($R^2 = 0.98$).

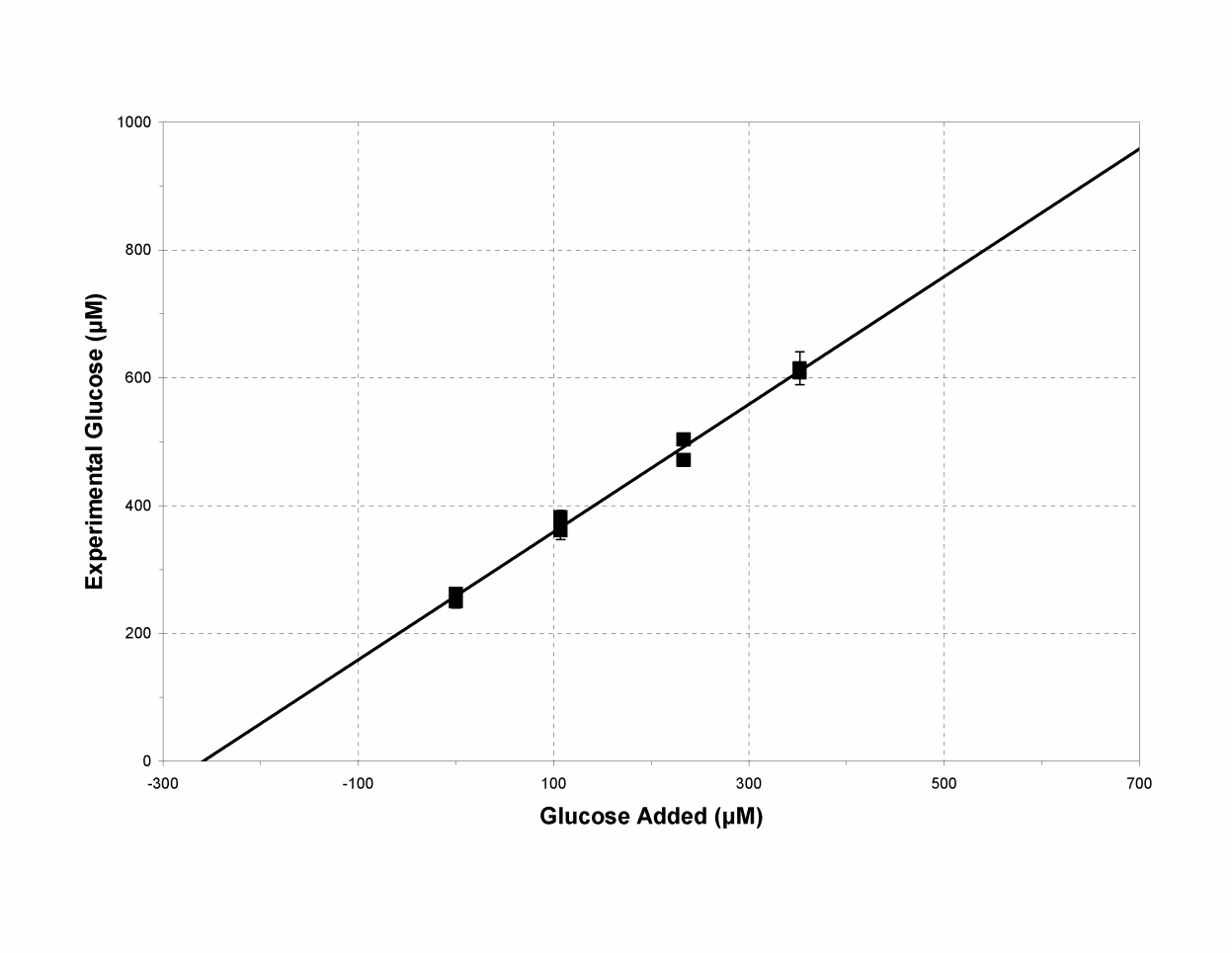

Figure 4.2: Duplicate samples of pooled, induced tears at four different concentrations of added glucose were analyzed. Error bars are plus/minus one standard deviation from the average value of each sample. Linear regression analysis gave an equation of y = 0.99 x + 256 (R^2 = 0.99) and a recovery range of 94% to 111% of the glucose spike.

A recovery experiment was performed on another pooled sample of onion-induced tears. The tears were spiked with aqueous glucose solutions to increase the glucose concentration by 0, 107, 233, and 352 μM. Linear regression of measured versus added glucose gave an equation of $y = 0.99\ x + 256$ ($R^2 = 0.99$) (Figure 4.2). We also determined that the induced tear fluid contained 256 μM glucose.

The average relative standard deviation over the three 6.5 μL injections of the diluted tear samples studied with concentrations greater than 50 μM glucose was 4%. For the samples studied with concentrations less than 50 μM glucose, the average relative standard deviation of the three measurements was 15%. The FDA currently requires self-blood-glucose monitors to have an accuracy of within 15%. Within one standard deviation, the calibration curve is indistinguishable from $y = x$ and the recovery experiment shows 100% recovery of added glucose. We therefore feel confident using D-glucose-6,6-d_2 as the internal standard and the $y = x$ calibration curve to determine tear glucose concentrations.

We performed two studies on a non-diabetic subject who fasted overnight. During both sessions, which were separated by one week, three samples were taken from each eye. Samples from the same eye were collected at ten minutes intervals. The tear glucose concentration from this subject during the two sessions ranged from 13 to 51 μM with an average of 32 μM (Table 4.1). The concentration of tear glucose determined in this work for this non-diabetic subject is about four-fold less than the tear glucose concentrations recently reported[45]. Whereas previous studies used collection methods which either touched the eye or chemically stimulated tears[12-14], we use glass micro-capillaries to collect a single microliter volume of tear fluid from the tear meniscus without touching the eye. This decrease in reported tear glucose concentration is likely due to our less irritating method of tear collection. The onion-stimulated tears (from a different

subject) showed a seven to eight fold higher glucose concentration than in the absence of stimulation.

Table 4.1: Tear Glucose Concentration of a Non-diabetic Subject

	Session 1		Session 2	
Sample	Left Eye	Right Eye	Left Eye	Right Eye
1st	22	38	44	48
2nd	51	37	50	25
3rd	13	17	14	24

Note: Concentrations are micromolar.

4.5 CONCLUSION

In the present study we demonstrate a robust ESI-MS method for determining tear glucose concentration in tear fluid. Liquid chromatography separates glucose from the majority of salts and proteins, such as lyzosyme, globulin, and albumin, in tears reducing interference of the biological matrix on the sodiated-glucose signal. The resulting increase in the sensitivity and signal-to-noise ratio of glucose over data obtained without the column allows measurements of tear glucose concentrations as low as 10 μM (limit of quantification) by relying on an internal standard. We use a 1 μL tear sampling method that is minimally irritating to the eye. This method enables reliable studies of physiological tear glucose concentrations in non-stimulated tears. A preliminary study indicates that the physiological, baseline tear glucose concentration is

substantially below previous reports. Further studies are warranted to determine the inter- and intra-individual variation in baseline tear glucose concentration. This method will be used to establish normal values for tear glucose concentration and can monitor changes in tear glucose with changes in blood glucose. Application of this LC-MS method can help us to understand tear glucose physiology. Our future work will determine whether monitoring tear glucose concentration is a viable approach for non-invasive blood glucose monitoring. We are now using this method for tear glucose concentration measurements to examine a population of non-diabetic and diabetic subjects to determine their tear fluid glucose concentrations and their correlations of tear glucose with blood glucose.

4.6 ACKNOWLEDGEMENTS

The authors thank Kasi Somayajula for his consultation. This research was supported of the National Institutes of Health Grant DK-55348 to Sanford A. Asher.

5.0 MASS SPECTRAL DETERMINATION OF FASTING TEAR GLUCOSE CONCENTRATIONS IN NONDIABETIC VOLUNTEERS

This work was published as:

Justin T. Baca, Christopher R. Taormina, David N. Finegold, Joseph J. Grabowski, and Sandford A. Asher. *Clinical Chemistry.* **2007**, 53, 1370.[43]

5.1 ABSTRACT

Background: There is considerable disagreement regarding the concentration of glucose in tears and its relationship to the concentration in blood. Improved sampling and analysis methods may resolve these discrepancies and possibly provide a basis for in situ tear glucose sensors.

Methods: We used liquid chromatography (LC) with electrospray ionization mass spectrometry (ESI-MS) to determine glucose in 1-μL tear fluid samples obtained from 25 fasting study participants. Tear fluid was collected with microcapillaries and a slitlamp microscope.

Results: The median (range) of fasting tear glucose concentrations was 28 (7–161) μmol/L or 0.50 (0.13–2.90) mg/dL. The SD of tear glucose measurements for individuals varied linearly with the mean tear glucose concentration and was approximately half of the mean. We found no significant difference in tear glucose concentrations between contact lens users and nonusers (P = 0.715). We observed significant correlations between fasting blood and tear glucose concentrations (R = 0.50, P = 0.01).

Conclusions: Our tear fluid collection and analysis method enables reliable measurement of equilibrium, fasting tear glucose concentrations. These concentrations are lower than those previously reported for nondiabetic persons. Larger population studies are required to determine correlations between blood and tear glucose concentrations and to determine the utility of contact lens–based sensors for the monitoring of diabetes. Our methods are applicable for study of other tear fluid analytes and may prove useful for monitoring other disease states.

5.2 RESULTS AND DISCUSSION

Glucose has been a recognized component of tear fluid since the early 1900s, but disagreement continues regarding its concentration in tear fluid and its correlation with blood glucose concentration.[12,44,48,66-68] Literature reports of normal tear glucose concentrations range between 0 and 9.1 mmol/L (164 mg/dL), with median values of 110–280 μmol/L (1.98 and 5.04 mg/dL).[12,46] In a recent study of 121 persons, tear glucose concentrations ranged from below the limit of detection to 9.1 mmol/L (164 mg/dL).[46] Much of the difference in reported tear glucose concentrations is likely from the use of different tear collection techniques.[13] Collection techniques causing severe eye irritation such as filter paper collection[68] are associated with the highest tear glucose concentrations, whereas less irritating techniques (such as glass capillary collection) are associated with the lowest.[44,48] Chemically stimulated tears have increased tear glucose.[13,42] Reliable tear sampling may also be confounded by individual differences in tolerance to real or expected eye stimulation during sampling.

Improved tear fluid collection, and the ability to analyze very low volumes of tear fluid, may dramatically improve measurement of tear fluid glucose concentrations and help resolve the

reported discrepancies in basal tear glucose concentrations. Improved methods would also enable the study of physiologic glucose transport in the eye and advance the use of tear fluid as a surrogate for blood in measuring other clinically important analytes.

Some groups have tried to use tear glucose to diagnose diabetes[66,67], and others have proposed continuous monitoring of blood glucose concentrations by use of contact lenses with glucose sensors.[9,11,69,70] We recently reported a photonic crystal glucose-sensing material for noninvasive monitoring of glucose in tear fluid.[9] Detailed understanding of tear glucose concentration and its regulation is critical to developing noninvasive glucose sensors.

We recently developed an electrospray ionization mass spectrometry (ESI-MS) method for measuring glucose in 1-μL samples of collected tear fluid.[42] With this method, we studied basal tear glucose concentrations in healthy persons without diabetes.

We recruited volunteers (age 18–60 years) within and around the University of Pittsburgh. Persons with a history of diabetes were excluded. Blood and tear samples were obtained after participants had fasted overnight for at least 8 h. The samples were always collected in the same order: capillary blood from the finger pad, tear fluid from the left eye, and then tear fluid from the right eye. This sequence was repeated 3 times for each study participant, with at least 10 min between successive blood sample collections. Glucose in capillary blood was measured with an Accu-Chek® Compact glucometer (Roche), according to the manufacturer's protocol.

A total of 26 volunteers completed the study; 11 wore their usual contact lenses at the time of the study, and 15 did not wear contact lenses. The type of contact lenses worn were daily disposable (n = 1), daily wear (n = 6), extended wear (n = 1), and silicone hydrogel lenses (n = 2). Of the 15 non-contact lens wearers, 1 had a history of contact lens use, but did not wear

contacts on the day of the study. For 1 contact lens wearer, the collected tear samples were lost because of vial breakage before analysis. For 2 participants (1 from the contact lens group and 1 from the non-contact lens group), 1 of the 6 tear glucose samples was lost because of instrument failure. The tear glucose concentration statistics for these 2 participants were determined from only 5 samples. The University of Pittsburgh School of Medicine Institutional Review Board approved all clinical procedures, and all participants signed a detailed informed consent form.

Tear fluid samples of 1 μL were collected and analyzed by liquid chromatography ESI-MS as previously reported.[42] Three aliquots of each tear sample were injected into the analyzer to determine the mean glucose concentration. Our study found much lower tear fluid glucose concentrations for healthy individuals than did previous studies (Figure 5.1).

The population median (range) of the tear glucose concentrations were 28 (7–161) μmol/L [0.50 (0.13–2.90) mg/dL]. The distribution of mean tear glucose concentrations was highly skewed; <28 μmol/L (0.50 mg/dL) in 50% of the study participants and <42 μmol/L (0.76 mg/dL) in 80% of the study participants. Two individuals were observed rubbing their eyes during the course of the study, and they had the highest mean (SD) tear glucose concentrations: 128 (75) and 161 (71) μmol/L or 2.31 (1.35) and 2.90 (1.28) mg/dL.

Because the SD of the mean tear glucose concentration for each participant was proportional to the mean for each participant, a natural log transformation was applied to the tear glucose concentration values (Figures 5.2 and 5.3). After transformation, standard statistical methods were applied.

Contact lens use did not affect mean tear glucose ($P = 0.715$). Transformed tear glucose concentrations were significantly correlated with mean blood glucose ($R = 0.50$, $P = 0.01$, Figure 5.4A). This correlation for fasting tear and blood glucose is similar to that reported by Daum

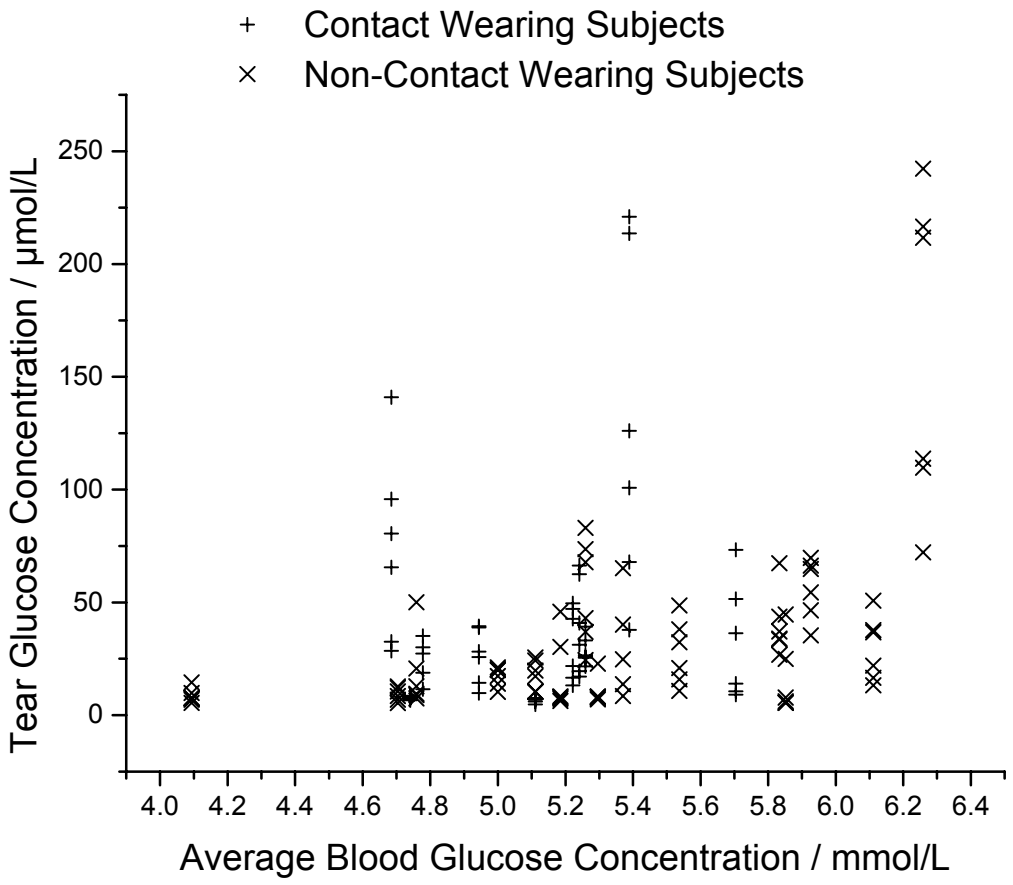

Figure 5.1: The six tear glucose concentrations determined for each subject are plotted against the subject's average blood glucose concentration. All tear glucose measurement for a given subject are in vertical alignment. Large variations occur in the value of the tear glucose concentrations for each subject between their eyes and between subsequent measurements of each eye over the course of the study (30-40 minutes). It should be noted that in all cases blood glucose concentration remains essentially constant over the measurement interval as subjects had fasted overnight.

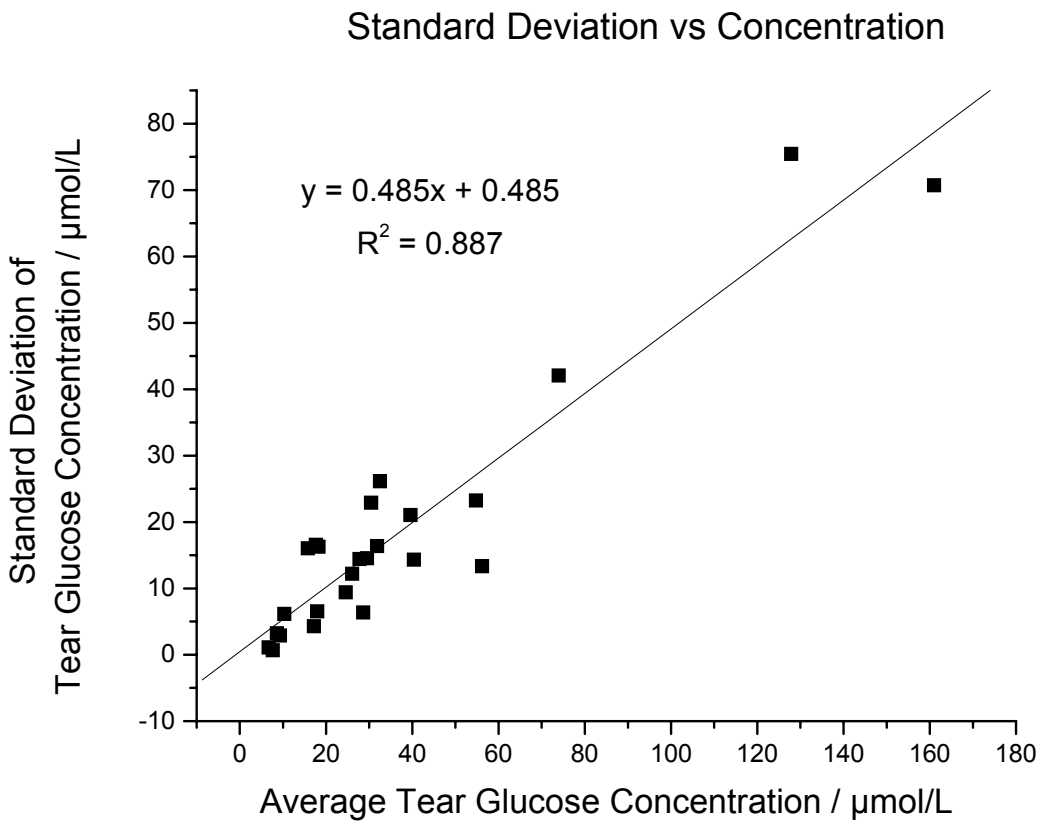

Figure 5.2: The standard deviations of the six tear fluid glucose measurements for each subject are linearly proportional to the mean value measured (~50% of the mean value).

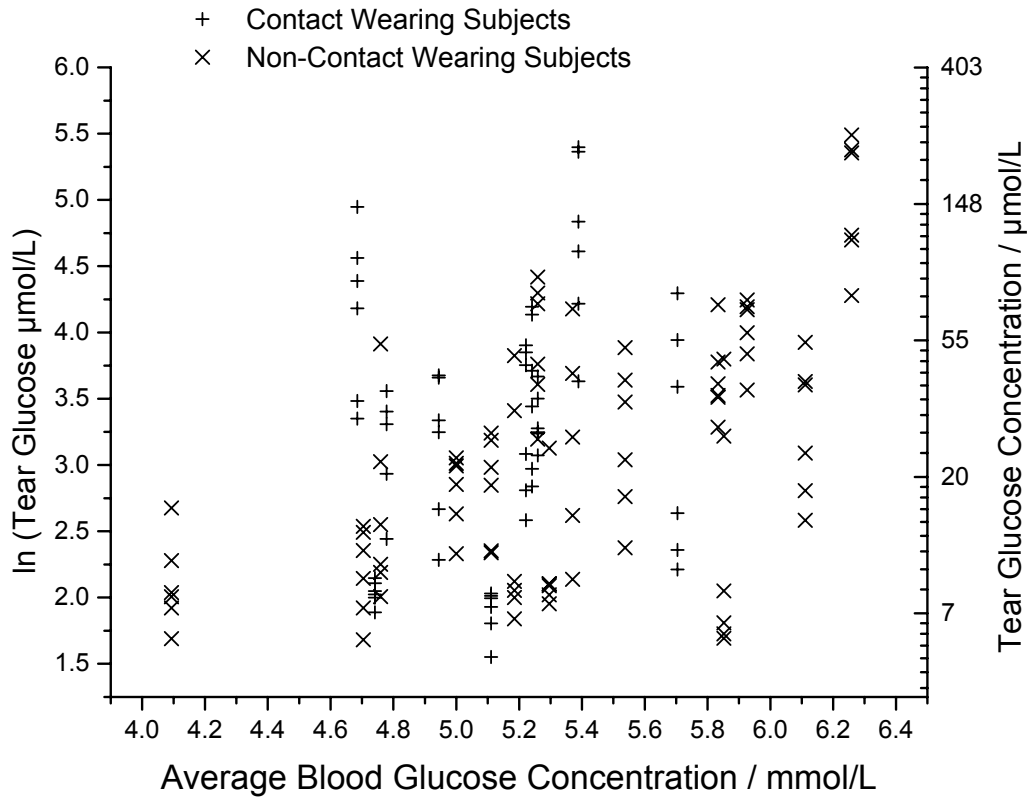

Figure 5.3: The transformed tear glucose values of the six tear glucose determinations for all subjects are plotted against the subject's average blood glucose concentration. There is significant variation in the tear glucose concentration measured in individual subjects over the course of the study (30-40 minutes). Note that all tear glucose measurements for a given subject are in vertical alignment. The average natural log transformed tear glucose value for non-contact-wearing subjects was 3.1 ± 0.8, and 3.2 ± 0.8 for contact-wearing subjects (mean ± SD).

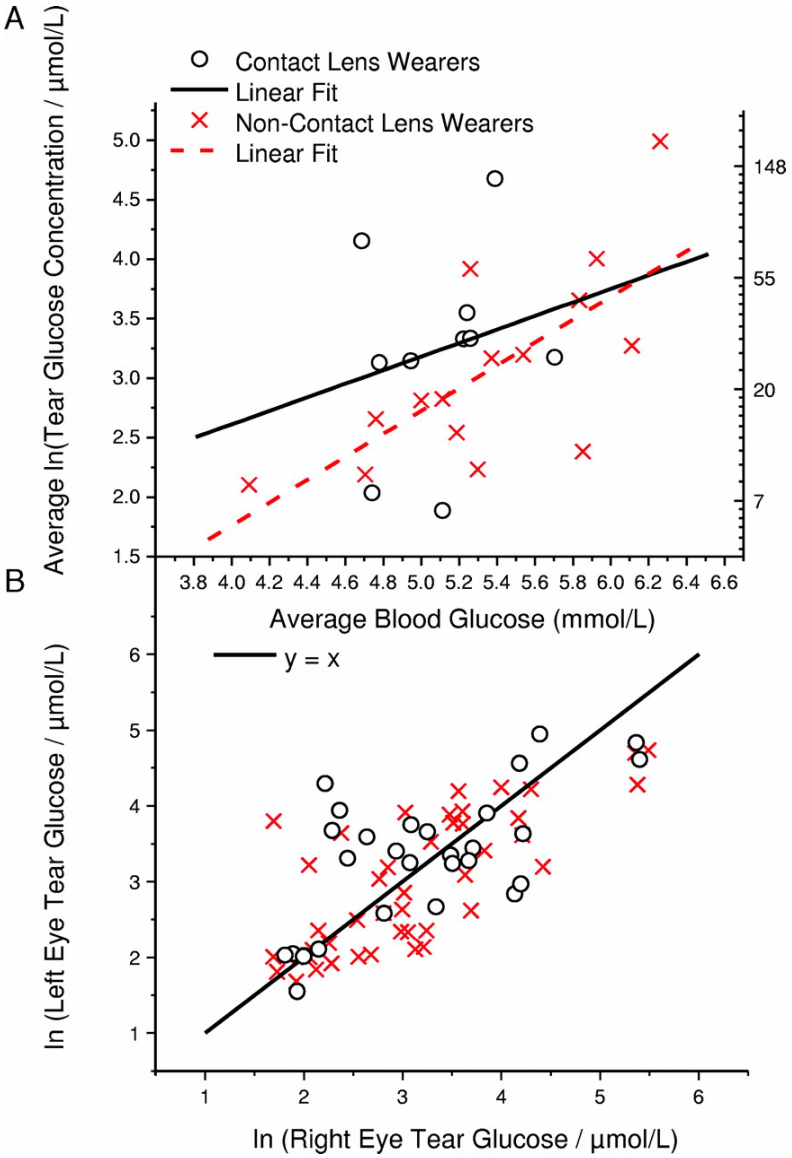

Figure 5.4: (*A*) Correlation (*P* = 0.01) between the mean *ln*(tear glucose concentration) and the mean blood glucose concentration. A linear regression for all participants gives *y* = 0.80x – 1.07 (*R* = 0.50). (*B*) Linear regression for the subpopulations of contact wearers and non-contact wearers gives *y* = 0.570*x* + 0.332 (*R* = 0.22) for contact lens wearers and *y* = 0.961*x* – 2.079 (*R* = 0.70) for non-contact wearers. No significant differences were observed between right and left eyes (*P* = 0.76, two-tailed paired *t*-test), but results may differ at any given time. The left and right tear glucose determinations that are closest in time are plotted against each other. There are hence 3 data points for each study participant.

and Hill of $R = 0.53$ for blood and tear glucose measurement variations throughout the day. However, they reported a mean (SD) population tear fluid glucose concentration of 420 (355) μmol/L or 7.57 (6.40) mg/dL.

The glucose concentrations in the right and left eyes were highly correlated within individuals (Figure 5.4B). There was no evidence that eye-to-eye variation in individual study participants differed significantly from variation in a single eye over time. Furthermore, we observed no evidence that variation in tear glucose concentration between individuals with similar blood glucose concentrations was greater than variation in tear glucose concentration within an individual.

The correlation between the transformed tear glucose value and the average blood glucose concentration appears to be stronger for non-contact lens wearers than for participants wearing contact lenses ($R = 0.70$ vs $R = 0.22$). However, analysis of covariance does not indicate a significant difference ($P = 0.63$).

The ESI-MS method used here enables reliable determination of basal tear glucose concentrations in fasting individuals. Study participants had fasted overnight, and had stable blood glucose concentrations over the brief course of the study. We observed much lower basal tear glucose concentrations than previously reported for healthy individuals. This difference is likely a result of our sampling methods, which were less irritating than earlier methods that stimulated tear production chemically or with filter paper.[13] If our collection method had caused significant irritation, we would have expected tear glucose concentrations to increase over the course of the study.

We observed no evidence of such an increase (Figure 5.5). We observed significant variation in tear glucose concentrations between the 2 eyes of individual study participants, as

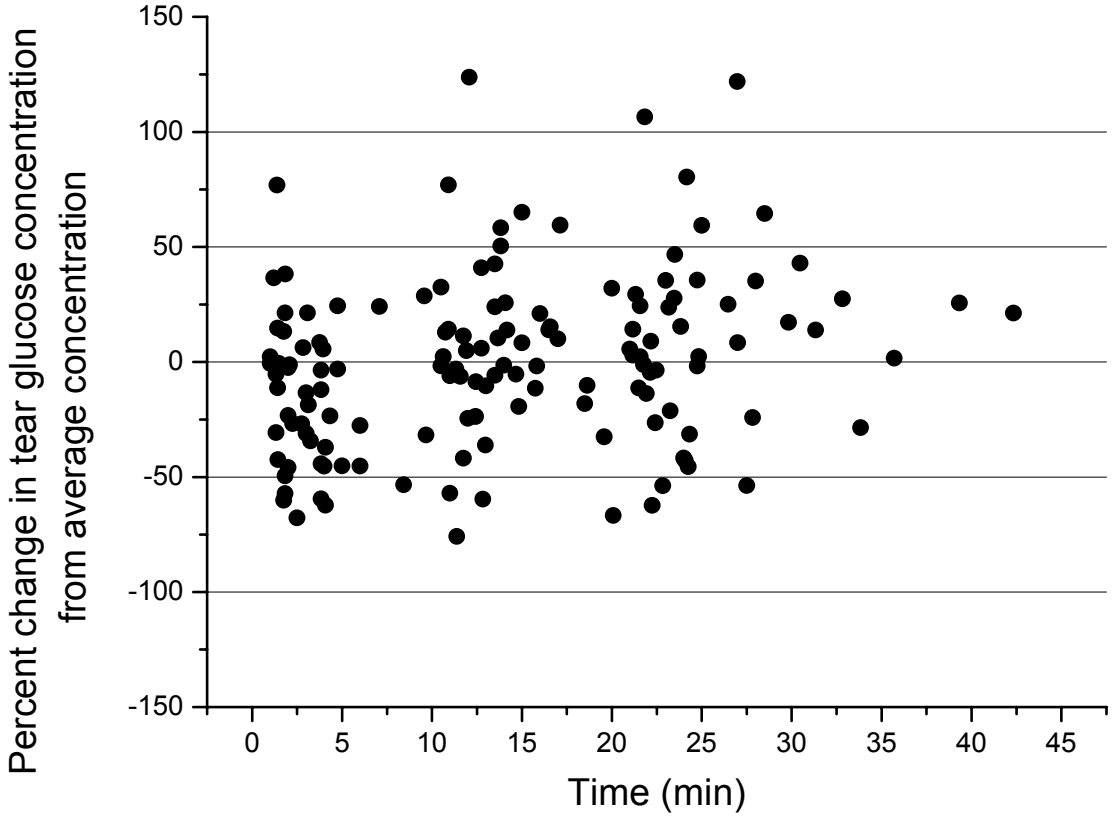

Figure 5.5: A plot of the relative difference in tear glucose concentration from the average tear glucose value for each subject versus time does not show a significant trend. If the sampling procedure caused significant irritation to the eye, we would expect an overall relative increase in tear glucose concentration with time.

well as over time within a single eye. During this study, we were cognizant of potential confounding events such as yawning and eye rubbing. Although the 2 individuals who rubbed their eyes during the study had the highest glucose concentrations, events like these do not explain the large within-individual differences observed.

Variations in tear glucose concentrations within a single individual must derive from the sum of the biological variance and any variances associated with sampling and measurement. The error in our tear fluid collection volumes was negligible[42]; the SD observed for an individual was <3 times the SD of the 3 replicate mass spectral measurements of a single tear fluid sample. The relative SDs of these 3 replicates varied somewhat with glucose concentration but had a median value of 14%. Thus, the observed SD in tear glucose measurements derive mainly from actual variations of the glucose concentration in the different tear fluid samples.

We did not observe a systematic increase over time in glucose concentration variations that could result from the effect of tear depletion during repeated measurements. Tear glucose concentration appeared to vary randomly over the repeated sampling events.

We observed variations in tear glucose concentrations among fasting individuals and a significant correlation between *ln*(tear glucose concentration) and blood glucose concentration. Mean fasting tear glucose concentrations did not differ significantly in relation to contact lens use. Further studies are needed to investigate the apparent difference in the correlation between tear glucose and blood in these subpopulations.

The extremely low glucose concentrations in tear fluid, more than 100 times lower than in blood, raise questions about the physiologic role of tear glucose. Future studies are needed to address the correlation between tear and blood glucose in hypoglycemic and hyperglycemic states and in the presence of diabetes.

5.3 FUNDING AND ACKNOWLEDGEMENTS

Grant funding/support: This research was supported by the National Institutes of Health Grant DK-55348 (to S.A.A.).

Financial Disclosures: S.A.A. is the scientific founder of Glucose Sensing Technologies LLC, a company developing glucose-sensing contact lenses.

Acknowledgments: We thank Drs. Gary Foulks and Cholappadi Sundar-Raj for helpful discussions and critical reviews of the manuscript.

6.0 PEPTIDES

Neuropeptides are a diverse class of inter-neuron-signaling molecules which participate in various physiological functions.[5,15-17] Direct analysis of the neuropeptide content of a biological fluid would prove invaluable to the understanding of neurological functions. In conjunction with Dr. Michael's group, this study analyzes interstitial fluid adjacent to unharmed cells in the brain of a rat. Previous studies have used microdialysis to collect samples in vivo.[5,18] The large size of the microdialysis probe relative to the rat brain has been shown to damage cells upon insertion.[19] The damaged cells could alter the concentrations of neuropeptides in the interstitial fluid through the exposure of the cell's interior. To minimize the damage to the brain, smaller tapered fused silica capillaries instead of a microdialysis probes can be used to sample fluid. The ESI-MS based analysis of these samples is ideal due to the small volume and low concentrations.

6.1 EXPERIMENTAL

The experiments were conducted with the instrumentation described in Chapter 2.4. The peptides and chemicals were purchased from Sigma Chemical Company (St. Louis, MO). They were dissolved in water and then co-solvent (methanol or acetonitrile) and the acid or base were added. All of the enkephalin standards were sprayed from a New Objective capillary tip with an

orifice of 10 μm with 2.0 kV applied to the spray tip and with a flow rate of 100 nL/min set on the syringe pump. Data were collected for five minutes and all scans were averaged to provide the spectra.

The dynorphin standards for the HP LCMS were dissolved in water (10 μM) and injected directly into the solvent flow of 60% water containing 1% acetic acid and 40% acetonitrile. The instrument used a flow rate of 400 μL/min and 3.0 kV applied to the spray tip. The dynorphin standards for the SWISS-484 were dissolved in water (10 μM) and diluted to provide a 1% acetic acid and 50% methanol solution. The solutions were sprayed from a New Objective tip with a 15 μm orifice with 3.0 kV applied and at a flow rate of 300 nL/min.

The CID experiments were performed with a pressure of $3x10^{-5}$ Torr of argon gas. The pole biases of the octopole and Q3 were set at -20V and -30V respectively. The experiments with the sodiated leucine-enkephalin differed from this only in that the pole biases were set to -10V and -15V respectively for higher resolution spectra.

The experiments with the rat brain fluid also followed the general procedure as stated in Chapter 2.4. The rat brain was infused with the standard for one hour at a rate of 100 nL/min (6 μL volume total injected). Once the hour passed the collection of the fluid began and lasted an hour at a rate of 7 nL/min (0.42 μL volume total collected). The samples contained in the fused silica capillaries were attached to a PEEK connector and sprayed through a New Objective tip with a 10 μm orifice. A flow rate of 50 nL/min was applied to the solution with a syringe pump and 2.0 kV was applied on the tip. For the CID experiments for the rat brain experiments had pressures in the CID chamber and voltages of the pole biases of 3x10-5 Torr, -20V (O), and -25V (Q3) or 5x10-5 Torr, -10V (O), and -15V (Q3).

6.2 PEPTIDE CHARACTERIZATION

To assess the abilities of the SWISS-484, the spectra of known peptide solutions were acquired. The majority of the tests of these solutions dealt with the constituents of the solvent. Experiments were performed on leu-enkephalin, met-enkephalin, dynorphin A, and dynorphin B. The ideal conditions to obtain spectra for identification generally were found to consist of a micromolar peptide concentration, a solvent containing 25-50% organic co-solvent (i.e., methanol or acetonitrile), and addition of acid to promote protonation in the spray process. If sodium ions are in the solution the sodiated ion will appear in the spectra and at the expense of the signal of the protonated ion. Millimolar concentrations of salt in the solution or lack of a co-solvent adversely affects the ion signal by yielding an assortment of cluster ions and a significantly smaller signal-to-noise ratio for any individual peak.

A second goal of the characterization studies was to optimize the collision induced dissociation (CID) parameters for quantitation experiments. These experiments were performed on the enkephalins and the dynorphins. The protonated ions of the peptides produced typical product ions in the form of Roepstorff's nomenclature (y_2, b_3, a_2).[71] The sodiated ions showed rather high specificity in accord with previous work by Westmore[72] and Beauchamp.[34] The unique fragmentation of each peptide can be used to enhance quantitation through increased signal-to-noise and ion selectivity. Selected ion monitoring (SIM), multiple ion monitoring (MIM), and selected reaction monitoring (SRM) can be used toward this end. All three of these methods are utilized to determine the best route to quantify neuropeptides in interstitial brain fluid.

6.2.1 Solvent Effects

Leucine-enkephalin and methionine-enkephalin are pentapeptides and differ only in their C-terminal amino acid. Leucine-enkephalin (LEnk) has the N to C sequence of tyrosine-glycine-glycine-phenylalanine-leucine and the mono-isotopic molecular weight of 555.3 Daltons. Methionine-enkephalin (MEnk) has the N-to-C sequence of tyrosine-glycine-glycine-phenylalanine-methionine and the mono-isotopic molecular weight of 573.2 Daltons. Spectra were first taken with the SWISS-484 with micromolar concentrations of the peptides in 100% water. Direct injections into the mass spectrometer were made without any modifications to the solutions. In these spectra the protonated species (MW + 1) is the most intense ion, 556.3 Daltons for LEnk and 574.2 Daltons for MEnk (Figure 6.1). Along with these peaks are the sodiated ion (MW + 23) and the substitution of a sodium for a proton to the sodiated ion (MW – 1 + 46). These additional peaks show that the solutions were not devoid of all salt ions.

The addition of an organic co-solvent of methanol or acetonitrile and acid proved to enhance the overall intensity of the peaks, especially the protonated species (Figure 6.2a). Further experiments with the organic solvent showed that adding approximately 1% acid and 10 to 50% by volume organic co-solvent to obtained the best signal-to-noise ratio of a protonated ion. The addition of salt to the solution typically provides a spectrum with the corresponding analyte-salt cation adduct as shown in Figure 6.2b. With artificial cerebrospinal fluid (aCSF, Table 6.1) as the solvent, the high concentration of sodium ions depletes the protonated species, promotes the sodiated species to the most intense ion, and causes the additional substitution of sodium ions for protons on the molecule. The use of certain salts in electrospray ionization solutions results in aggregates that can overwhelm the analyte peaks. The addition of 20 μM of sodium acetate to the solution provides spectra (Figure 6.2c) only with the salt cluster peaks

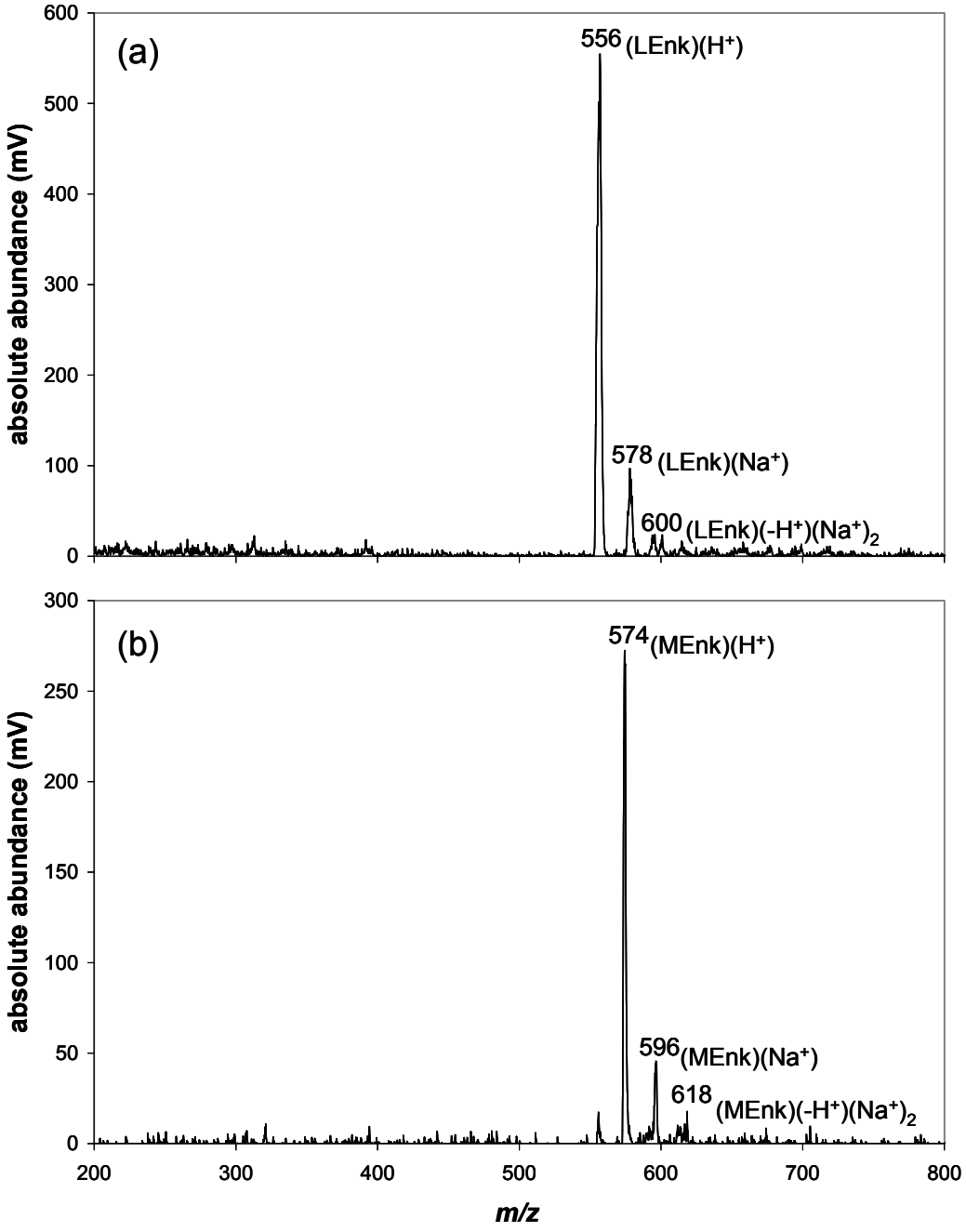

Figure 6.1: Spectra of (a) 63 µM leucine-enkephalin and (b) 300 µM methionine-enkephalin in water

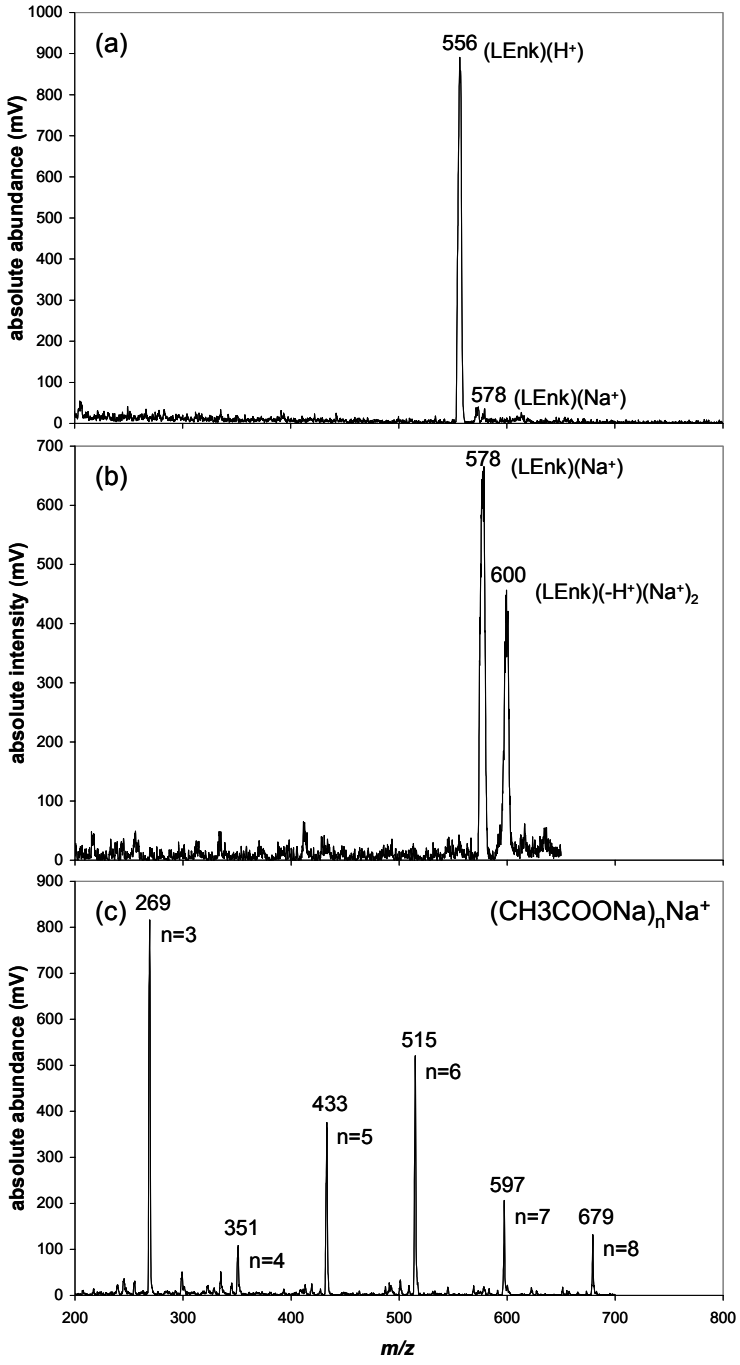

Figure 6.2: Solvent dependence of spectra with leucine-enkephalin in (a) 13% methanol and 1% acid (55 µM LEnk), (b) 100% aCSF (63 µM LEnk), and (c) 20 µM sodium acetate (10 µM LEnk, n signifies the number of sodium acetates in the sodiated sodium acetate cluster, LEnk was not observed).

Table 6.1: Ion content of aCSF

Salt ion	Concentration in aqueous solution (mM)
Sodium	147.3
Calcium	1.6
Potassium	2.7
Chloride	150.9
Magnesium	2.1
Phosphate buffer	2.3

with pH adjusted to 7.4 with sodium hydroxide

$(CH_3COONa)_nNa^+$ where $2 < n < 8$. The elimination of salts from solutions prior to ESI-MS analysis would be beneficial for the observance of the protonated analyte. One way to remove salts from a sample is with the use of Millipore's Ziptips, which are essentially small chromatography columns. Following the procedure provided by Millipore, ESI-MS solutions can be produced where the majority of the peptides are protonated rather than sodiated. For example a sample of 10 μM LEnk in aCSF gives a spectrum (Figure 6.3a) with different cationic species of leucine-enkephalin and a poor signal-to-noise ratio. After the use of a Ziptip, the solution provides a spectrum (Figure 6.3b) with increased signal-to-noise ratio of the protonated peak.

Another neuropeptide dynorphin A (2147.53 Daltons) is a heptadeca-peptide with the N to C sequence of YGGFLRRIRPKLKWDNQ in single letter amino acid format. In the spectra obtained on the commercial HP LC-MS instrument the double, triple, and quadruple charged ions are seen (Figure 6.4a) whereas on the SWISS-484 only the triply and quadruply charged

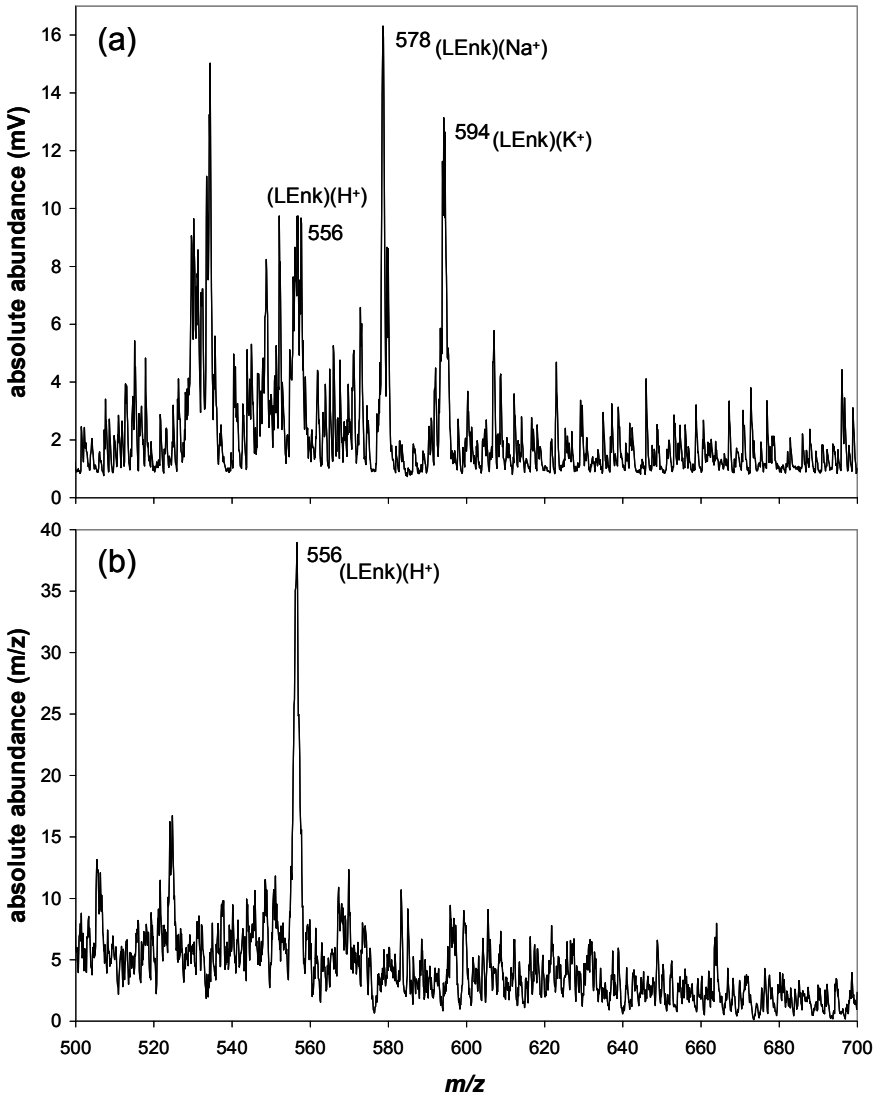

Figure 6.3: Spectra of 10 µM leucine-enkephalin in 100% aCSF (a) before use of Ziptip and (b) after use of Ziptip (50% methanol and 1% acetic acid).

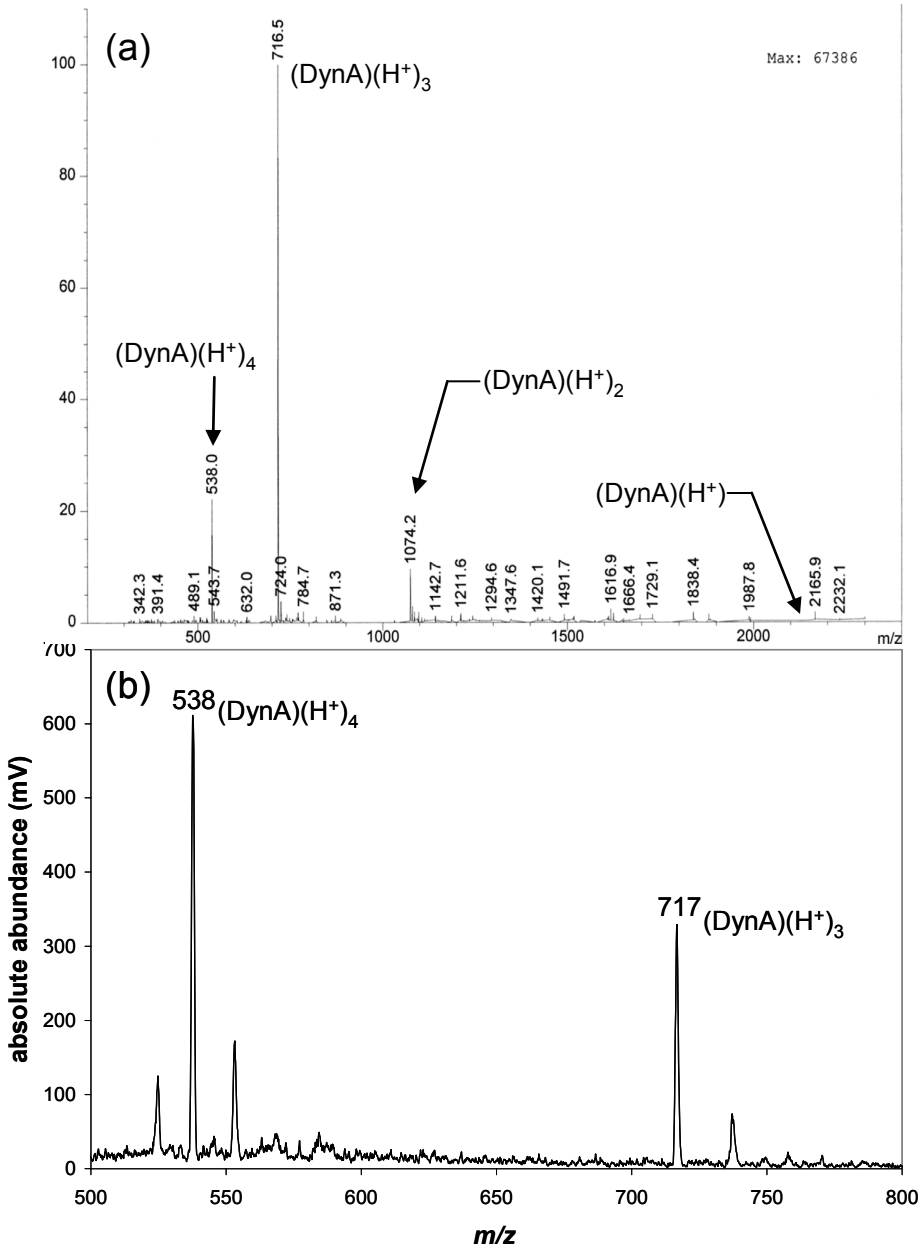

Figure 6.4: Spectra of dynorphin A obtained on the (a) HP LC-MS (10 µM) and the (b) SWISS-484 (5 µM).

molecule appear (Figure 6.4b). This difference is likely due to a difference in the addition of acid. With the HP LCMS, acid was not added to the peptide solution but was in the mobile phase, while the experiment with the SWISS-484 was a direct injection of a solution with 1% by volume of acetic acid added. The abundance of acid in the latter will lower the pH and provide more protons to increase the charge on the molecule.

6.2.2 Collision Induced Dissociation

The SWISS-484 has a triple multipole setup with the octopole acting as a collision cell allowing the obtainment of ion structure information through collision induced dissociation (CID). Figures 4.5 and 4.6 show the CID spectra of protonated leucine-enkephalin and protonated methionine-enkephalin respectively. In the case of peptides, Roepstorff's nomenclature[71] is the generally accepted guide for ease of fragment ion identification. The A, B, and C fragment ions contain the N-terminal side of the parent peptide and the X, Y, and Z fragment ions contain the C-terminal side. The protonated enkephalins fragment readily with the collision cell at a pressure of $3x10^{-5}$ Torr of argon gas. The A_4 and B_4 ions are the most abundant of the fragments which is in agreement with the literature.[72] As shown by Beauchamp[34] the sodiated peptide ions have a specific fragmentation pathway. The ions sequentially fragment down the amino acid bonds starting at the C-terminal. A single collision of sodiated methionine-enkephalin with a neutral produces *m/z* 465.2 and a second collision with the fragment ion and a neutral will provide *m/z* 318.1 (Figure 4.7). With a single spectrum containing the protonated and sodiated ions, subsequent MIM and SRM can be performed on both ions in the same scan showing the difference in fragmentation. In the case of an unknown peptide, the fragmentation can ease the interpretation of the ion's sequence and structural aspects.

Fragment	MW
Y5	555.6
Z5	540.6
B5	539.6
A5	511.6
C4	441.5
B4	426.5
X4	420.5
A4	398.5
Y4	392.5
Z4	377.4
X3	363.4
Y3	335.4
Z3	320.4
X2	306.4
C3	294.3
B3	279.3
Y2	278.4
Z2	263.3
A3	251.3
C2	237.3
B2	222.2
A2	194.2
C1	180.2
B1	165.2
X1	159.2
A1	137.2
Y1	131.2
Z1	116.2

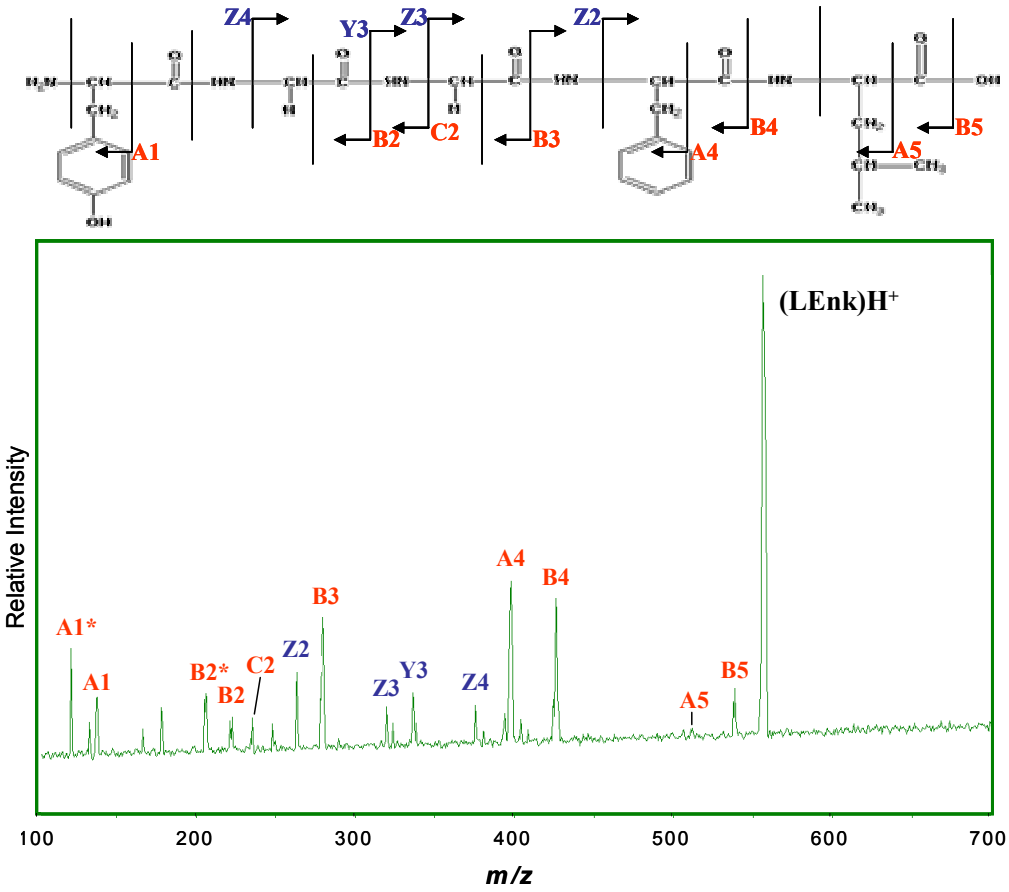

Figure 6.5: Collision induced dissociation of protonated leucine-enkephalin (LEnk) sprayed from a solution of 18 µM LEnk in 75:25 methanol:water with 1% acetic acid. The list on the left represents all of the possible A, B, C, X, Y, and Z fragments. The structure on top is LEnk with the observed fragments. Each vertical line with an arrow indicates the protonated peptide fragment that is observed (i.e., B5 is the protonated peptide without the C-terminal end OH group). The spectrum is the CID of LEnk with each fragment labeled. An asterisk (*) indicates a loss of NH_3 from that particular fragment.

Fragment	MW
Y5	573.7
Z5	558.7
B5	557.7
A5	529.7
C4	441.5
X4	438.5
B4	426.5
Y4	410.5
Z4	395.5
A4	398.5
X3	381.5
Y3	353.4
Z3	338.4
X2	324.4
Y2	296.4
C3	294.3
Z2	281.4
B3	279.3
A3	251.3
C2	237.3
B2	222.2
A2	194.2
C1	180.2
X1	177.2
B1	165.2
Y1	149.2
A1	137.2
Z1	134.2

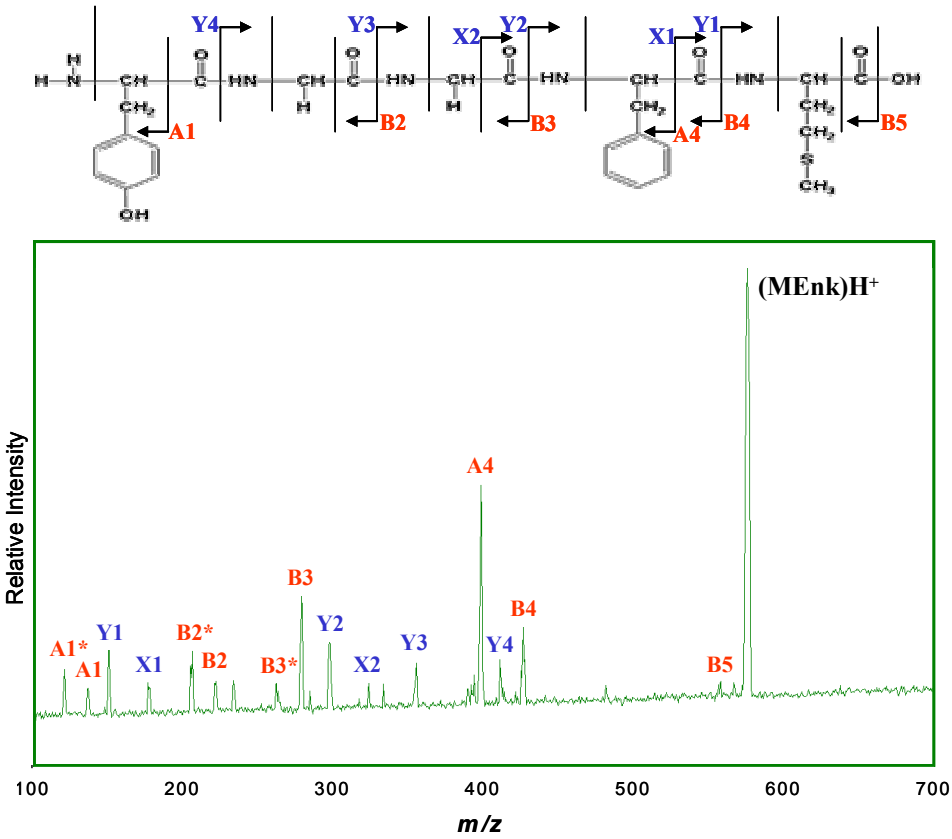

Figure 6.6: Collision induced dissociation of protonated methionine-enkephalin (MEnk) sprayed from a solution of 92 µM MEnk in 75:25 methanol:water with 1% acetic acid. The list on the left represents all of the possible A, B, C, X, Y, and Z fragments. The structure on top is MEnk with the observed fragments. Each vertical line with an arrow indicates the protonated peptide fragment that is observed (i.e., B5 is the protonated peptide without the C-terminal end OH group). The spectrum is the CID of MEnk with each fragment labeled. An asterisk (*) indicates a loss of NH_3 from that particular fragment.

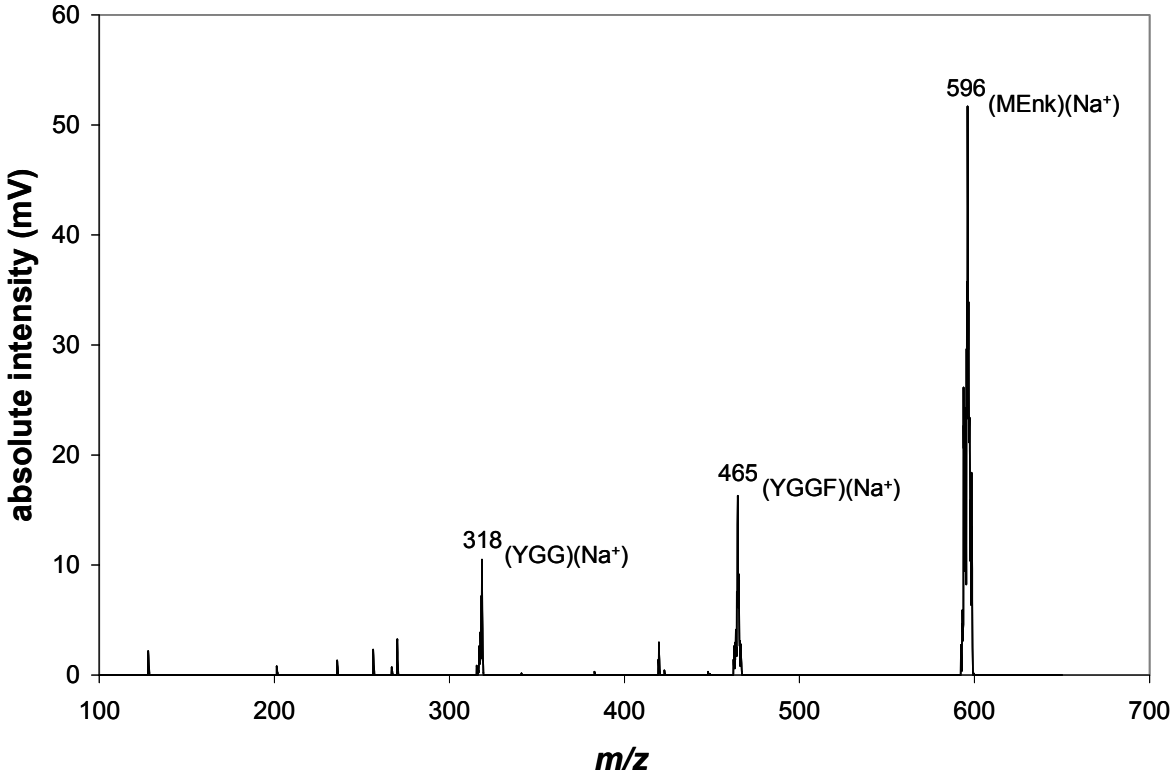

Figure 6.7: Collision induced dissociation of sodiated methionine-enkephalin (MEnk)

6.2.3 Internal Standard Calibration Curves

The main goal in the neuropeptide project is to quantitate peptides within biological fluids. It has been demonstrated that the most reliable calibration curve results from an internal standard.[2,39,53] The internal standard should be a molecule similar to the analyte being examined. An isotopically-labeled version of the analyte is often used to fulfill the internal standard criteria.[2,53]

As a test for reproducibility, methionine-enkephalin was used as the analyte and leucine-enkephalin was used as the internal standard. Solutions were made containing 16 μM of LEnk and 0.72 μM to 72 μM of MEnk in 49.5% water, 49.5% methanol, and 1% acetic acid. For each solution, three five-minute spectra were collected (Q1 scan, Q3 scan, and MIM scan of the two protonated enkephalins). The spectra were averaged and the heights of the protonated ions were plotted with and without the use of the internal standard (Figure 4.9). The curves show the use of the internal standard increases the reliability of the linear regression. Out of the three methods of collecting data, the Q3 scan has the best linear fit ($R^2 = 0.9843$). Combining the linear fit with sensitivity, indicated by the slope, the Q3 scanning of the ions would be the most accurate method.

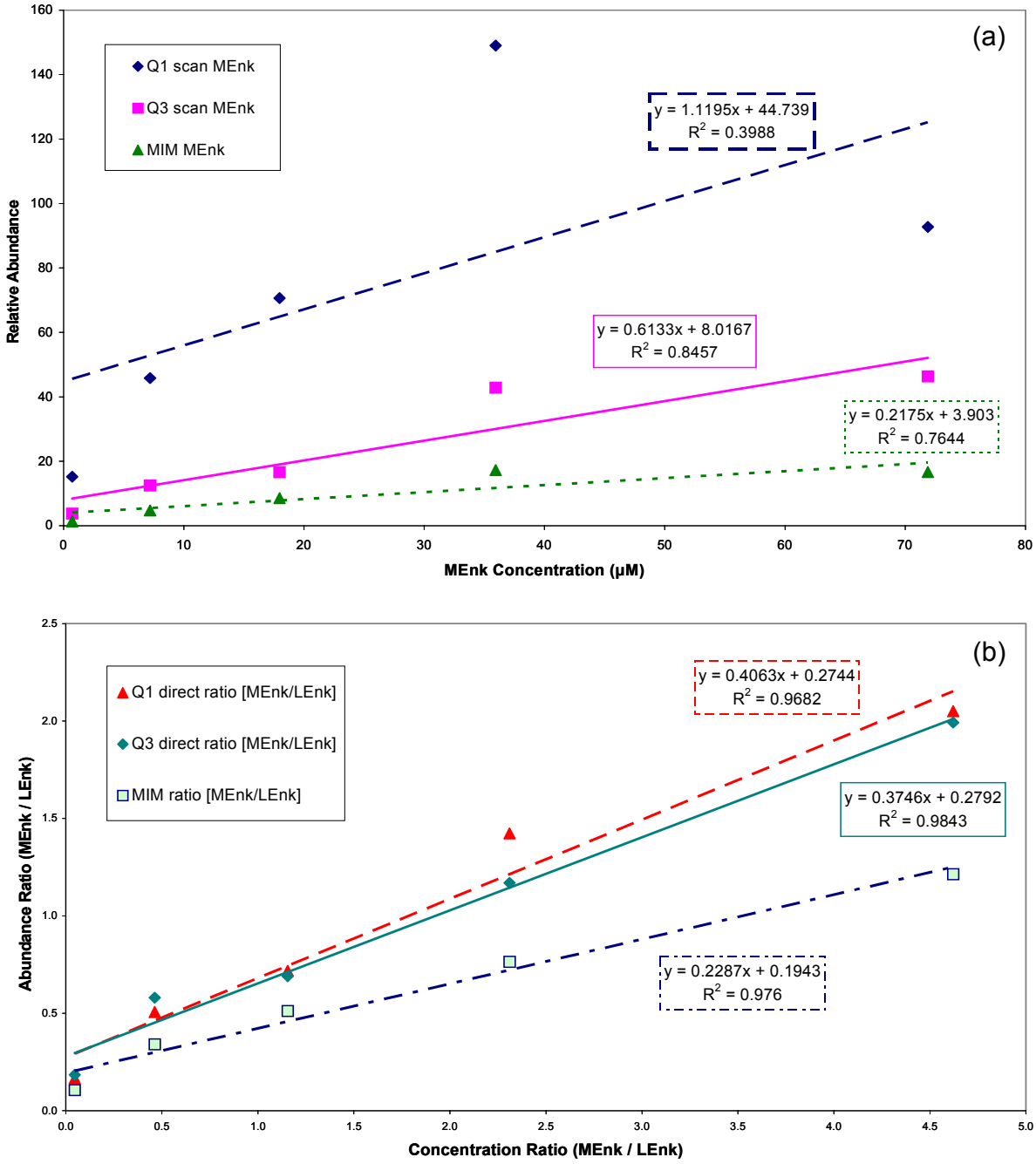

Figure 6.8: Calibration curve of (a) methionine-enkephalin abundance and (b) methionine-enkephalin abundance to leucine-enkephalin abundance ratio. The standard addition of leucine-enkephalin was at a concentration of 16 µM and the methionine-enkephalin concentration ranged from 0.72 µM to 72 µM.

6.3 BIOLOGICAL SAMPLES

Experiments were done on interstitial brain fluid of a rat obtained with a unique technique of collecting samples from the interstial fluid of the brain. A fused silica capillary with ID of 25 μm was tapered down to a thin OD wall at the tip of the capillary. These tips were then delicately placed into the surgically exposed brain tissue of the rat. The other end of the capillary was then connected to a syringe pump. Two of these capillaries were placed into the brain. One capillary was used to inject a known concentration of analyte at a rate of 100 nL/min and the second capillary was used to pull fluid at a rate of 7 nL/min. In these experiments, LEnk (YGGFL) or GGFL in aCSF solution were used as the injected analyte. After a collection time of 60 minutes the capillaries containing fluid were removed from the rat and were brought to the mass spectrometer. After removing the tapered capillary tip (necessary to ensure a good seal), the capillary was attached to a New Objective tip with a PEEK union. Each experiment progressed through a Q3 scan to SIM of the sodiated LEnk *m/z* 578 to CID of the sodiated LEnk *m/z* 578 and finally to SRM of the known fragment of sodiated LEnk *m/z* 465. The first two steps of the progression were initiated by a successful observation of *m/z* 578 in the spectra. A lack of 2-to-1 signal-to-noise ratio prompted the switch from CID to an SRM experiment to verify the *m/z* 578 peak as sodiated LEnk.

Through the course of these experiments, spectra were obtained in 11 of the 22 experiments. Failure to obtain spectra was due to either the lack of fluid uptake into the capillary or the failure to initiate the spray process. Scanning Q3 showed many peaks but only the *m/z* corresponding to the sodiated analyte could be seen as confirmation of the injected analyte in the collected sample. However, performing SIM, CID, and SRM on the *m/z* value did not provide a stable intensity for the selected ion or fragment ions. The correct fragment ion intermittingly

would be obtained for the analyte during CID and SRM but would quickly disappear. These inconsistencies in the data must be solved before the method can progress toward quantification.

One possibility to obtain consistent data is to separate the analyte from the other constituents of the sample. The high salt content in the samples will decrease the sensitivity of the method by the spread of ions and suppression of the electrospray as described in Chapter 3. Modifications to the capillary by creating a liquid chromatography-mass spectrometry system similar to Kennedy's instrumentation[5] should increase the probability of detection. The concentration and desalting of the analyte should enable the sensitivity to be increased and provide signal stability and more consistent data.

7.0 PROTEINS

There are hundreds of thousands of proteins expressed in the human brain alone. Many questions still remain on how all of these proteins originate form a much smaller set (~30,000) of proton coding genes.[73] A large amount of this diversity of gene expression is created by the splicing event, which is yet to be fully understood.[20] Polypyrimidine-tract-binding proteins (PTB) and neuroblastoma apoptosis-related protein (NAPOR) have been identified to have a role in the splicing mechanisms.[20,21] With the use of ESI-MS, these proteins' structural aspects important to splicing functions can be explored.

Proteins analyzed with ESI-MS are typically observed with multiple charges on them. The "envelope" of charges can be deconvoluted to provide a molecular weight for the protein without any charges. The proteins' amino acid sequence can be identified through a combination of digestion and collision-induced-dissociation (CID).[74] Also, the protein-RNA complex can be explored with the "soft ionizaton" of electrospray ionization which allows non-covalent binding to be transferred to the gas phase.[75]

In this study, well-documented proteins are explored on two electrospray-ionization mass spectrometers. These experiments facilitated the optimization of the instruments' parameters for protein analysis. The lesser known proteins, PTB and NAPOR, along with RNA are analyzed individually and in complexes with each other.

7.1 EXPERIMENTAL

The characterization proteins were obtained from Sigma Chemical Company (St. Louis, MO) and the neuroproteins were obtained from Dr. Paula Grabowski's group. The experiments performed on the HP LCMS were direct injections into the "mobile phase" flowing directly into the mass spectrometer. The injections were 1 μL in volume with the exception of the 5 μL injections in the PTB experiments. The solutions of standard proteins contained only water prior to the mixing with the "mobile phase" with the exception of pepsin which had 1% ammonium hydroxide added. The solutions of the neuroproteins and RNA had the 1% acetic acid or 1% ammonium hydroxide added prior to injection. The flow rate of the "mobile phase" was 0.4 mL/min. The "mobile phases" for the BSA, CA, and RNA experiments were water containing 0.1% triflouroacetic acid, 60% water containing 1% of acetic acid and 40% acetonitrile, and 60% water and 40% acetonitrile respectively. The experiments performed on the SWISS-484 were all direct injections under conditions stated previously in the SWISS-484 section. The flow rate for the experiments was 300 nL/min. For carbonic anhydrase, a 26 μM, 1% acetic acid, and 25% methanol aqueous solution was used with 3.0 kV applied to the tip with a 10 μm orifice. For cytochrome c, a 70 μM aqueous solution was used with 3.0 kV applied to the tip with a 10 μm orifice. For myoglobin, a 4.5 μM, 1% acetic acid, and 25% methanol aqueous solution was used with 2.0 kV applied to the tip with a 15 μm orifice. For NAPOR, a 5 μM, 1% acetic acid, 50% methanol, and 50% ammonium acetate solution was used with 2.0 kV applied to the tip with a 15 μM orifice.

7.2 CHARACTERIZATION PROTEINS

As with peptides, known solutions of proteins are used to characterize the capabilities of the SWISS-484. Cytochrome C, myoglobin, carbonic anhydrase II (CA), pepsin, and bovine serum albumin (BSA) were used to this end. These proteins range in molecular weight from 12 kiloDaltons to 67 kiloDaltons. Micromolar protein concentrations in a solution with 10-50% co-solvent and ~1% acid or base provided the best signal-to-noise ratios. The spectra of CA, pepsin, and BSA were also obtained from the HP LC-MS in order to compare the two instruments. Experiments with CA were performed under positive ion conditions and produced an envelope with a range of 20 to 40 charges (Figure 5.1a). Experiments with Pepsin were performed under negative ion conditions and produced an envelope with a range of 25 to 42 charges (Figure 5.2).[76] Experiments with BSA were performed under positive ion conditions and produced an envelope with a range of 35 to 60 charges (Figure 5.3) as in the literature.[77] Among other things, these three experiments demonstrate that the larger the protein is, the greater the number of charges it can accommodate. Using MagTran to deconvolute the envelope of peaks, the average MW of the parent ion was less than a tenth of a percent different from the expected value. The spectra of cytochrome C (Figure 5.4), myoglobin (Figure 5.5), and CA (Figure 5.1b) were obtained using the SWISS-484. All three experiments were performed in the positive ion mode. The spectra had charge ranges of 7-14 for cytochrome C, 12-25 for myoglobin, and 20-35 for CA. All of these spectra are consistent with spectra found in the literature.[78] The percent difference from the assigned protein's MW to the known value is greater, around 1%, in the SWISS-484 data than in the HP data. However, the obtained spectra give an indication of the SWISS-484's capabilities for viewing the molecular weights of proteins.

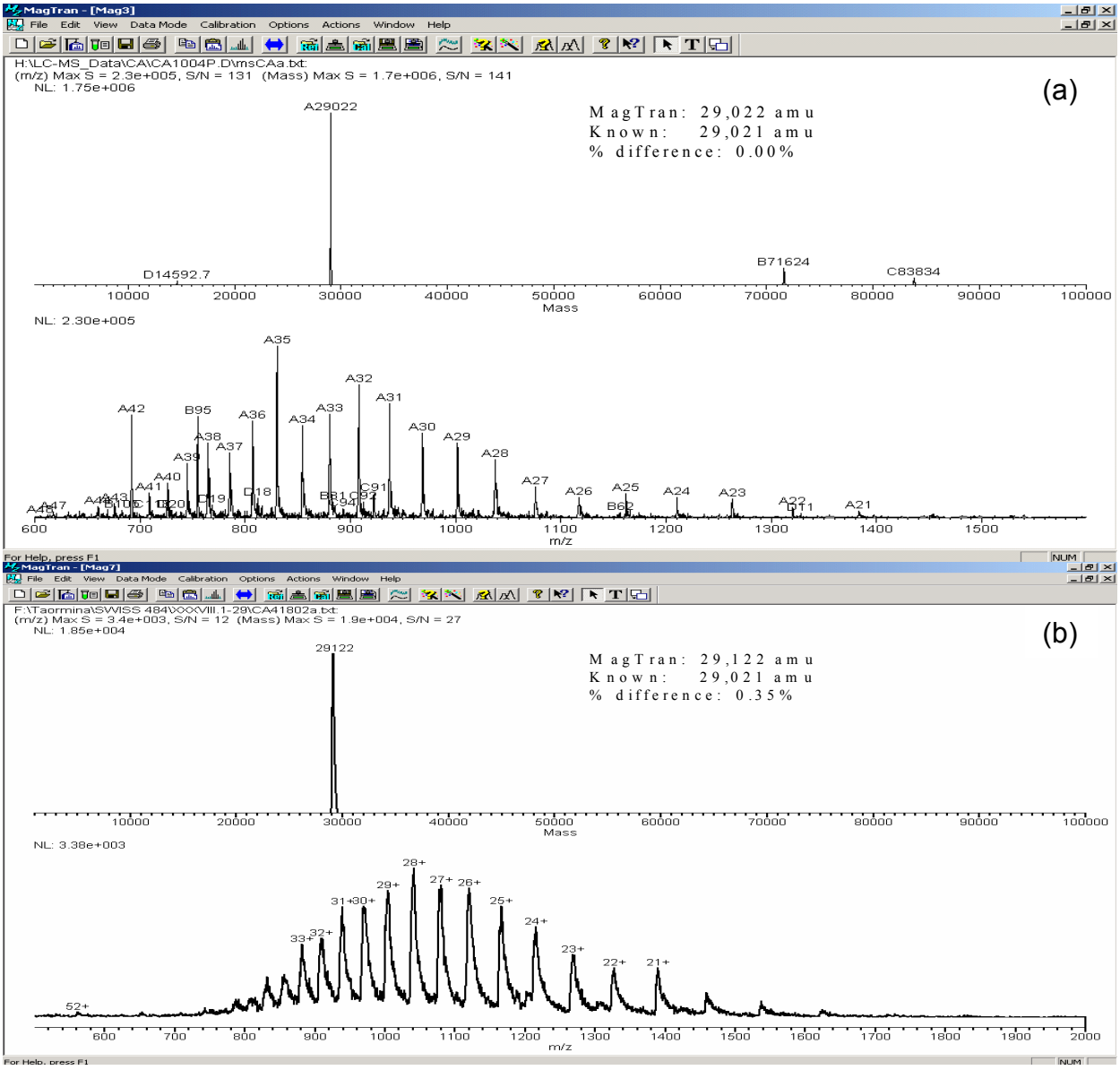

Figure 7.1: Spectra of carbonic anhydrase II obtained on the (a) HP LCMS (34 µM) and the (b) SWISS-484 (26 µM) each deconvoluted by MagTran. The lower spectra for each experiment are the raw data with letters (A, B, C …) signifying an "envelope" and numbers (15, 16, 17 …) signifying the number of protons on the structure. The upper spectrum for each experiment is the deconvoluted output showing the molecular weight each "envelope" represents. The intensity of each molecular weight provides the total abundance of the "envelope". MagTran was only able to find one "envelope" in the spectrum from the SWISS-484 so there are no letters associated with the charges.

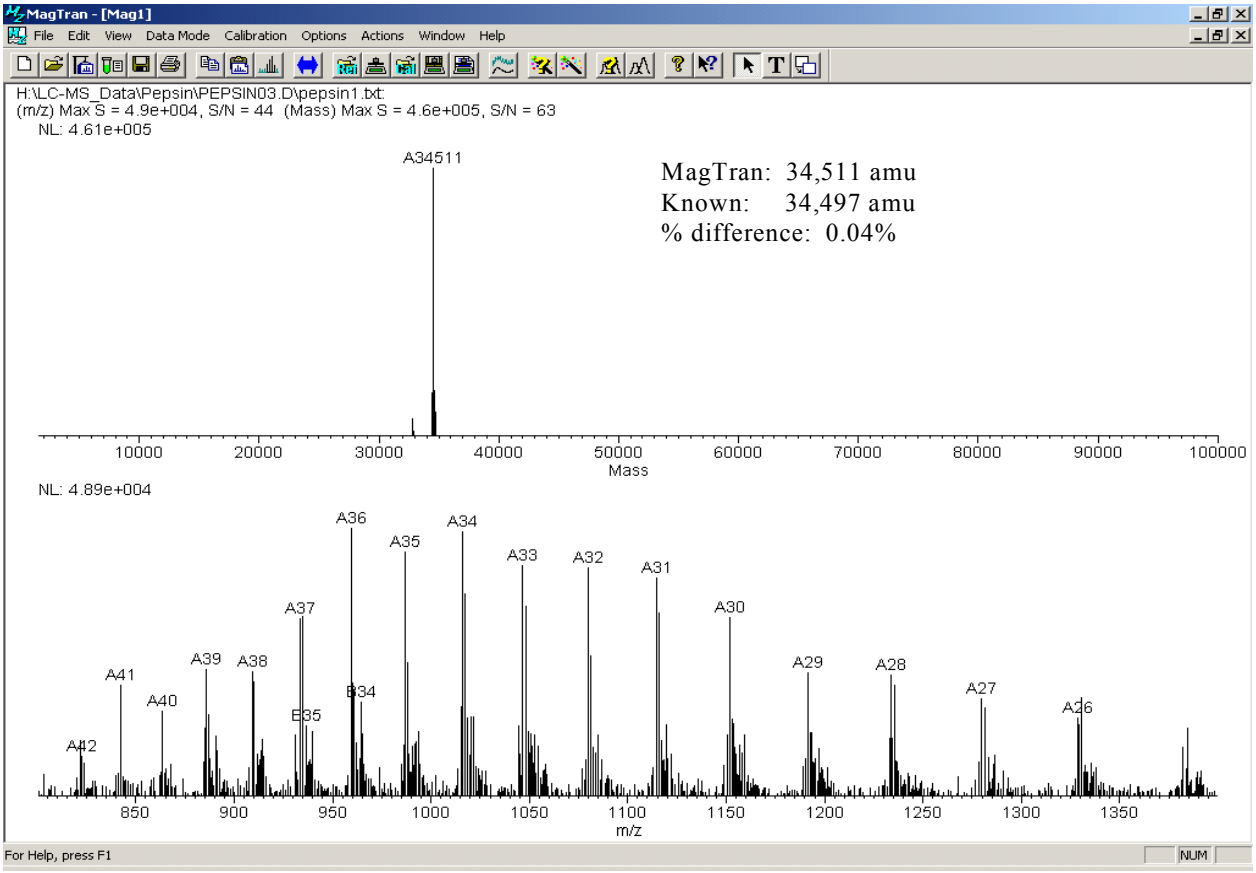

Figure 7.2: Spectrum of 58 µM pepsin in 1% NH_4OH obtained from the HP LCMS and deconvoluted by MagTran. The lower spectrum is the raw data with letters (A, B, C …) signifying an "envelope" and numbers (20, 21, 22 …) signifying the number of protons missing from the structure. The upper spectrum for each experiment is the deconvoluted output showing the molecular weight each "envelope" represents. The intensity of each molecular weight provides the total abundance of the "envelope".

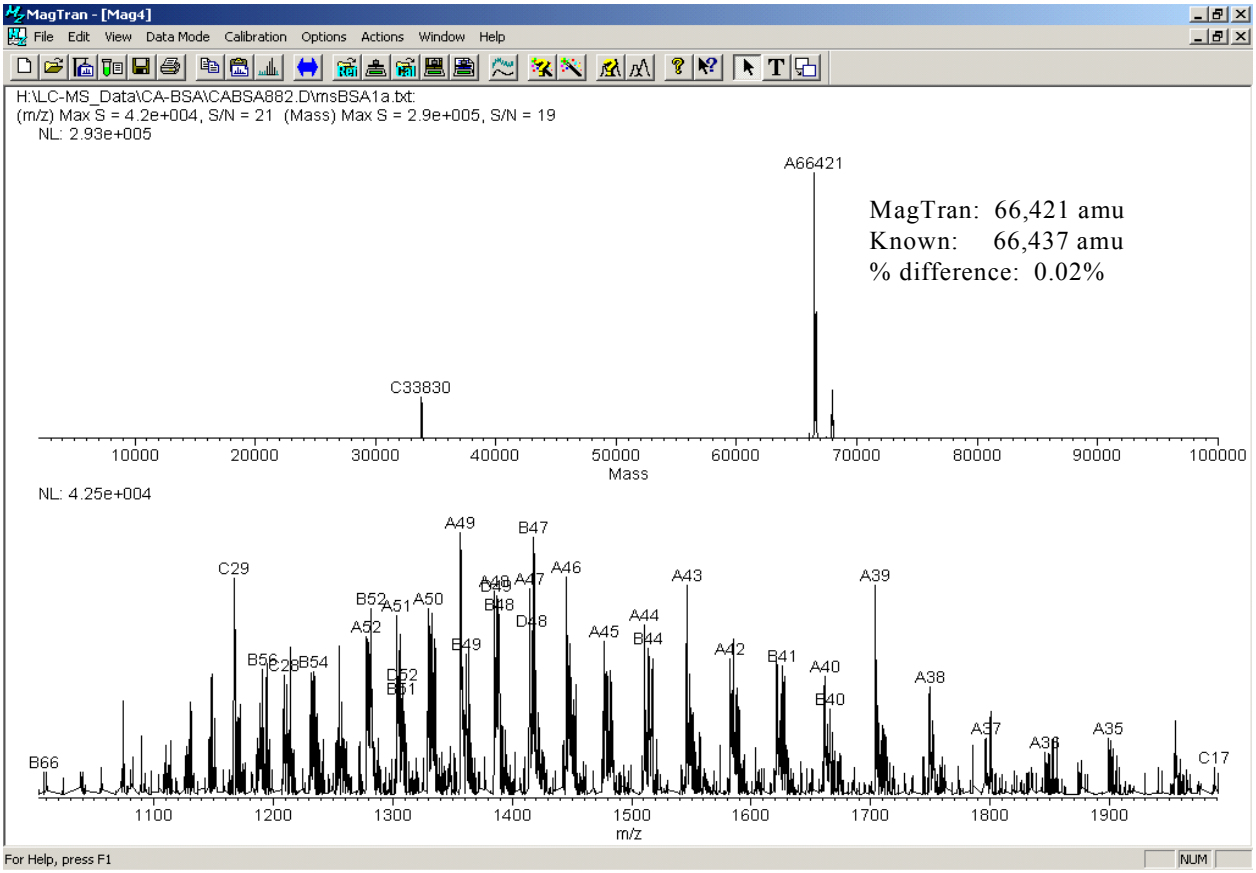

Figure 7.3: Spectrum of 45 µM bovine serum albumin obtained from the HP LCMS and deconvoluted by MagTran. The lower spectrum is the raw data with letters (A, B, C …) signifying an "envelope" and numbers (42, 43, 44 …) signifying the number of protons on the structure. The upper spectrum for each experiment is the deconvoluted output showing the molecular weight each "envelope" represents. The intensity of each molecular weight provides the total abundance of the "envelope".

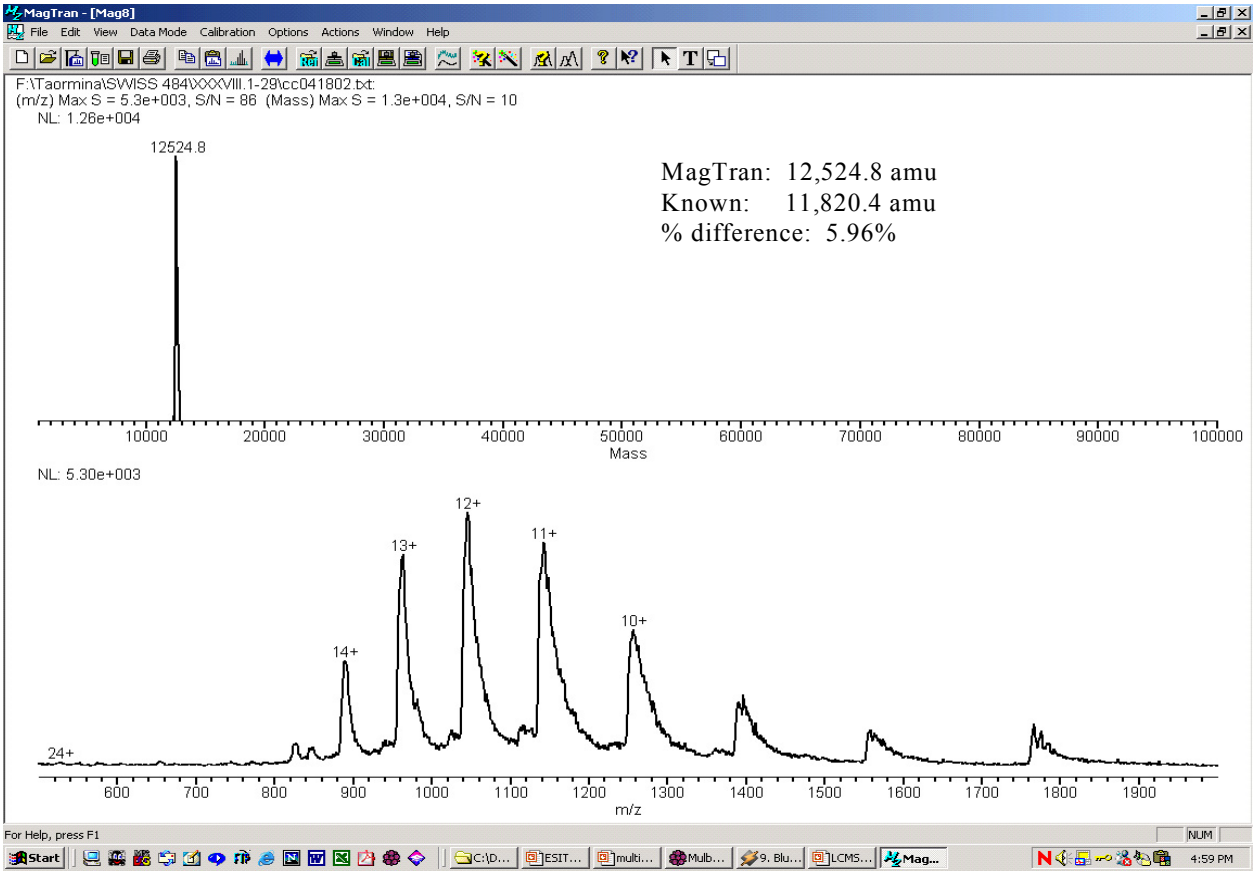

Figure 7.4: Spectrum of 70 µM horse heart cytochrome C in water obtained from the SWISS-484 and deconvoluted by MagTran. The lower spectrum is the raw data with numbers (10, 11, 12 …) signifying the number of protons on the structure. The upper spectrum for each experiment is the deconvoluted output showing the molecular weight each "envelope" represents. The intensity of each molecular weight provides the total abundance of the "envelope". MagTran was only able to find one "envelope" in the spectrum so there are no letters associated with the charges.

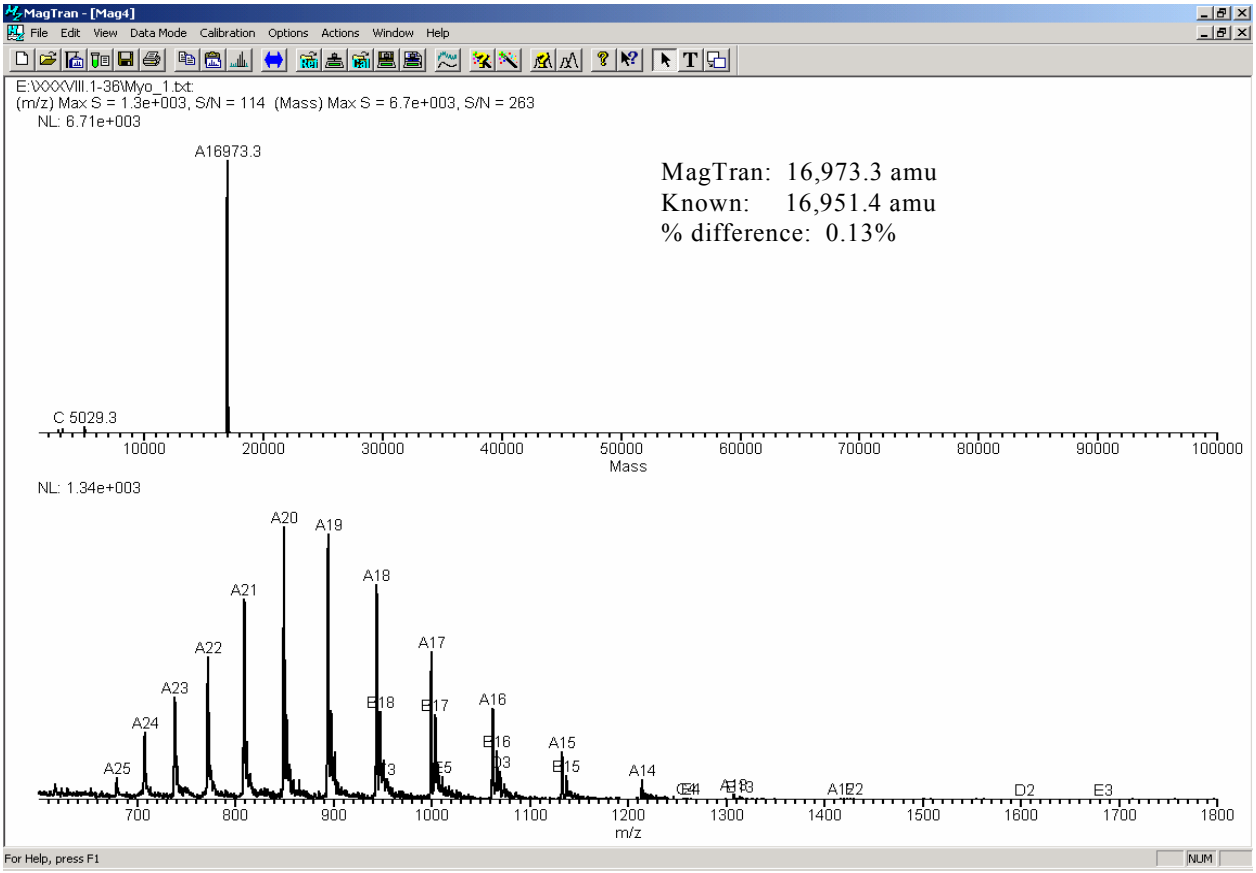

Figure 7.5: Spectrum of 4.5 µM myoglobin in 25:75 methanol:water with 1% acetic acid obtained from SWISS-484 and deconvoluted by MagTran. The lower spectrum is the raw data with letters (A, B, C …) signifying an "envelope" and numbers (15, 16, 17 …) signifying the number of protons on the structure. The upper spectrum for each experiment is the deconvoluted output showing the molecular weight each "envelope" represents. The intensity of each molecular weight provides the total abundance of the "envelope".

7.3 BACTERIALLY GROWN PROTEINS

Most of the work on the unknown samples has been performed on the HP LC-MS. Samples of polypyrimidine tract binding (PTB) A1 and A2 proteins and neuroblastoma apoptosis-related (NAPOR) protein have been tested. The samples were first received in TRIS buffer. The presence of TRIS proved to be fatal to the MS analysis of the proteins (including with the commercial instrument). The solution was dialyzed to remove TRIS and reanalyzed. Both PTBs provided spectra with a wide range of charge (z) values (Figure 5.6). The deconvolution gave a molecular weight with a mass percent difference from the expected value of less than 5%. The spectra of NAPOR is poorly resolved (Figure 5.7a) compared to the reference proteins examined. The most abundant molecular weight does match the predicted molecular weight of the protein with a high accuracy, 0.06% mass difference. NAPOR was examined on the SWISS-484 but an envelope of ions was not obtained (Figure 5.7b). These spectra provide only a small amount of data for the protein; CID must be performed to complete the structural analysis.

The CID process would be more helpful if the protein is digested into smaller fragments before collision induced dissociation. Without digestion the intact protein would require a high collision energy to provide a good spectrum of fragments. Even with efficient fragmentation, the spectrum would have a large number of peaks. In such a case, overlapping and poor signal-to-noise ratios would likely combine to make the spectrum indecipherable. Digesting the proteins will provide peptides that can be separately identified by CID. With the amino acid sequence of the peptides known, the protein sequence can be pieced back together.

A seventeen nucleotide RNA known to bind to these neuroproteins was obtained from Dr. Paula Grabowski's group. An additional goal was to determine the extent of complexation of PTB and NAPOR proteins with that RNA molecule. Since RNA is a highly negative charged

structure, the use of negative ion mode is regarded as the ideal route[79]. At present negative ion spectra of proteins have only been obtained on the HP LC-MS. The spectra of the RNA were acquired in the negative ion mode (Figure 5.8). To date, MS observation of the complex between the RNA and proteins has not been successful.

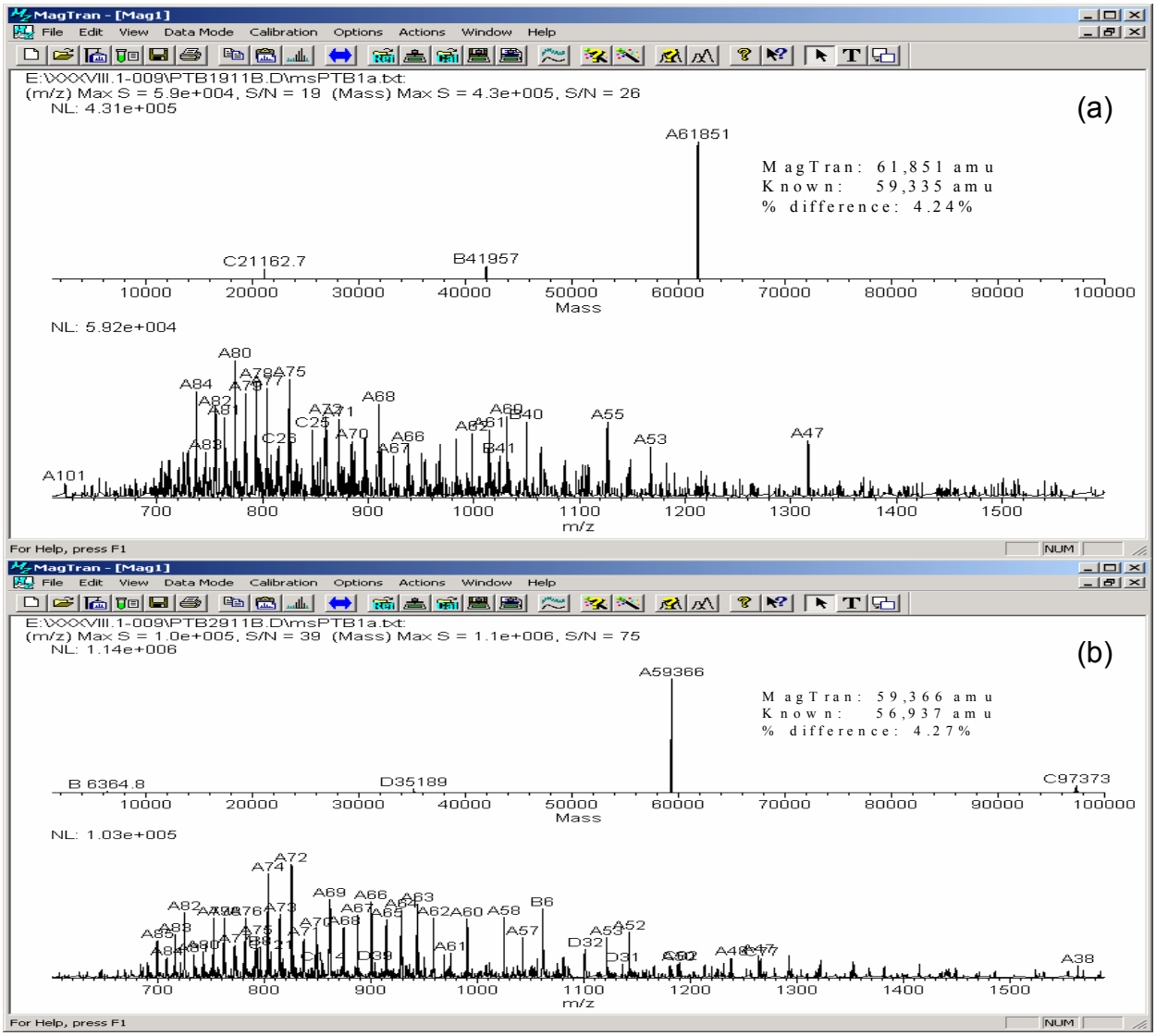

Figure 7.6: Spectra of 10 µM polypyrimidine tract binding proteins, (a) PTB A1 and (b) PTB A2, in 1% acetic acid obtained form the HP LCMS and deconvoluted by MagTran. The lower spectra for each protein are the raw data with letters (A, B, C …) signifying an "envelope" and numbers (70, 71, 72 …) signifying the number of protons on the structure. The upper spectrum for each experiment is the deconvoluted output showing the molecular weight each "envelope" represents. The intensity of each molecular weight provides the total abundance of the "envelope".

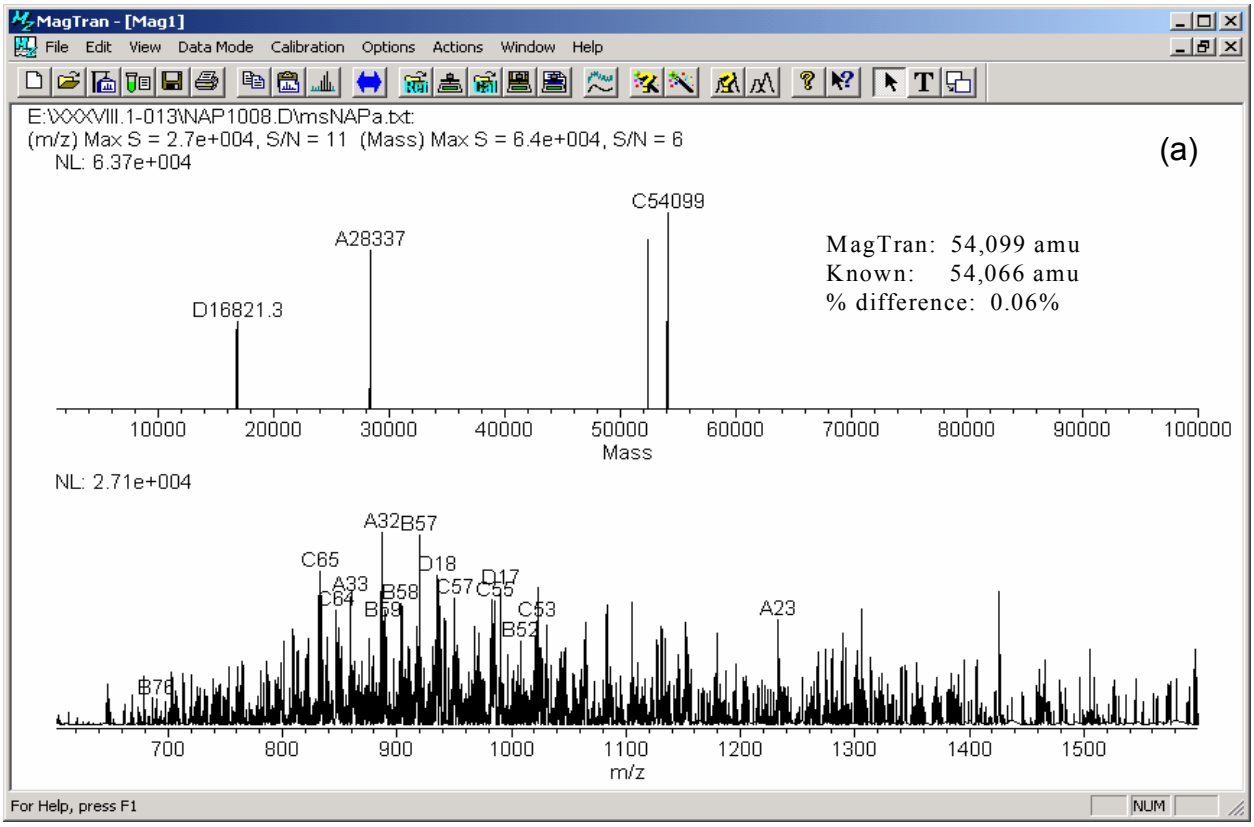

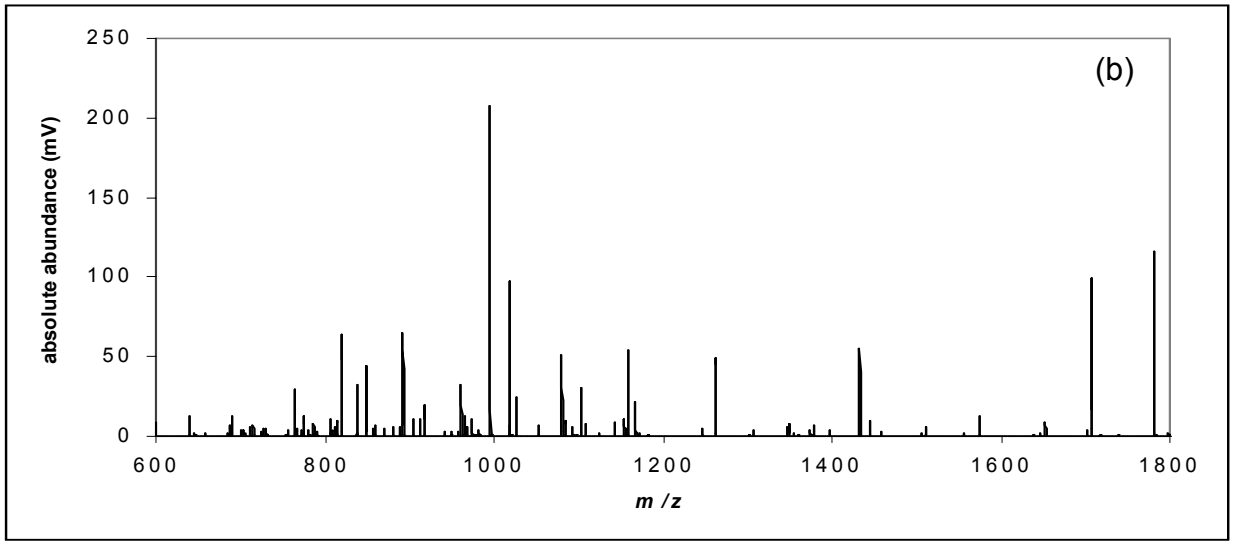

Figure 7.7: Spectra of NAPOR obtained from (a) HP LCMS (10 µM) and deconvoluted by MagTran and (b) SWISS-484 (5 µM) which MagTran was unable to deconvolute.

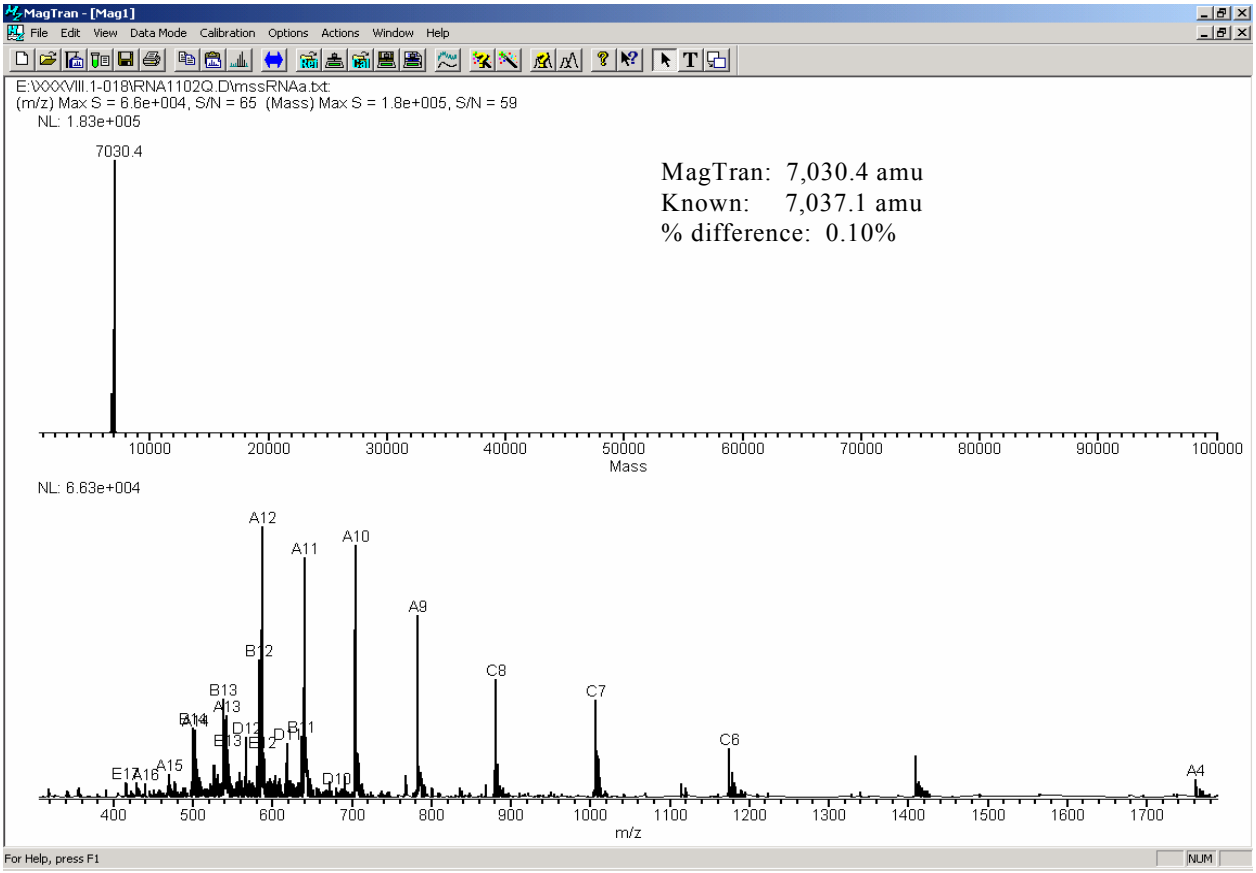

Figure 7.8: Spectra of the 64 µM seventeen nucleotide RNA obtained from the HP LCMS and deconvoluted by MagTran. The lower spectrum is the raw data with letters (A, B, C …) signifying an "envelope" and numbers (8, 9, 10 …) signifying the number of protons missing from the structure. The upper spectrum for each experiment is the deconvoluted output showing the molecular weight each "envelope" represents. The intensity of each molecular weight provides the total abundance of the "envelope".

APPENDIX A

TEAR GLUCOSE MEAL STUDIES

To gauge the blood-tear glucose correlation, meal studies were carried out on non-diabetic and diabetic subjects. The studies consisted of the patient fasting overnight and providing blood and tear samples before and after intake of a set amount of sugar drink (Meal). Samples were taken in sets with one set defined as blood, left eye tears, and then right eye tears. Three sets were taken prior to the meal for most of the studies and then about twelve sets after the meal. Blood glucose concentration was determined by either venous blood sampling with use of the glucose oxidase method or a pin prick along with the use of a glucose meter. Tear glucose concentrations were obtained by sampling with a one microliter capillary and use of the mass spectrometry method described in Chapter 4. The meal for studies without using the C_{18} column was 1 gram of glucose within the drink per 1 kilogram of the subject's body weight. The studies with the C_{18} column had a meal which consisted of an intake of 75 grams of glucose contained in the drink, which resembles a glucose tolerance test used to diagnose diabetes. Meal studies were performed on thirteen subjects prior to the use of the C_{18} column in the glucose method (Figures A.1-13) and three studies were performed after the column addition (Figures A.14-16). The figures are arranged to show the deviation from the averaged pre-meal glucose concentrations

but also the absolute values. For each study, the data is separated into the three graphs one each for blood glucose concentration, left eye glucose concentration, and right eye glucose concentration. The thirteen studies completed before the final method was established contain an average baseline (pre-meal) value of glucose in tears of 150 μM. It was determined after the final method was established that baseline glucose values are on average 28 μM. The baseline values for the experiments prior to the use of the column are more than likely at the limit of detection for the method. All data was used to further the understanding of the tear glucose concentrations and helped to provide the conclusions in Chapter 4. In addition, it can be seen that each subject had a different rise and fall of glucose concentration within blood and tears. The method was approved by the University of Pittsburgh Institutional Review Board #011108.

Figure A.1: Meal study of subject 1 (non-diabetic)

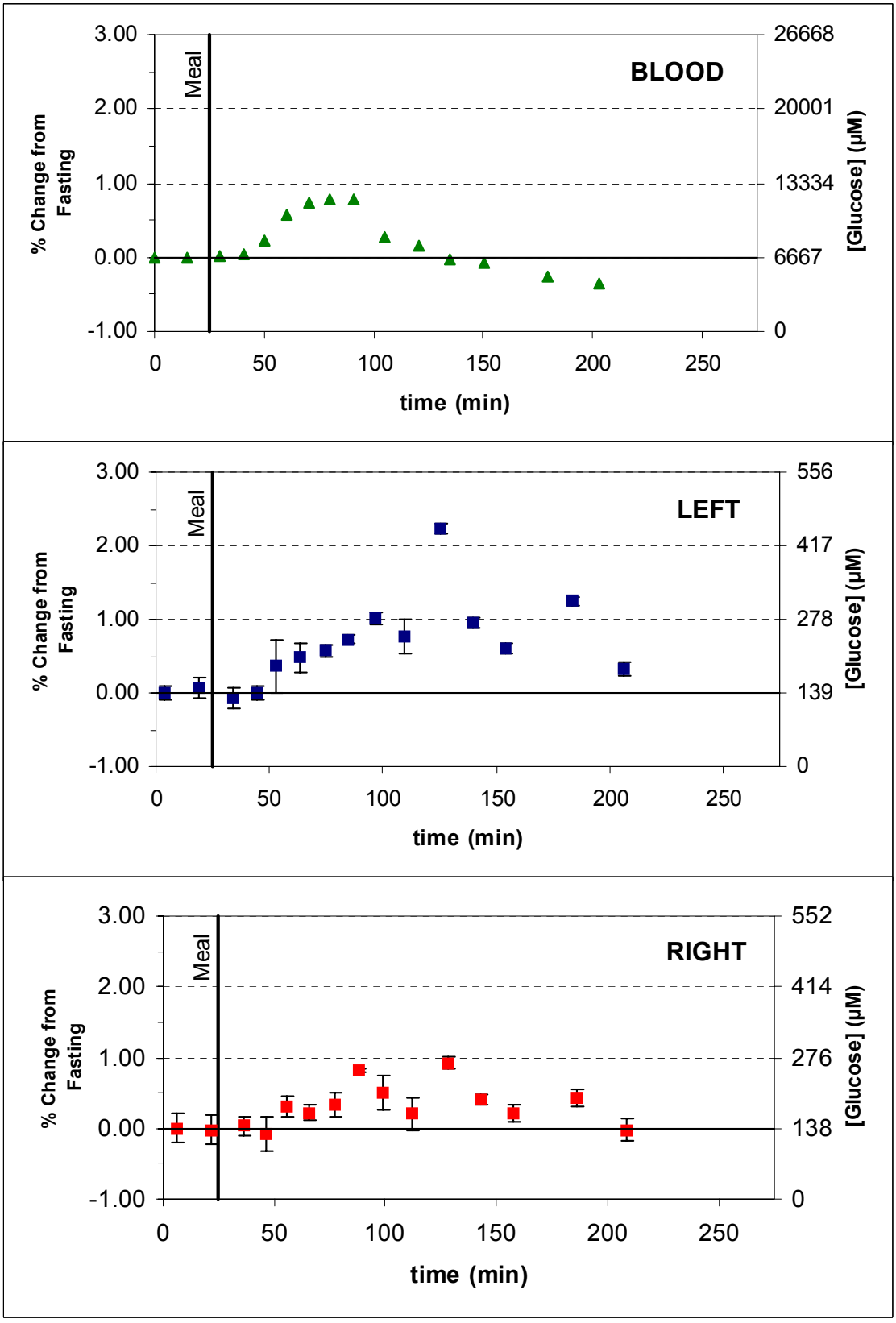

Figure A.2: Meal study of subject 2 (non-diabetic)

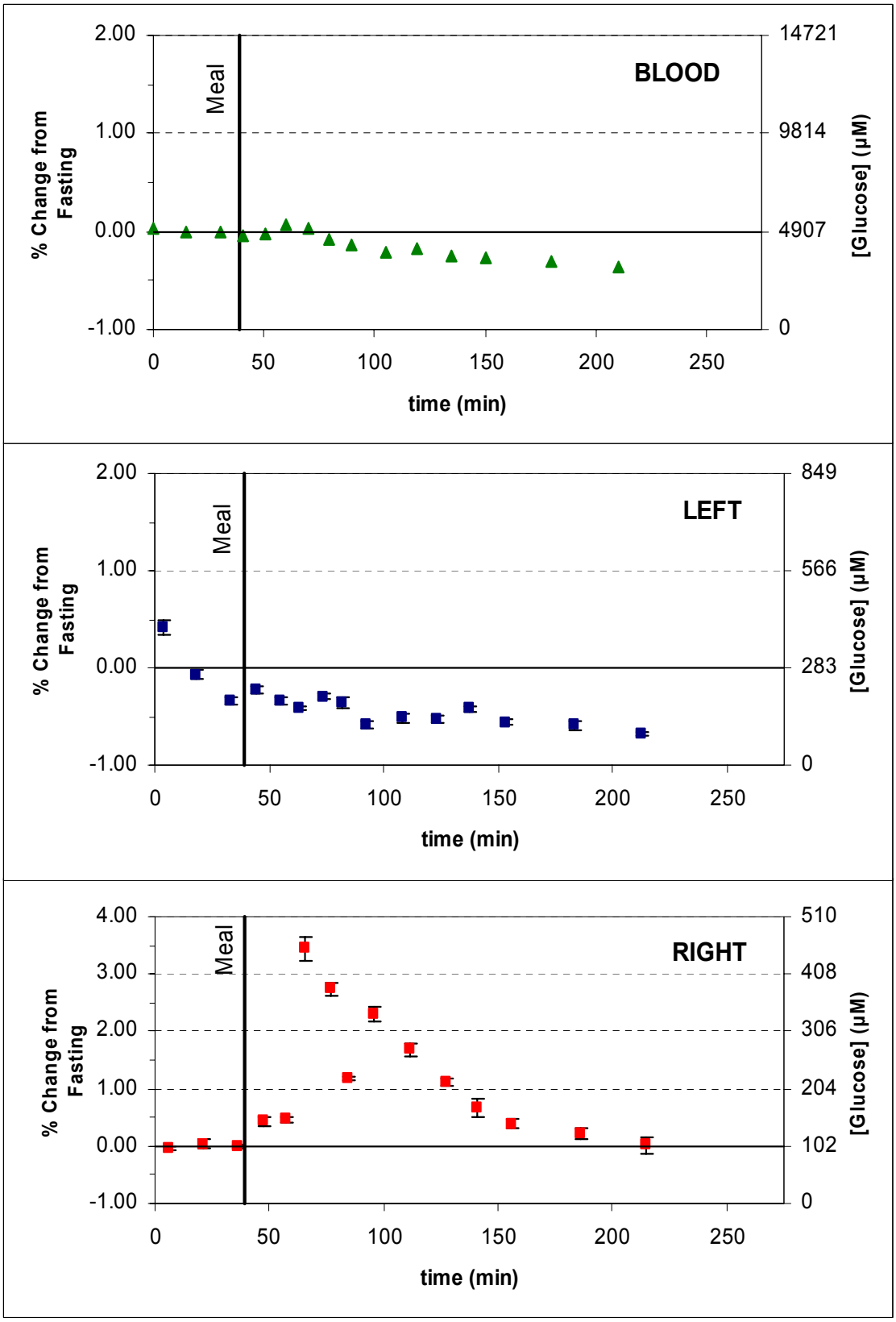

Figure A.3: Meal study of subject 3 (non-diabetic)

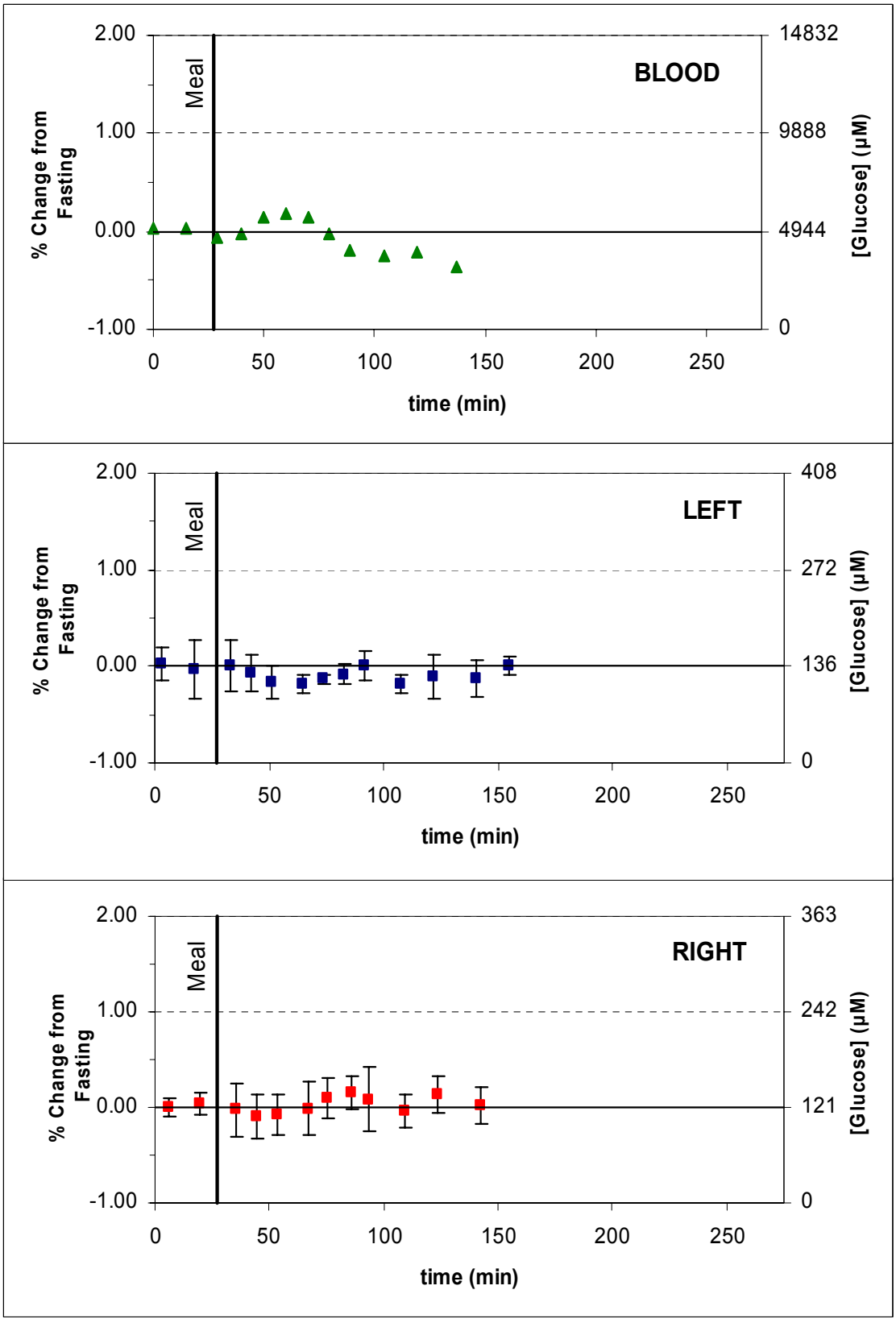

Figure A.4: Meal study of subject 4 (non-diabetic)

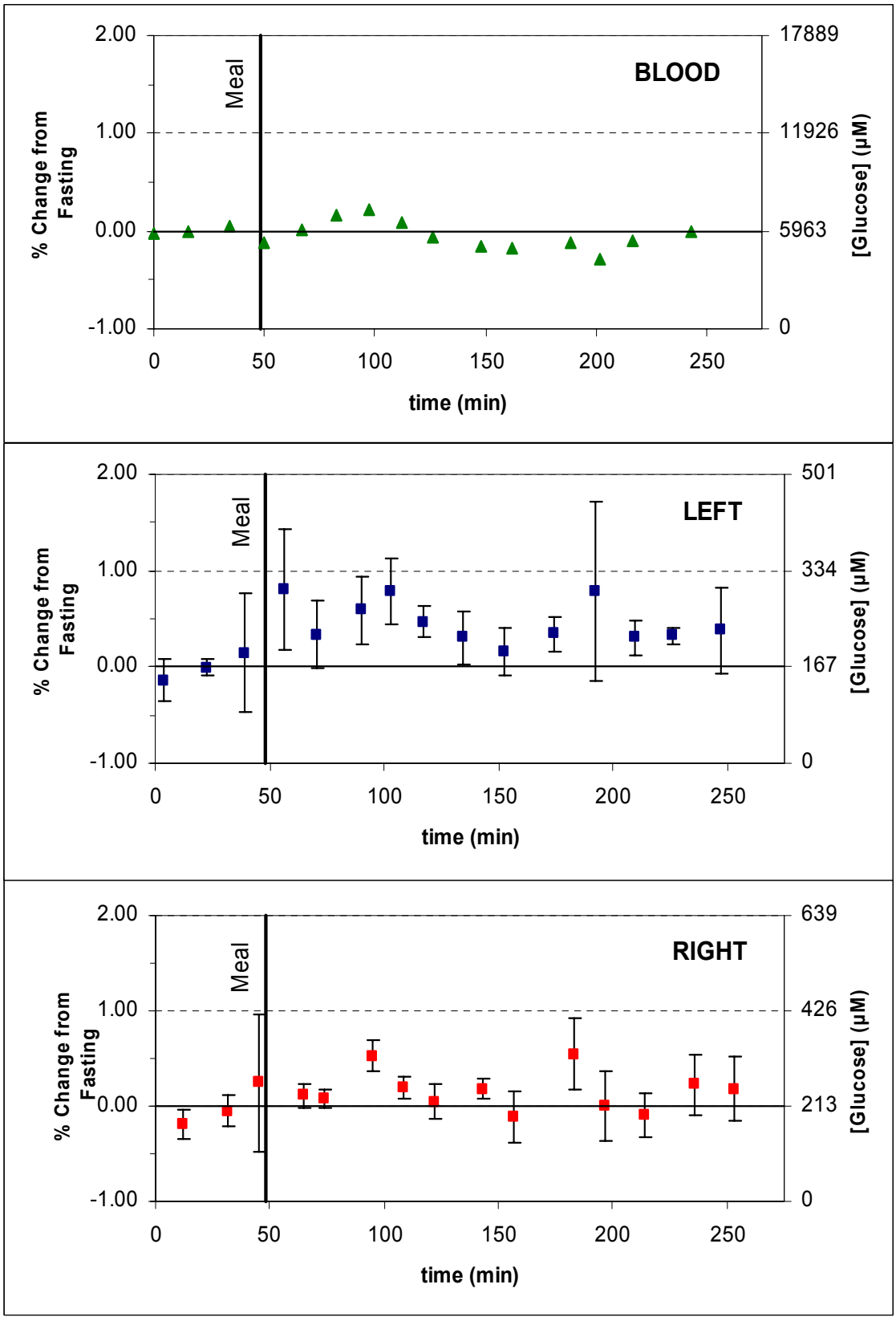

Figure A.5: Meal study of subject 5 (non-diabetic)

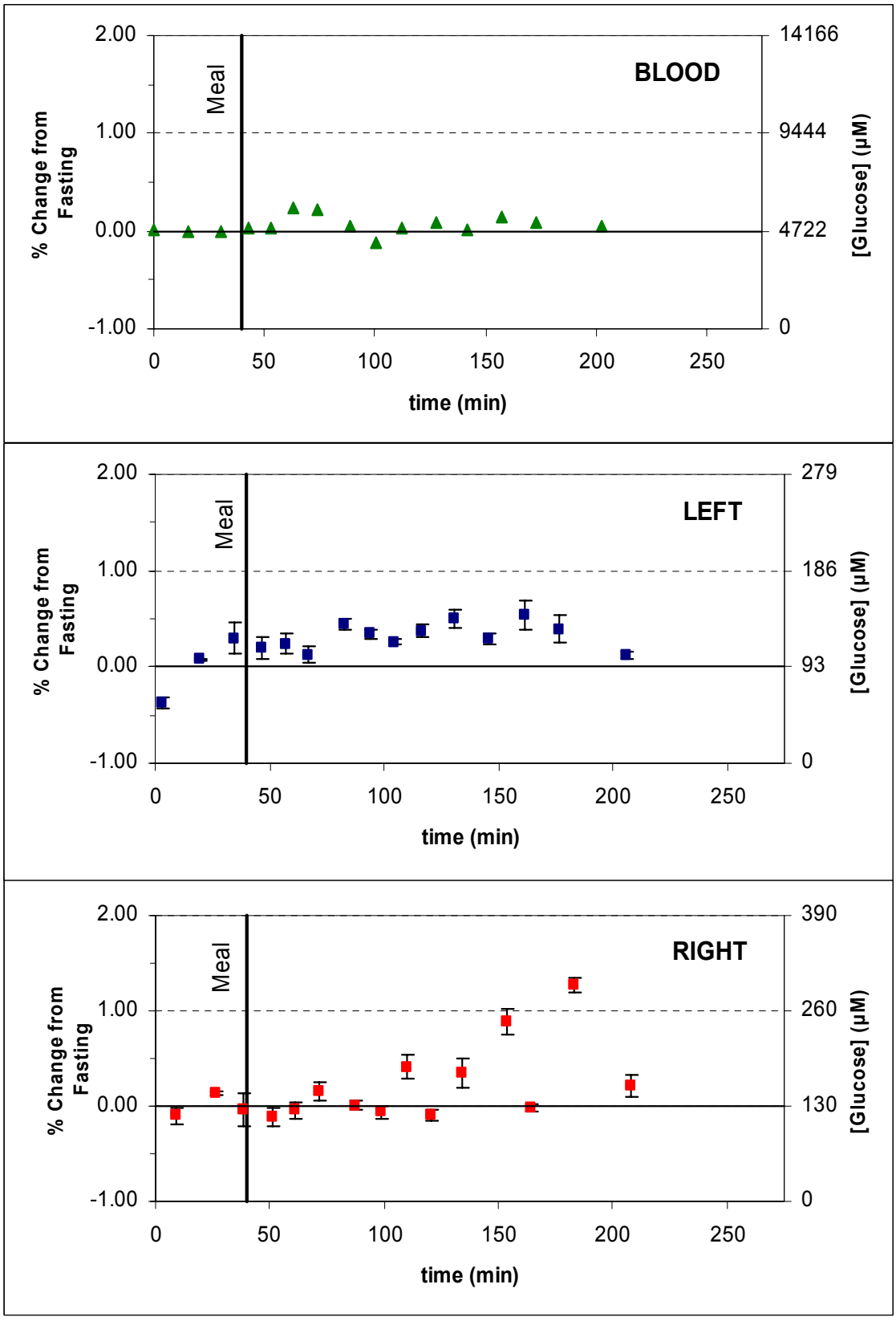

Figure A.6: Meal study of subject 6 (non-diabetic)

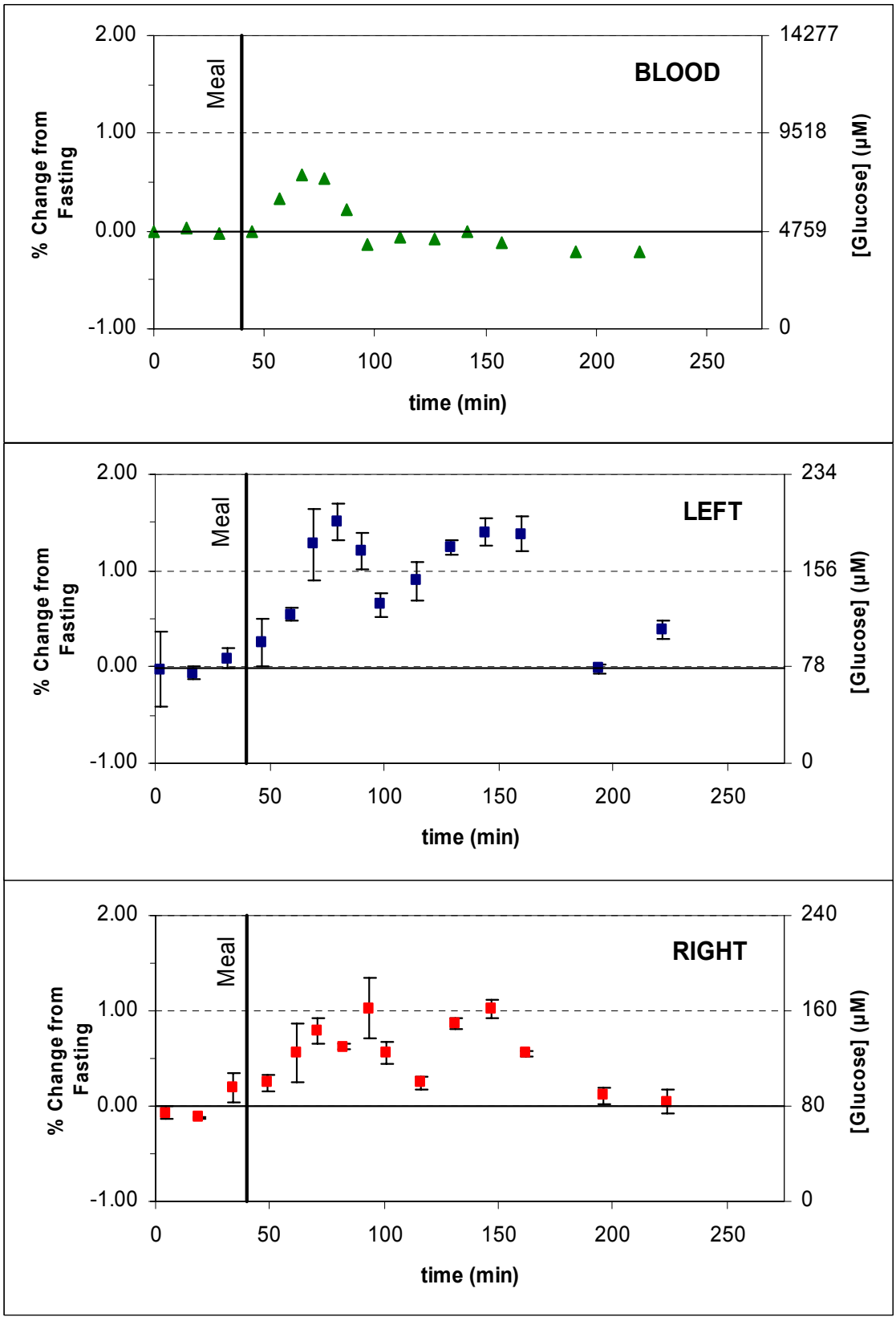

Figure A.7: Meal study of subject 7 (non-diabetic)

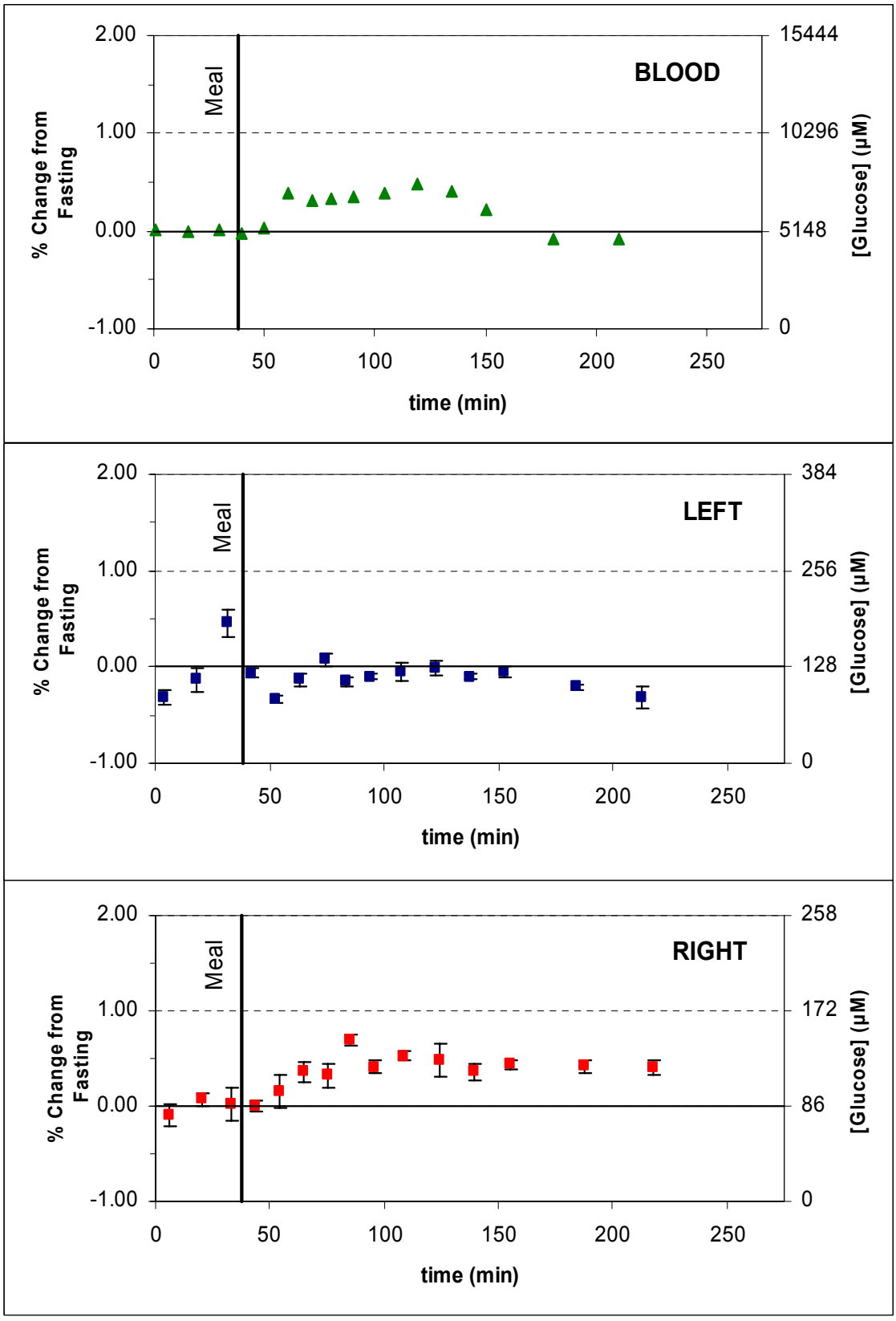

Figure A.8: Meal study of subject 8 (non-diabetic)

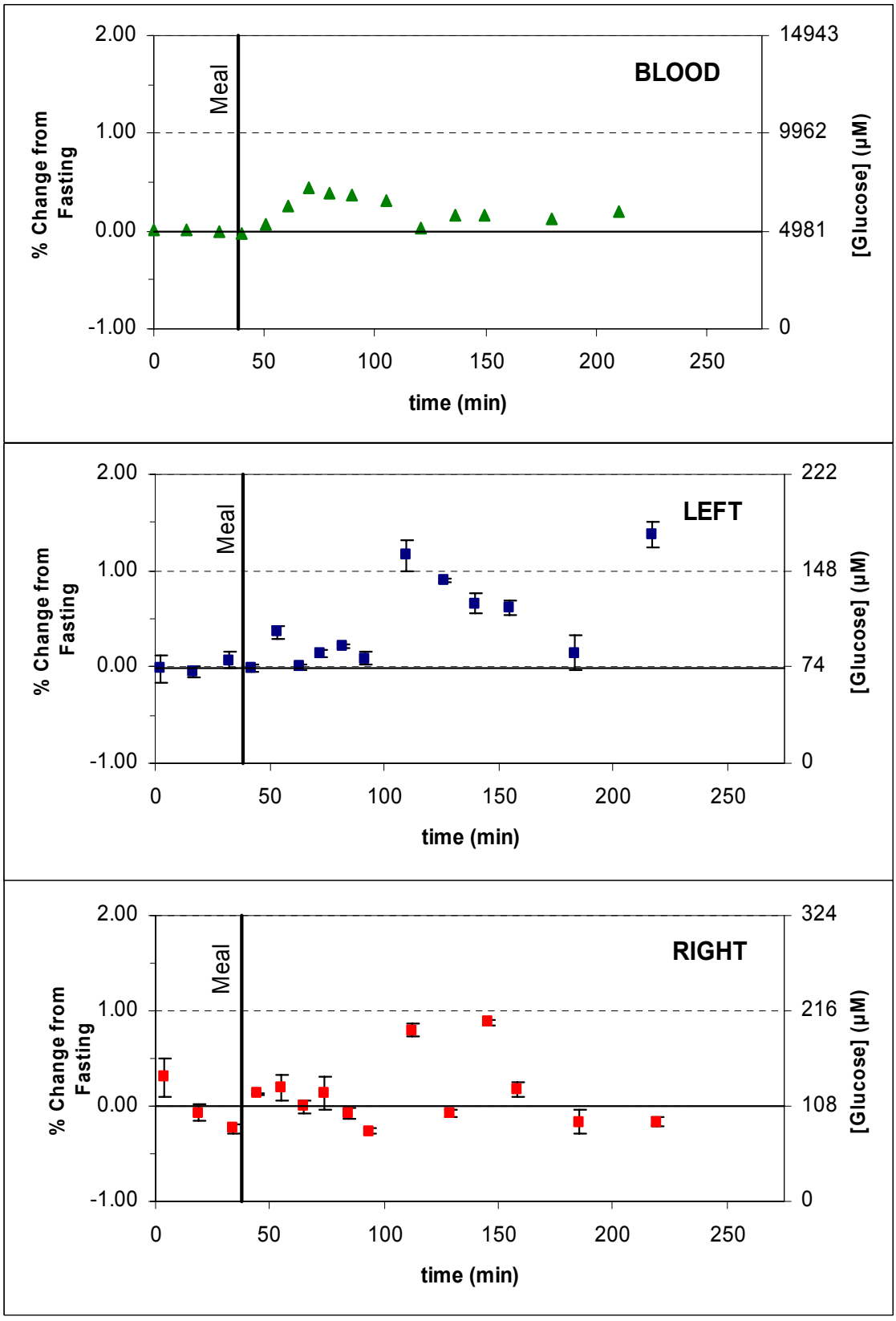

Figure A.9: Meal study of subject 9 (diabetic)

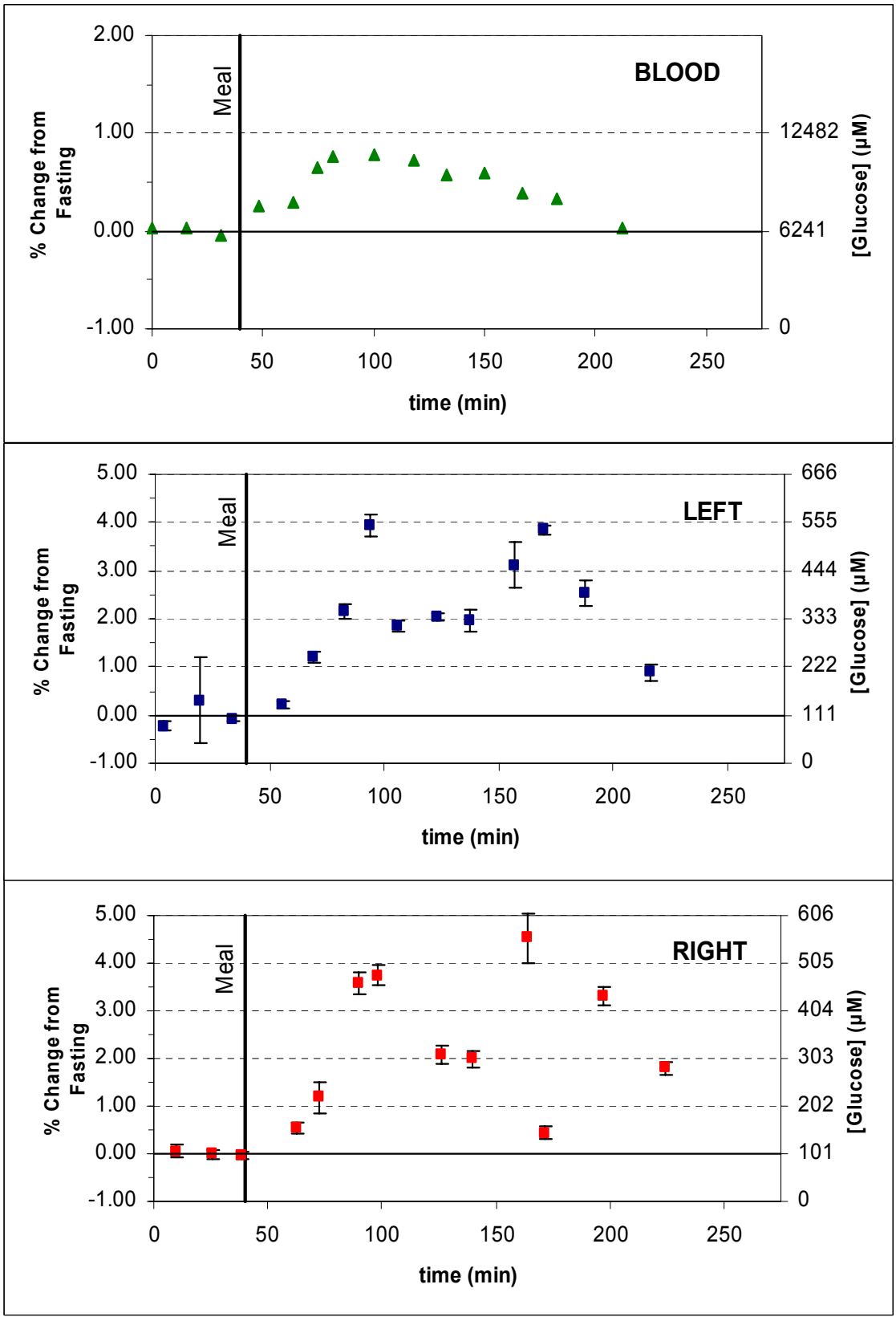

Figure A.10: Meal study of subject 10 (diabetic)

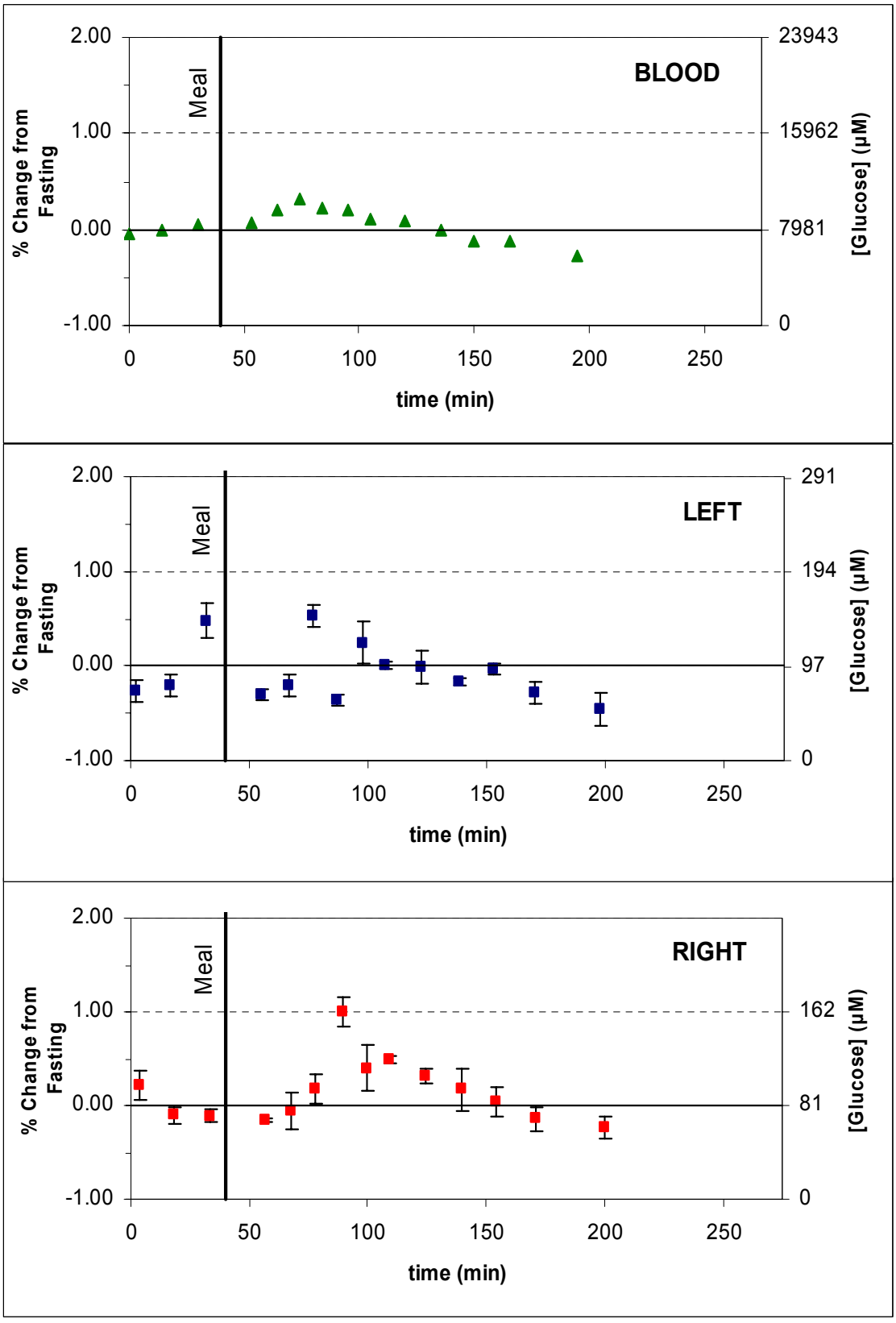

Figure A.11: Meal study of subject 11 (diabetic)

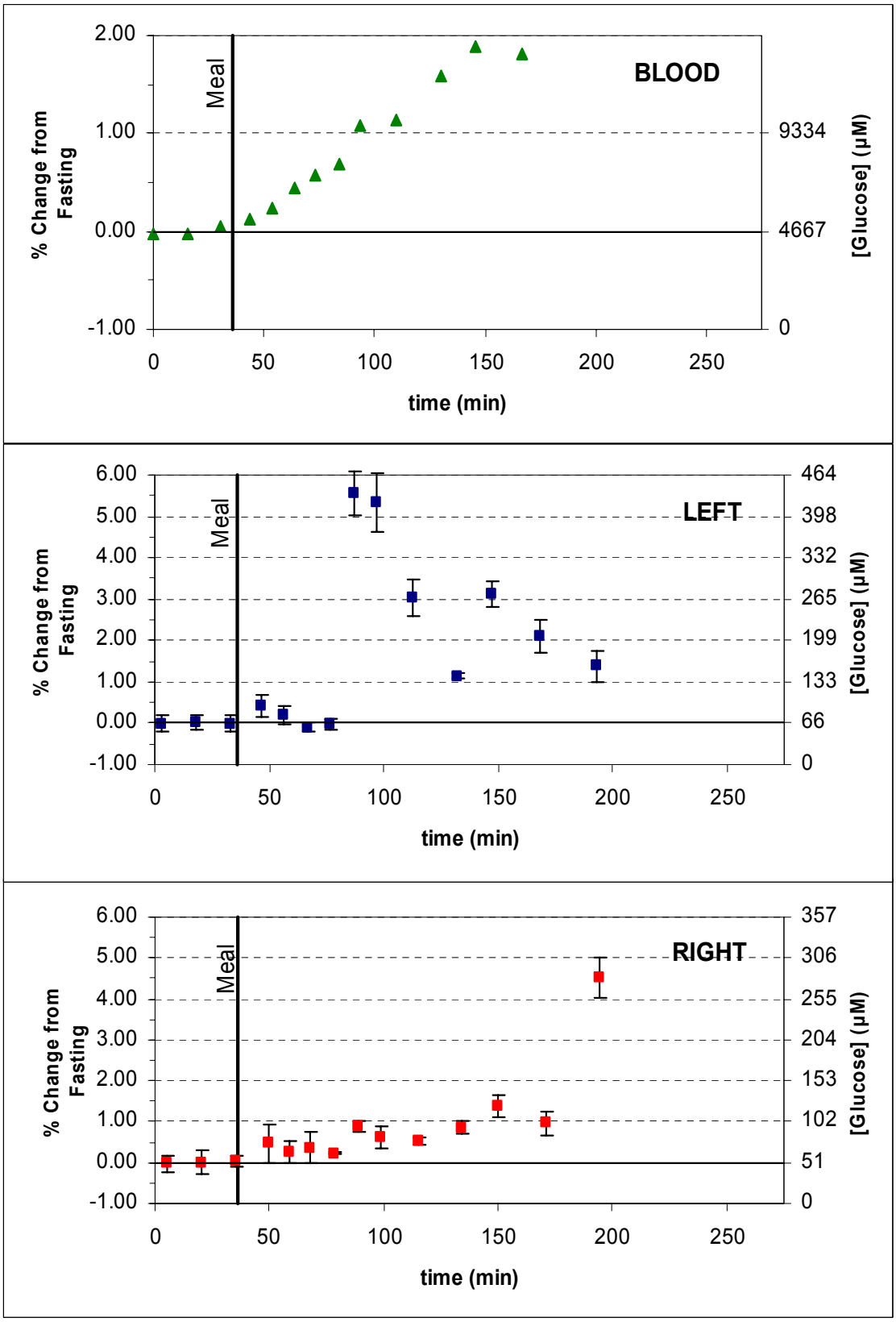

Figure A.12: Meal study of subject 12 (diabetic)

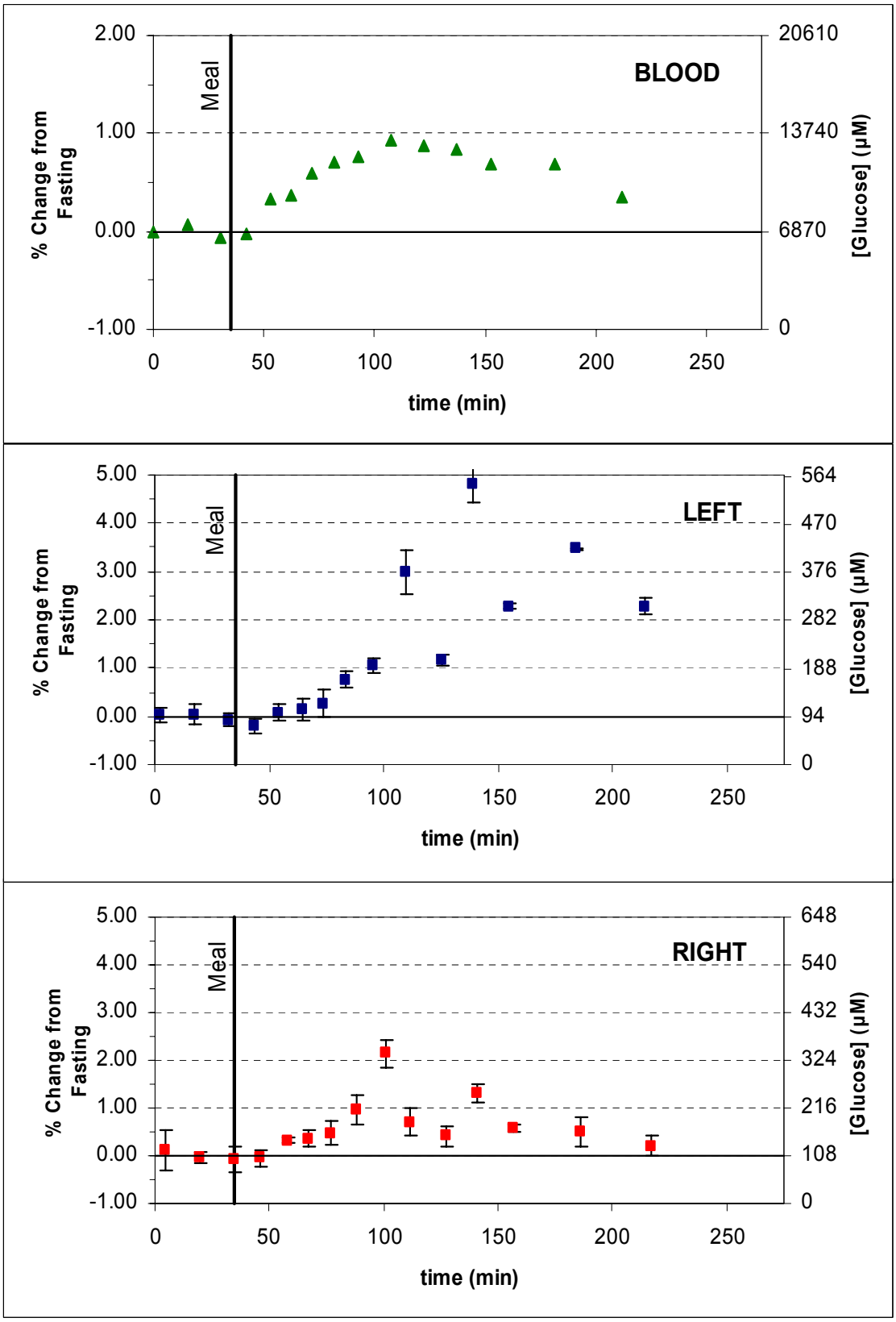

Figure A.13: Meal study of subject 13 (diabetic)

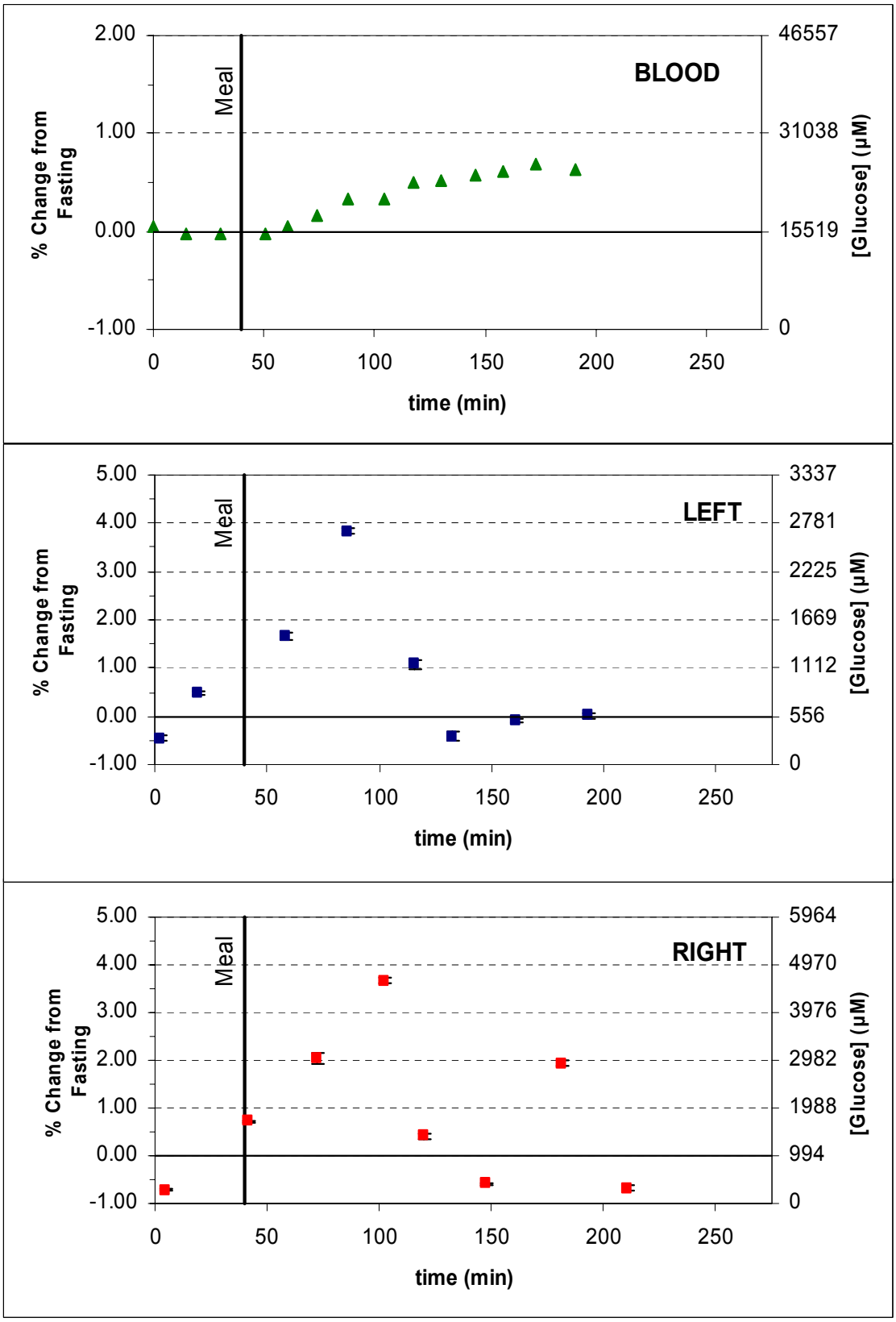

Figure A.14: Meal study of subject 1 (non-diabetic) with column

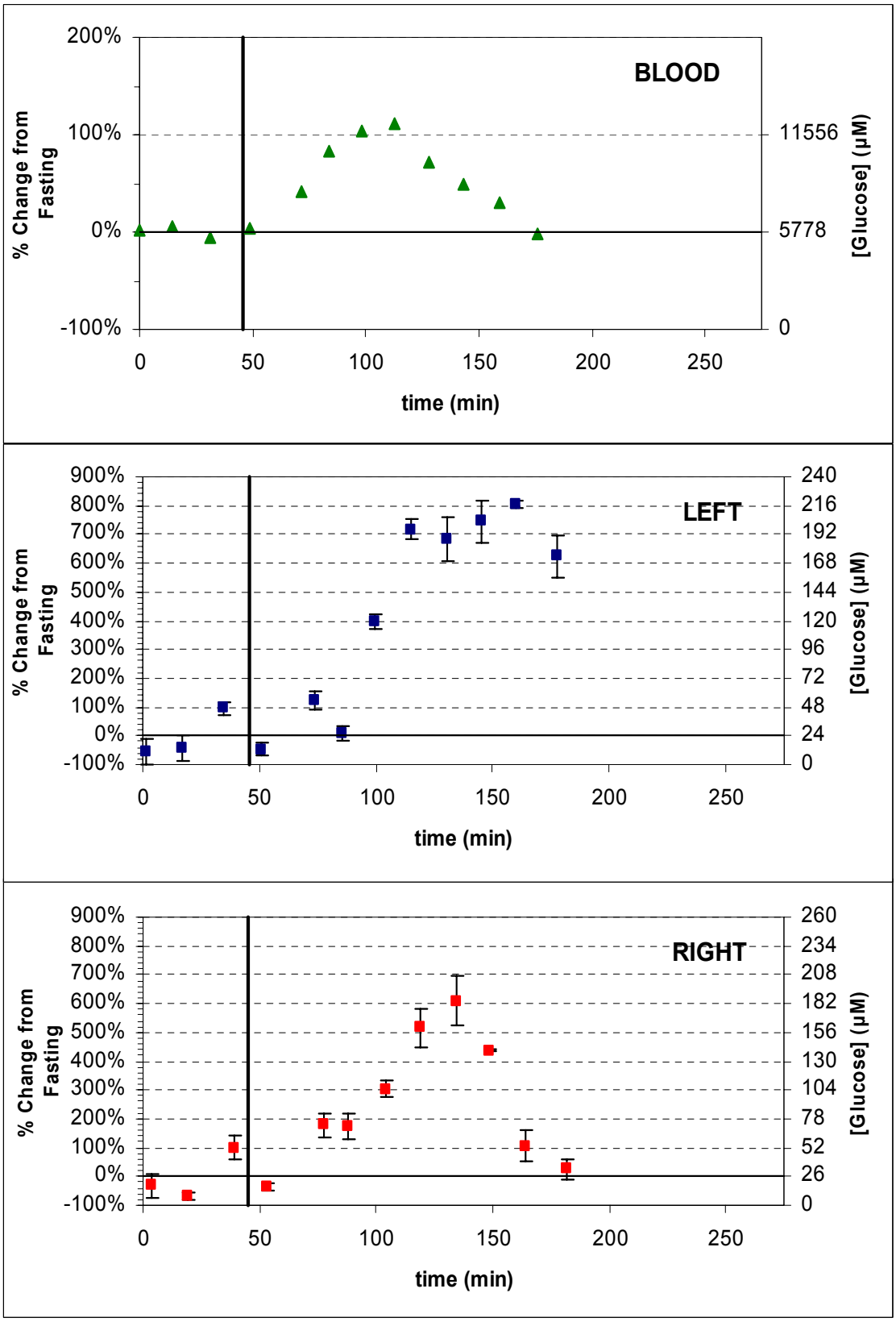

Figure A.15: Meal study of subject 10 (diabetic) with column

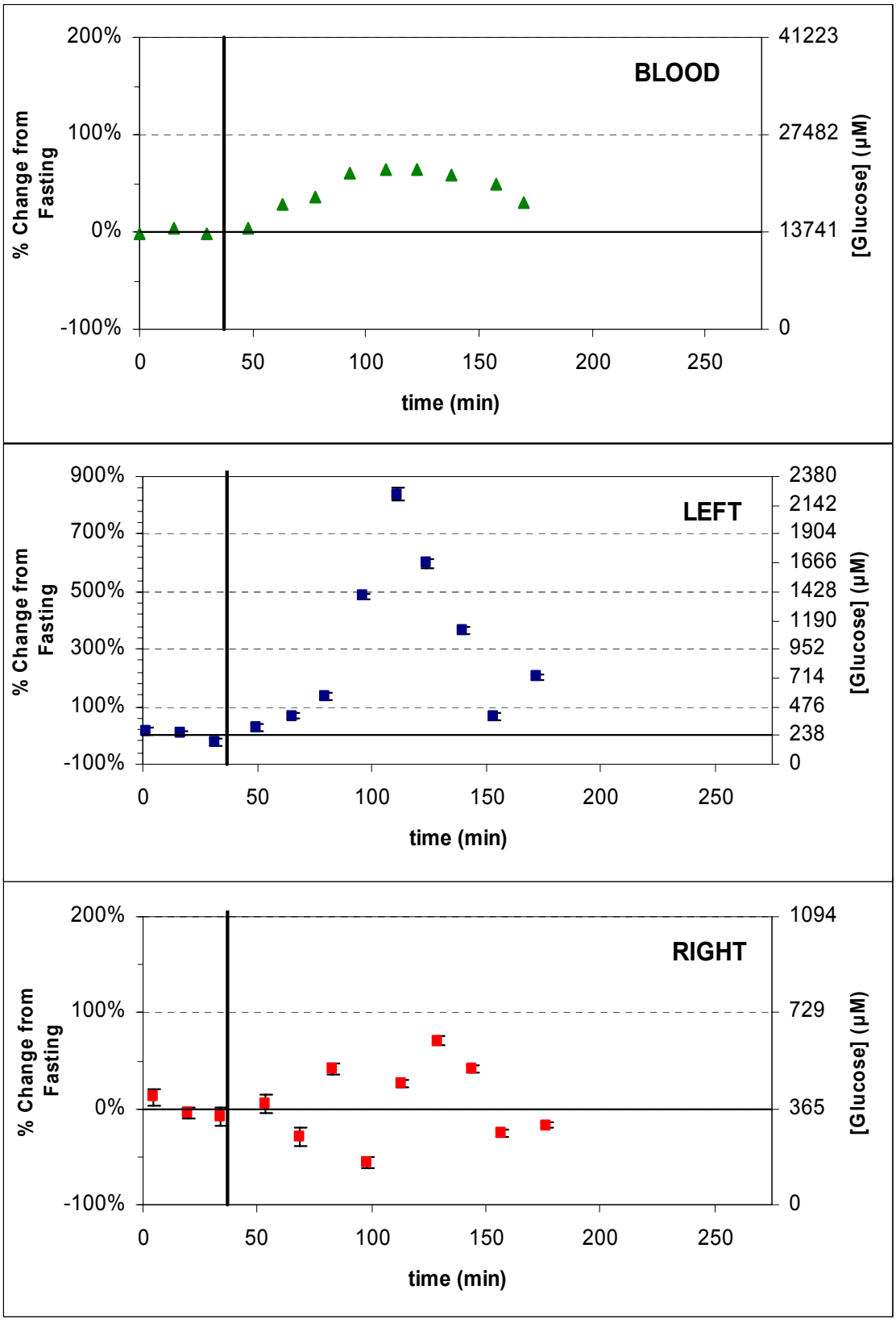

Figure A.16: Repeat meal study of subject 1 (non-diabetic) with column

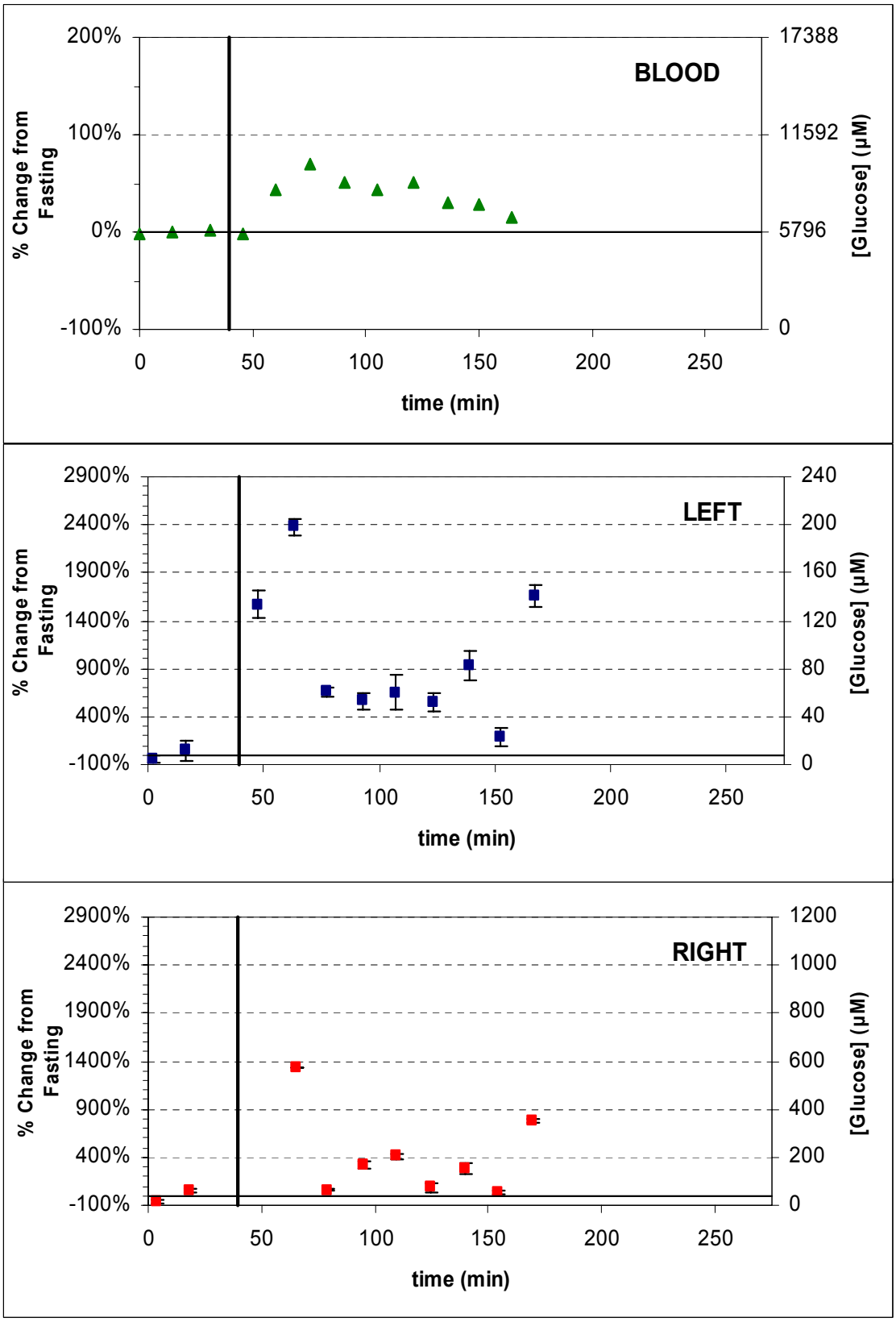

APPENDIX B

ANALYSIS OF SILYL CONTAINING REACTION COMPOUNDS

The ideal method to analyze volatile organic compounds would provide qualitative and quantitative analysis of any volatile organic compound and their isomers even in a complex mixture. H_3O^+ has been used within chemical-reaction mass spectrometry to this end[22]; however, it is susceptible to clustering reactions which complicates analysis. An alternative approach is to use a silyl-transfer reagent. It has been shown that ionic reaction complexes containing a silicon atom have a high exchange of functional groups.[23,80-83] The products of the chemical reaction between the silyl containing ion and the volatile organic compound could provide the differentiation between analytes or tandem mass spectrometry could provide unique fragment ions.[84] To further this objective, this study explores three silyl transfer reagents.

Three silyl containing compounds (hexamethyldisiloxane, tert-butoxy trimethylsilane, and 2-trimethylsiloxy-propene) were analyzed with tandem mass spectrometry preceded with different ionization techniques. Hexamethyldisiloxane ($(CH_3)_3SiOSi(CH_3)_3$) was tested due to its similarity to water[23] and the other two compounds are related to hexamethyldisiloxane. Compared to hexamethyldisiloxane, Tert-butoxy trimethylsilane ($(CH_3)_3SiOC(CH_3)_3$) has a carbon substituted for a silicone and 2-trimethyldisiloxy-propene ($(CH_3)_3SiOSi(CH_3)CH_3$) has

lost CH_4. The three ionization techniques used were electron ionization, atmospheric-pressure chemical ionization, and electrospray ionization. Ions resulting from these techniques were subjected to collision-induced-dissociation to determine their structure. Collision-induced-dissociation was also performed on the electron ionization ions of hexamethyldisiloxane with acetone-d_6 and propanal (instead of argon) as the collision gas to determine if isomeric determination could be achieved.

B.1 EXPERIMENTAL

Hexamethyldisiloxane, 2-trimethylsiloxy-propene, propanal, and acetone-d_6 were purchased from Sigma-Aldrich (St. Louis, MO). Tert-butoxy trimethylsilane was purchased from Oakwood Products, Inc. (West Columbia, SC). Argon was purchased from National Valley Gas, Inc. (Pittsburgh, PA). Electron ionization experiments were either performed on the SWISS-484 with the ionization source mounted directly on the first quadrupole casing (Figure B.1) or on a triple multipole at Extrel CMS (Pittsburgh, PA) with 100 eV set as the ionization energy. All electrospray ionization experiments were performed on the HP LCMS with flow-injection analysis. Injections into the HP LCMS were 1 μL in volume of pure analyte and the flow rate of the "mobile phase" was 0.4 mL/min of 50% water and 50% acetonitrile. The atmospheric-pressure chemical ionization experiments were performed on the SWISS-484 with a custom built source (Figure B.2). The source is similar to the electrospray source described previously but the high-voltage is placed on a corona needle situated in-between the analyte delivery capillary and the mass spectrometer capillary inlet. 4.5 kV was placed on the corona needle and a flow rate of 0.5 μL/min was used through the 25 μm tipped analyte delivery capillary. All experiments used

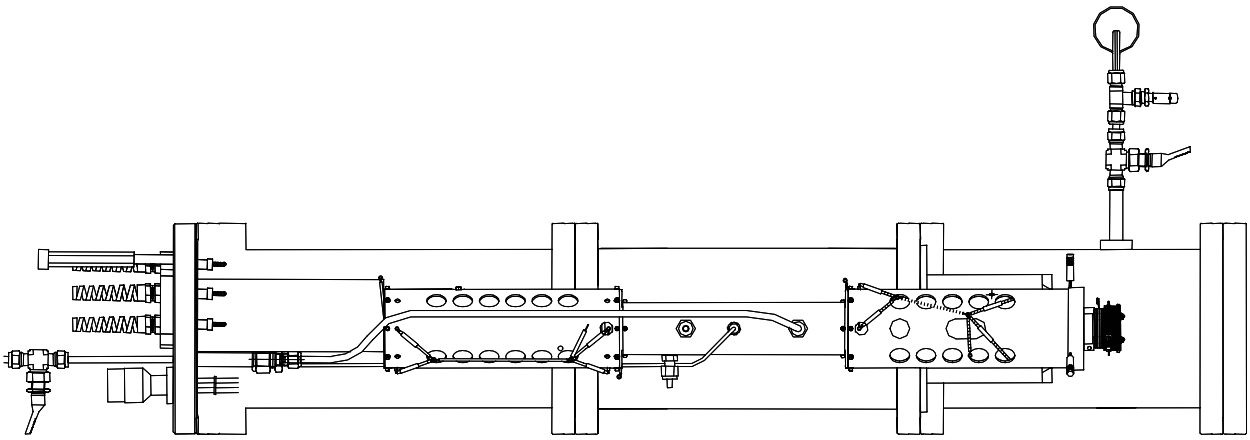

Figure B.1: SWISS-484 with EI source and volatile sample inlet.

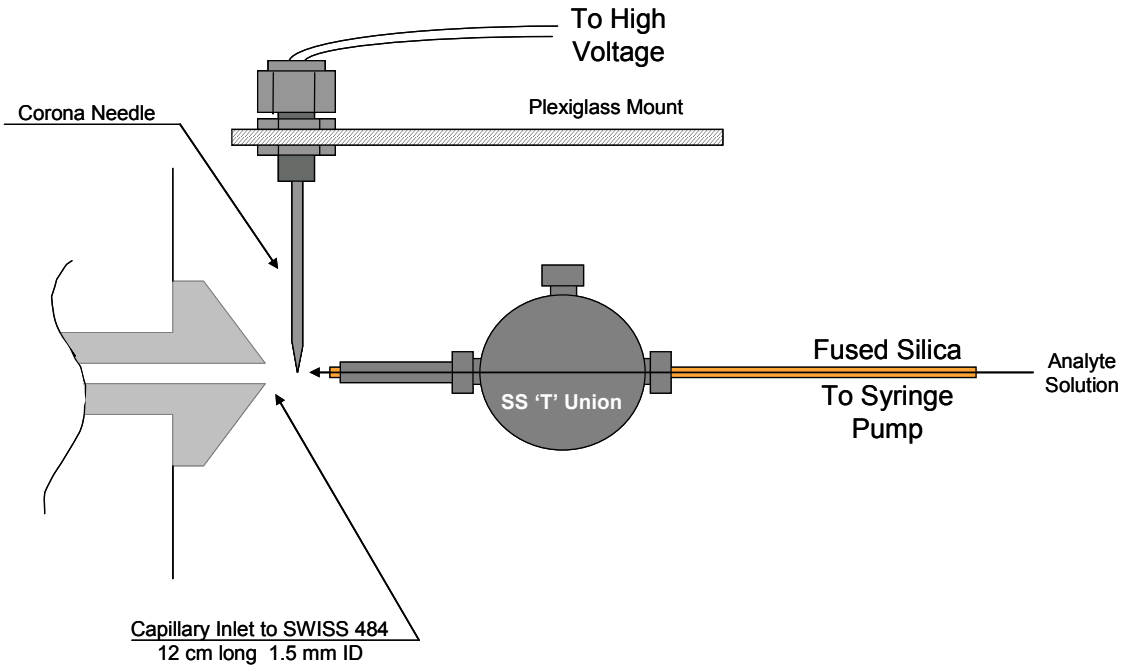

Figure B.2: Atmospheric-pressure ionization source for the SWISS-484

100% of the compound as the analyte solution. Tandem mass spectrometry experiments had a collision gas pressure about 1 x 10^{-5} torr.

B.2 RESULTS AND CONCLUSIONS

The EI experiments on the three silyl compounds resulted in data similar to research previously reported.[80,85] With hexamethyldisiloxane as the analyte, *m/z* values of 147 (loss of a methyl group), 131 (loss of a methyl and methane), and 73 (trimethylsilane ion) were observed (Figure B.3a). With tert-butoxy trimethylsilane as the analyte, *m/z* values of 131 (loss of a methyl group), 75 (proposed to be $(CH_3)_3COH_2^+$ due to its isotopic ratio), and 73 (trimethylsilane ion) were observed (Figure B.4a). With 2-trimethylsiloxy-propene as the analyte, observed *m/z* values and the proposed structures for each are *m/z* 130 $[(CH_3)_3SiOC(CH_3)CH_2]^+$, *m/z* 115 $[(CH_3)_3SiOCCH_2]^+$, *m/z* 99 $[CH_3(CH_2)SiOCCH_2]^+$, *m/z* 85 $[CH_3SiOCCH_2]^+$, *m/z* 73 $[(CH_3)_3Si]^+$, and m/z 59 $[H(CH_3)_2Si]^+$ (Figure B.5a).

The protonated analyte was observed for both hexamethyldisiloxane (Figure B.3b) and tert-butoxy trimethylsilane (Figure B.4b). In the tert-butoxy trimethylsilane spectrum *m/z* 91 was also observed. This ion is attributed to fragmentation in the source and proposed due to its isotopic ratio to be $[(CH_3)_3SiOH_2]^+$. In the 2-trimethylsiloxy-propene spectrum only *m/z* 102 was observed (Figure B.5b). Conflicting data was obtained for the structure of this ion. In the fragmentation study on *m/z* 102 (Figure B.6c) loss of 29 (*m/z* 73) and 57 (*m/z* 45) are observed. With these observed fragments, $[(CH_3)_3SiOCH]^+$ is proposed to be m/z 102. However, the isotopes of *m/z* 102 (i.e., *m/z* 103 and 104) are not consistent with having silicon in the molecular formula. The other compound's fragmentation studies proved to be consistent with the

protonated analyte (Figure B.6). The ESI data obtained on the HP LCMS were identical to the APCI data obtained on the SWISS-484.

Fragmentation studies on the EI ions of hexamethyldisiloxane were performed with organic carbonyl compounds as the collision gas. $[(CH_3)_3SiOSi(CH_3)_2]^+$, $[(CH_3)_2SiOSi(CH_3)CH_2]^+$, and $[(CH_3)_3Si]^+$ were selected in Q1 and allowed to collide with d_6-acetone or propanal in the collision cell. The main change from the traditional CID spectrum with argon as the collision gas is the presence of the adduct of the Q1 selected ion and the organic compound. When $[(CH_3)_3SiOSi(CH_3)_2]^+$ is selected, in addition to the adduct the loss of a methyl group from the adduct is observed in both carbonyl cases (Figure B.7). Also a unique ion is observed for each carbonyl. For d_6-acetone, the exchange of CD_3 groups is apparent at *m/z* 137, while for propanal the loss of an ethyl group from the adduct is observed. When $[(CH_3)_2SiOSi(CH_3)CH_2]^+$ is selected additional ions are observed but none could be attributed to the carbonyls (Figure B.8). When $[(CH_3)_3Si]^+$ is selected and d_6-acetone is used as the collision gas the exchange of the deuterated methyl group is once again observed (Figure B.9). If propanal is used instead the only additional ion is the loss of 14 from the adduct.

At present the only apparent isomer differentiation is with the use of hexamethyldisiloxane, however a more intense signal would be beneficial. Ideally, fragmentation of the adduct ions would provide a more intense signal and possibly better compound distinction from all three silyl ions. To perform this analysis on a triple multipole instrument the adduct ions would need to be formed prior to Q1.

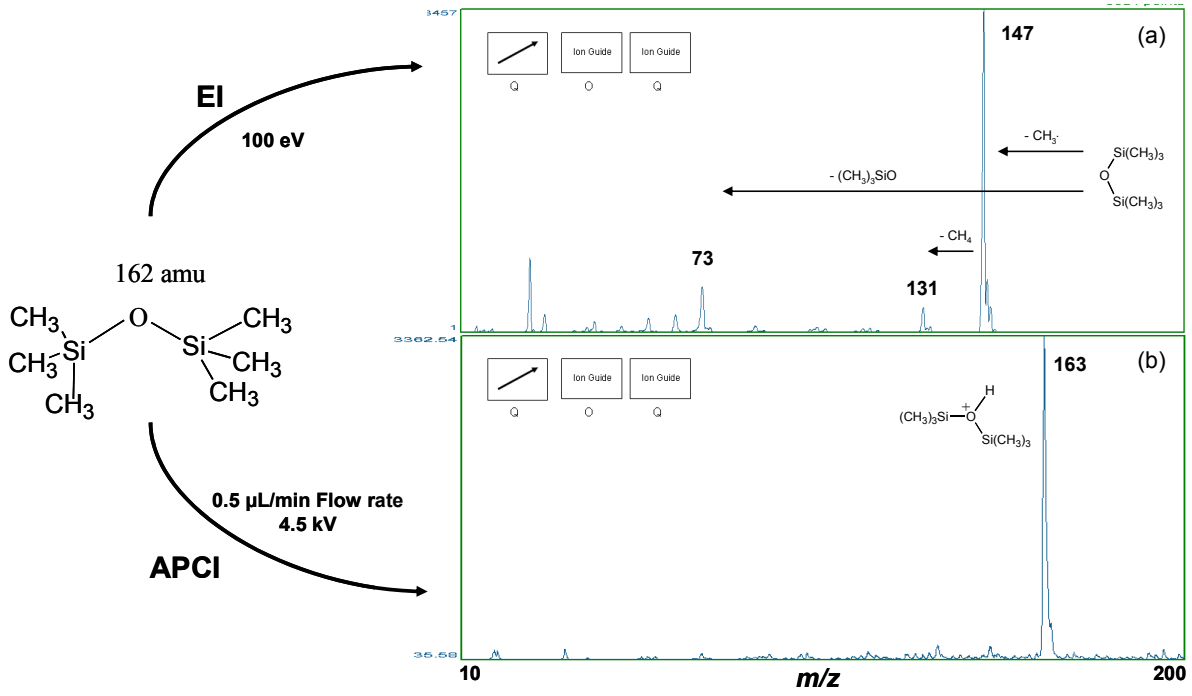

Figure B.3: Ionization of hexamethyldisiloxane by (a) EI and (b) APCI

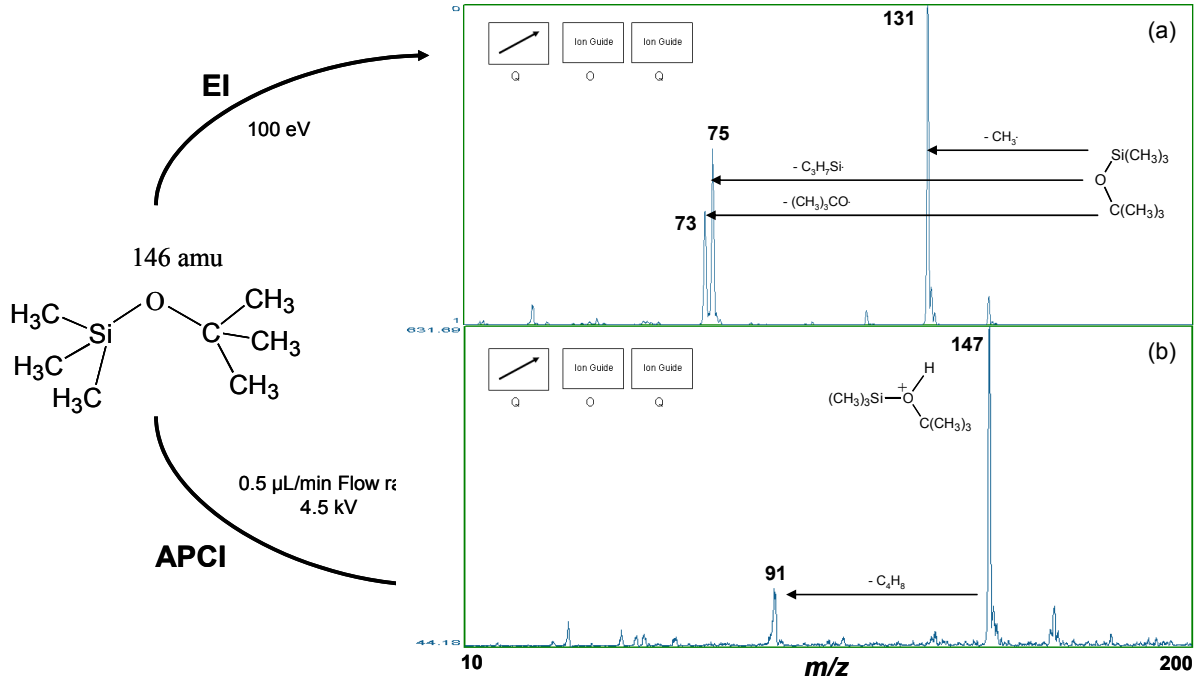

Figure B.4: Ionization of tert-butyoxy trimethylsilane by (a) EI and (b) APCI

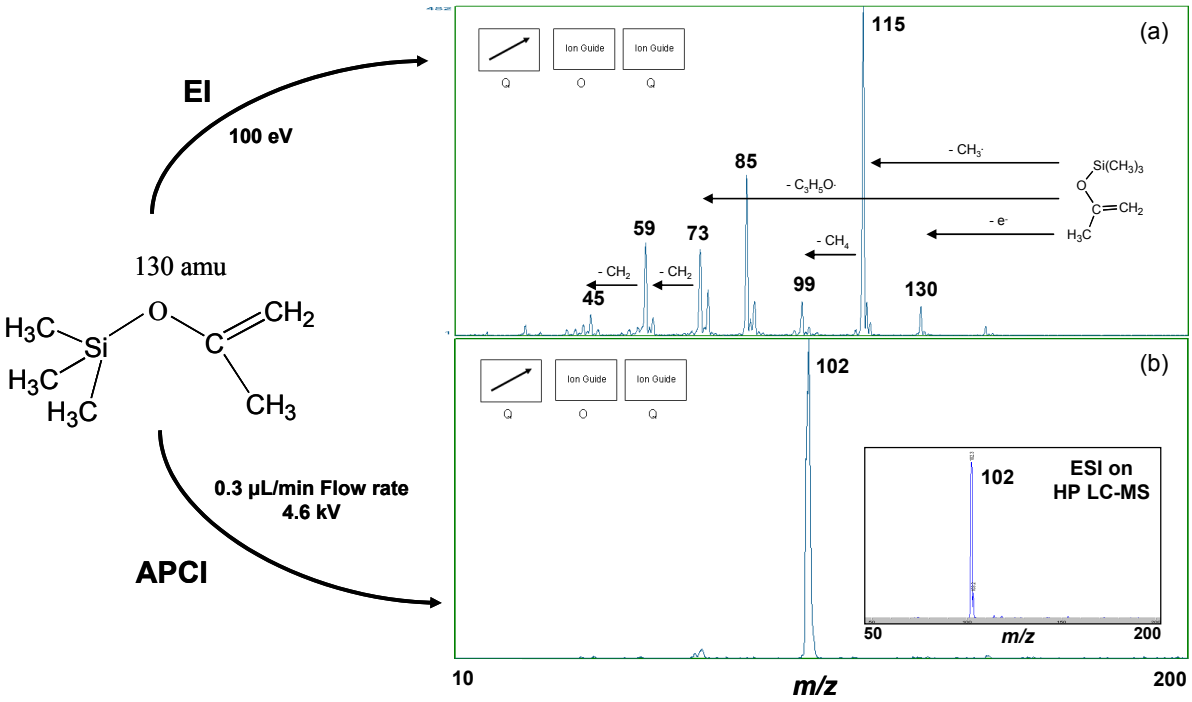

Figure B.5: Ionization of 2-trimethylsiloxy-propene by (a) EI and (b) APCI

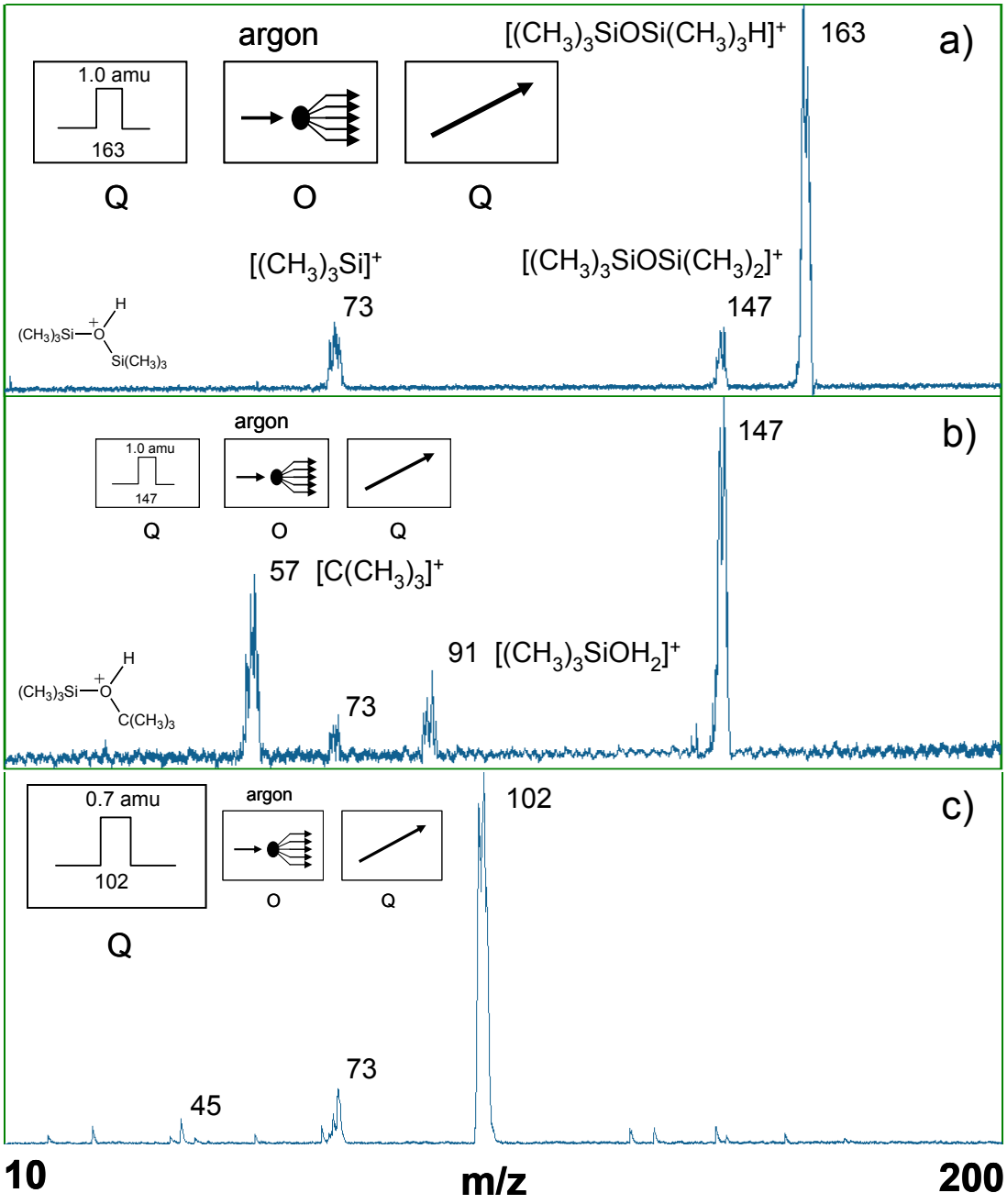

Figure B.6: CID of (a) protonated hexamethyldisiloxane, (b) protonated tert-butoxytrimethylsilane, and (c) *m/z* 102 from the APCI of 2-trimethylsiloxy-propene.

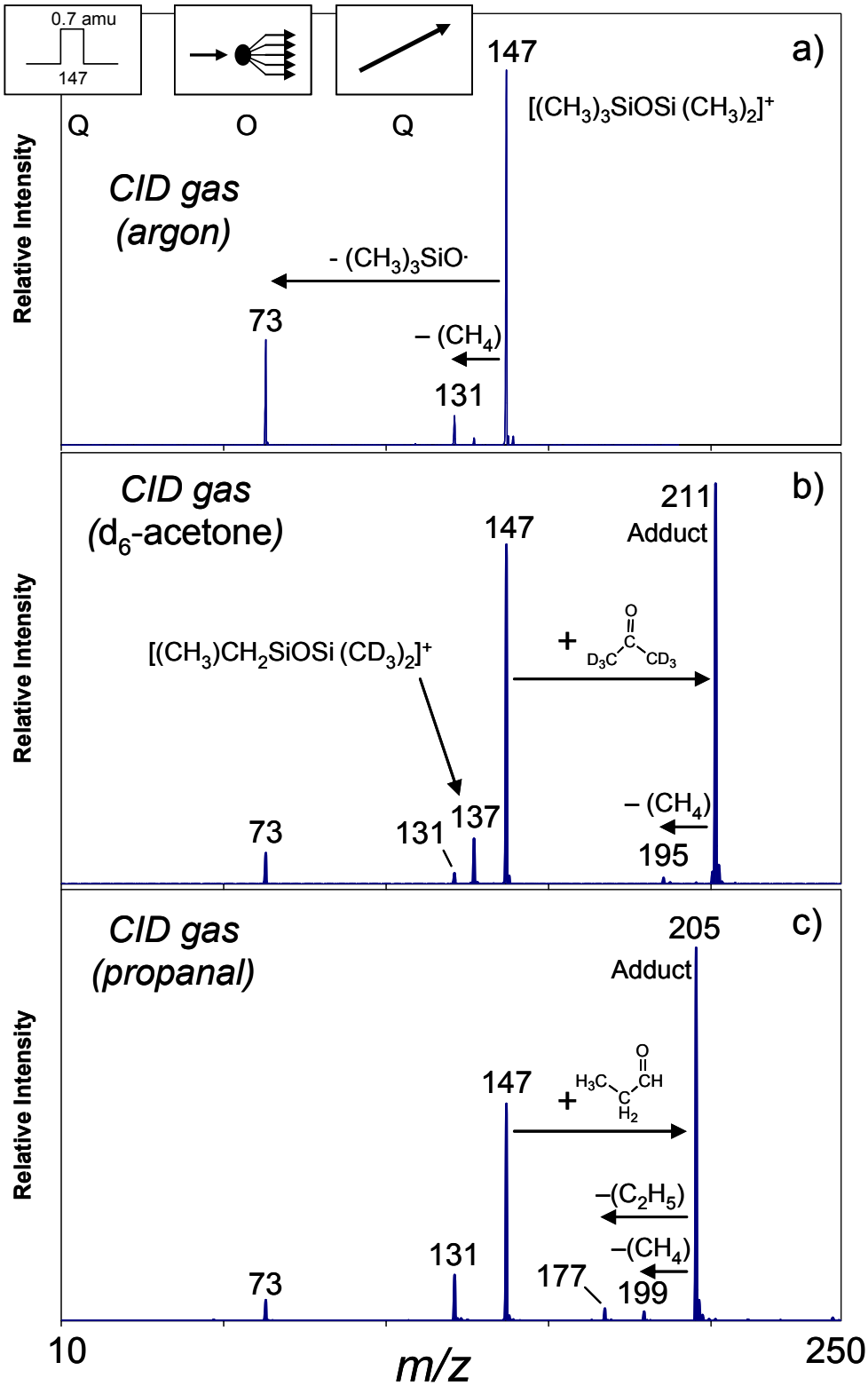

Figure B.7: CID experiments of $[(CH_3)_3SiOSi(CH_3)_2]^+$ with the collision gas being (a) argon, (b) d_6-acetone, and (c) propanal.

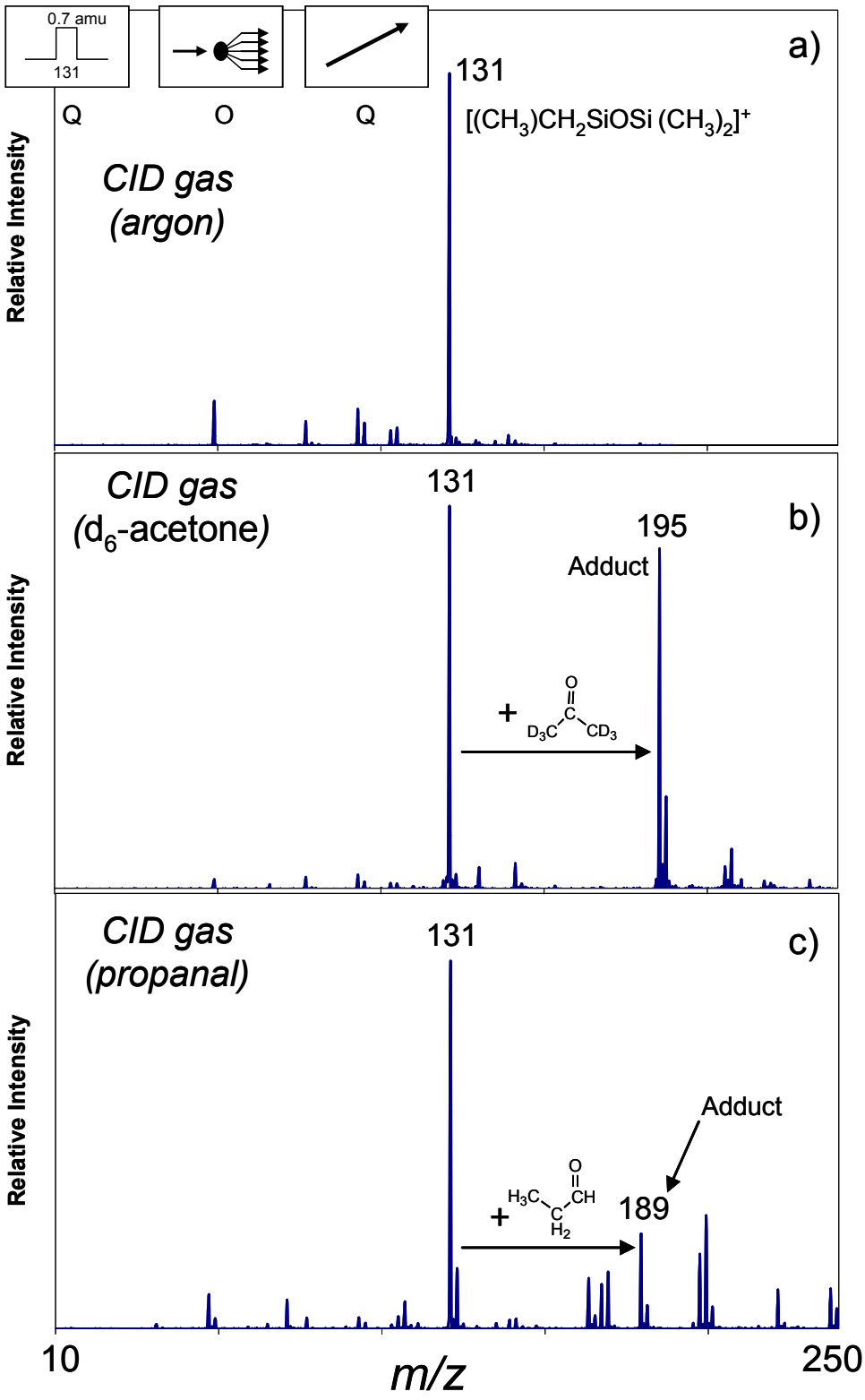

Figure B.8: CID experiments of $[(CH_3)_2SiOSi(CH_3)CH_2]^+$ with the collision gas being (a) argon, (b) d_6-acetone, and (c) propanal.

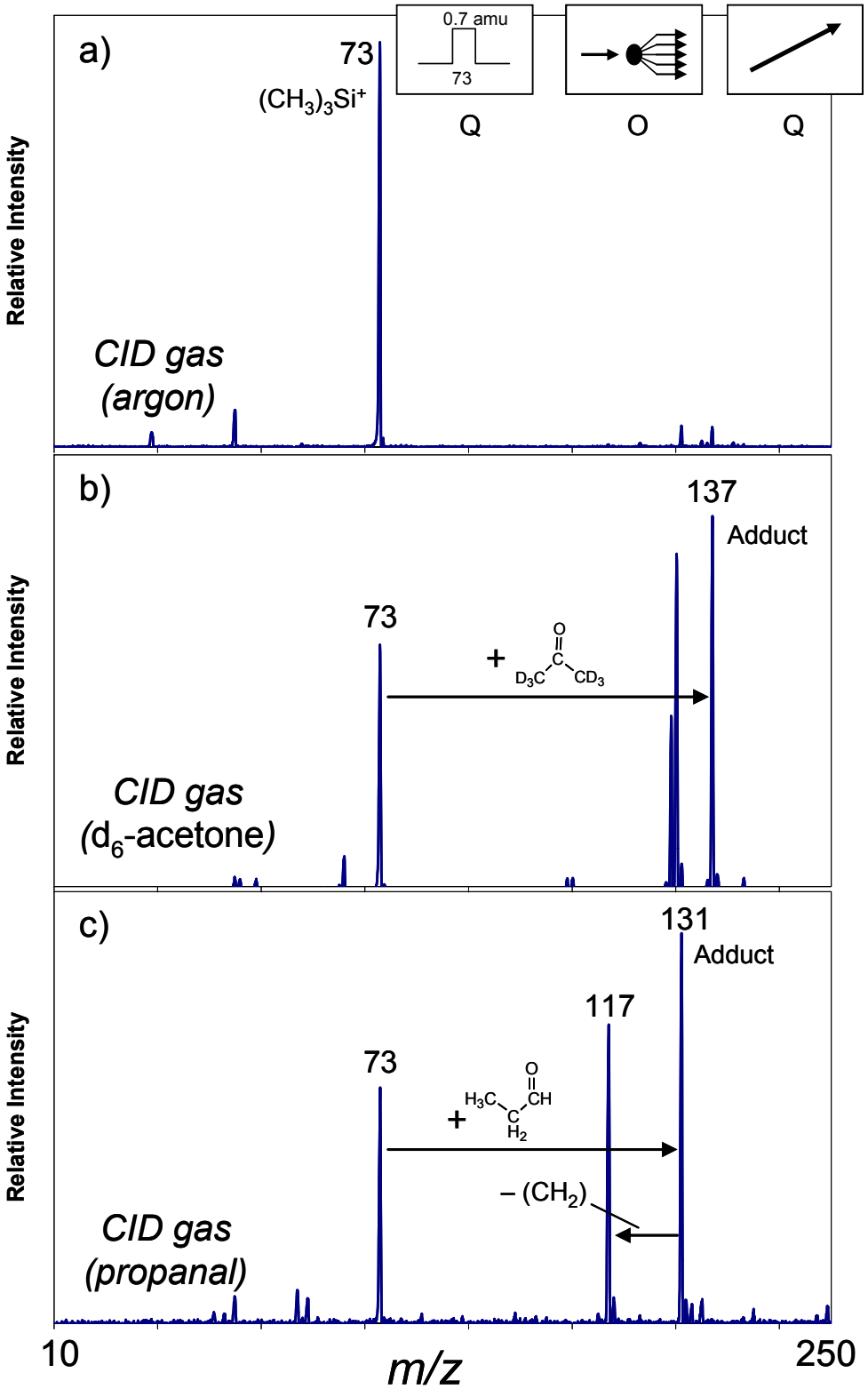

Figure B.9: CID experiments of $[(CH_3)_3Si]^+$ with the collision gas being (a) argon, (b) d_6-acetone, and (c) propanal.

BIBLIOGRAPHY

(1) Johnson, J. V.; Yost, R. A.; Kelley, P. E.; Bradford, D. C. *Analytical Chemistry* **1990**, *62*, 2162-72.

(2) Crowther, J.; Adusumallt, V.; Mukherjee, T.; Jordan, K.; Abuaf, P.; Corkum, N.; Goldstein, G.; Tolan, J. *Analytical Chemistry* **1994**, *66*, 2356-61.

(3) Wilm, M.; Shevchenko, A.; Houthaeve, T.; Breit, S.; Schweigerer, L.; Fotsis, T.; Mann, M. In *Nature (London)*, 1996; Vol. 379, pp 466-9.

(4) Juraschek, R.; Dulcks, T.; Karas, M. *Journal of the American Society for Mass Spectrometry* **1999**, *10*, 300-8.

(5) Haskins, W. E.; Wang, Z.; Watson, C. J.; Rostand, R. R.; Witowski, S. R.; Powell, D. H.; Kennedy, R. T. *Analytical Chemistry* **2001**, *73*, 5005-14.

(6) Feng, B.; Smith, R. D. *Journal of the American Society for Mass Spectrometry* **2000**, *11*, 94-9.

(7) Shamoon, H. D., H.; Fleischer, N.; Engel, S.; Saenger, P.; Strelzyn, M.; Litwak, M.;; Wylierosett, J. F., A.; et al. *New England Journal of Medicine* **1993**, *329*, 977-86.

(8) Badugu, R.; Lakowicz, J. R.; Geddes, C. D. *Analytical Chemistry* **2004**, *76*, 610-8.

(9) Alexeev, V. L.; Das, S.; Finegold, D. N.; Asher, S. A. *Clinical Chemistry* **2004**, *50*, 2353-60.

(10) Badugu, R.; Lakowicz, J. R.; Geddes, C. D. *Current Opinion in Biotechnology* **2005**, *16*, 100-7.

(11) March, W. F.; Mueller, A.; Herbrechtsmeier, P. *Diabetes Technology & Therapeutics* **2004**, *6*, 782-9.

(12) Daum, K. M.; Hill, R. M. *Investigative Ophthalmology & Visual Science* **1982**, *22*, 509-14.

(13) Van Haeringen, N. J.; Glasius, E. *Albrecht von Graefes Archiv fuer Klinische und Experimentelle Ophthalmologie* **1977**, *202*, 1-7.

(14) Kilp, H.; Heisig, B. *Albrecht von Graefes Archiv fuer Klinische und Experimentelle Ophthalmologie* **1975**, *193*, 259-67.

(15) Frecska, E.; Davis, K. L. In *Neuropeptides and Psychiatric Disorders*; Nemeroff, C. B., Ed.; American Psychiatric Press: Washington, DC, 1991, pp 169-92.

(16) Capper, S. J. *Progress in Brain Research* **1986**, *66*, 317-30.

(17) Terenius, L. *Progress in Brain Research* **1992**, *92*, 375-84.

(18) Emmett, M. R.; Andren, P. E.; Caprioli, R. M. *Journal of Neuroscience Methods* **1995**, *62*, 141-7.

(19) Khan, A. S.; Michael, A. C. *TrAC, Trends in Analytical Chemistry* **2003**, *22*, 503-8.

(20) Zhang, W.; Liu, H.; Han, K.; Grabowski, P. J. *RNA* **2002**, *8*, 671-85.

(21) Valcarcel, J.; Gebauer, F. *Current Biology* **1997**, *7*, R705-R8.

(22) Zhao, J.; Zhang, R. *Atmospheric Environment* **2004**, *38*, 2177-85.

(23) Fleming, I. *Chemical Society Reviews* **1981**, *10*, 83-111.

(24) Cole, R. B., Ed. *Electrospray Ionization Mass Spectrometry: Fundamentals, Instrumentation, and Applications*; John Wiley & Sons, Inc.: New York, 1997.

(25) Fenn, J. B.; Mann, M.; Meng, C. K.; Wong, S. F.; Whitehouse, C. M. *Science (Washington, DC, United States)* **1989**, *246*, 64-71.

(26) Kebarle, P.; Peschke, M. *Analytica Chimica Acta* **2000**, *406*, 11-35.

(27) Dole, M.; Mack, L. L.; Hines, R. L.; Mobley, R. C.; Ferguson, L. D.; Alice, M. B. *J. Chem. Phys.* **1968**, *49*, 2240-9.

(28) Schmelzeisen-Redeker, G.; Buetfering, L.; Roellgen, F. W. *International Journal of Mass Spectrometry and Ion Processes* **1989**, *90*, 139-50.

(29) Iribarne, J. V.; Thomson, B. A. *J. Chem. Phys.* **1976**, *64*, 2287-94.

(30) Thomson, B. A.; Iribarne, J. V. *Journal of Chemical Physics* **1979**, *71*, 4451-63.

(31) Labowsky, M.; Fenn, J. B.; Fernandez de la Mora, J. *Analytica Chimica Acta* **2000**, *406*, 105-18.

(32) Hoffmann, E. d.; Stroobant, V. *Mass Spectrometry: Principles and Applications*, Second Edition ed.; John Wiley & Sons, LTD: New York, 2002.

(33) Wilm, M.; Mann, M. *Analytical Chemistry* **1996**, *68*, 1-8.

(34) Lee, S.-W.; Kim, H. S.; Beauchamp, J. L. *Journal of the American Chemical Society* **1998**, *120*, 3188-95.

(35) Nesatyy, V. J. *Journal of Mass Spectrometry* **2001**, *36*, 950-9.

(36) Dawson, P. H., Ed. *Quadruple Mass Spectrometry and its applications*; Elsevier Scientific Publishing Compnay: New York, 1976.

(37) March, R. E.; Hughes, R. *Quadruple Storage Mass Spectrometry*; Wiley-Interscience, 1989.

(38) Caprioli, R. M.; Malorni, A.; Sindona, G., Eds. *Selected Topics in Mass Spectrometry in the Biomolecular Sciences*; Kluwer Academic Publishers, 1997.

(39) Chavez-Eng, C. M.; Schwartz, M.; Constanzer, M. L.; Matuszewski, B. K. *Journal of Chromatography B* **1999**, *721*, 229-38.

(40) Zhang, Z.; Marshall, A. G. *Journal of the American Society for Mass Spectrometry* **1998**, *9*, 225-33.

(41) U.S. Department of Health and Human Services, National of Institutes of Health, National Institute of Diabetes and Digestive and Kidney Diseases, National Diabetes Information Clearinghouse, 2005.

(42) Taormina, C. R.; Baca, J. T.; Finegold, D. N.; Asher, S. A.; Grabowski, J. J. *Journal of the American Society for Mass Spectrometry* **2007**, *18*, 332-6.

(43) Baca, J. T.; Taormina, C. R.; Finegold, D. N.; Grabowski, J. J.; Asher, S. A. *Clinical Chemistry* **2007**, *53*, 1370-2.

(44) Jin, Z.; Chen, R.; Colon, L. A. *Analytical Chemistry* **1997**, *69*, 1326-31.

(45) Chen, R.; Jin, Z.; Colon, L. A. *Journal of Capillary Electrophoresis* **1996**, *3*, 243-8.

(46) Lane, J. D.; Krumholz, D. M.; Sack, R. A.; Morris, C. *Current eye research* **2006**, *31*, 895-901.

(47) Domschke, A.; March, W. F.; Kabilan, S.; Lowe, C. *Diabetes Technology & Therapeutics* **2006**, *8*, 89-93.

(48) LeBlanc, J. M.; Haas, C. E.; Vicente, G.; Colon, L. A. *Intensive Care Med* **2005**, *31*, 1442-5.

(49) Salpin, J.-Y.; Tortajada, J. *Journal of Mass Spectrometry* **2002**, *37*, 379-88.

(50) Fung, K. Y. C.; Morris, C.; Sathe, S.; Sack, R.; Duncan, M. W. *Proteomics* **2004**, *4*, 3953-9.

(51) Ham, B. M.; Jacob, J. T.; Keese, M. M.; Cole, R. B. *Journal of Mass Spectrometry* **2004**, *39*, 1321-36.

(52) Gilbard, J. P. *International Ophthalmology Clinics* **1994**, *34*, 27-36.

(53) Desiderio, D. M. *Journal of Chromatography B* **1999**, *731*, 3-22.

(54) Khalil, O. S. *Diabetes Technology & Therapeutics* **2004**, *6*, 660-97.

(55) Badugu, R.; Lakowicz, J. R.; Geddes, C. D. *Journal of Fluorescence* **2004**, *14*, 617-33.

(56) Clapperton, A. T.; Coward, W. A.; Bluck, L. J. C. *Rapid Communications in Mass Spectrometry* **2002**, *16*, 2009-14.

(57) Dube, G.; Henrion, A.; Ohlendorf, R.; Vidal, C. *Rapid Communications in Mass Spectrometry* **2001**, *15*, 1322-6.

(58) Lee, J.; Chung, B. C. *Journal of Chromatography, B: Analytical Technologies in the Biomedical and Life Sciences* **2006**, *831*, 126-31.

(59) Di Gioia, M. L.; Leggio, A.; Le Pera, A.; Liguori, A.; Napoli, A.; Siciliano, C.; Sindona, G. *Journal of Chromatography, B: Analytical Technologies in the Biomedical and Life Sciences* **2004**, *801*, 355-8.

(60) Rogatsky, E.; Jayatillake, H.; Goswami, G.; Tomuta, V.; Stein, D. *Journal of the American Society for Mass Spectrometry* **2005**, *16*, 1805-11.

(61) Wan, E. C. H.; Yu, J. Z. *Journal of Chromatography, A* **2006**, *1107*, 175-81.

(62) McIntosh, T. S.; Davis, H. M.; Matthews, D. E. *Analytical Biochemistry* **2002**, *300*, 163-9.

(63) Bruggink, C.; Maurer, R.; Herrmann, H.; Cavalli, S.; Hoefler, F. *Journal of Chromatography, A* **2005**, *1085*, 104-9.

(64) Guignard, C.; Jouve, L.; Bogeat-Triboulot, M. B.; Dreyer, E.; Hausman, J.-F.; Hoffmann, L. *Journal of Chromatography, A* **2005**, *1085*, 137-42.

(65) Zhu, J.; Cole, R. B. *Journal of the American Society for Mass Spectrometry* **2001**, *12*, 1193-204.

(66) Chatterjee, P. R.; De, S.; Datta, H.; Chatterjee, S.; Biswas, M. C.; Sarkar, K.; Mandal, L. K. *Journal of the Indian Medical Association* **2003**, *101*, 481-3.

(67) Sen, D. K.; Sarin, G. S. *British journal of ophthalmology* **1980**, *64*, 693-5.

(68) Gasset, A. R.; Braverman, L. E.; Fleming, M. C.; Arky, R. A.; Alter, B. R. *American journal of ophthalmology* **1968**, *65*, 414-20.

(69) Badugu, R.; Lakowicz, J. R.; Geddes, C. D. *Journal of Fluorescence* **2003**, *13*, 371-4.

(70) March, R. E.; Mueller, A.; Herbrechtsmeier, P., Philadelphia 2001; American Diabetes Association; A125.

(71) Roepstorff, P. *Biomedical Mass Spectrometry* **1984**, *11*, 601.

(72) Tang, X.; Ens, W.; Standing, K. G.; Westmore, J. B. *Analytical Chemistry* **1988**, *60*, 1791-9.

(73) Grabowski, P. J.; Black, D. L. *Progress in Neuobiology* **2001**, *65*, 289 - 308.

(74) Shevchenko, A.; Wilm, M.; Vorm, O.; Mann, M. *Analytical Chemistry* **1996**, *68*, 850-8.

(75) Potier, N.; Donald, L. J.; Chernushevich, I.; Ayed, A.; Ens, W.; Arrowsmith, C. H.; Standing, K. G.; Duckworth, H. W. *Protein Science* **1998**, *7*, 1388-95.

(76) Loo, J. A.; Loo, R. R. O.; Light, K. J.; Edmonds, C. G.; Smith, R. D. *Analytical Chemistry* **1992**, *64*, 81-8.

(77) Loo, J. A.; Pesch, R. *Analytical Chemistry* **1994**, *66*, 3659-63.

(78) Loo, J. A.; Udseth, H. R.; Smith, R. D. *Analytical Biochemistry* **1989**, *179*, 404-12.

(79) Hofstadler, S. A.; Griffey, R. H. *Chemical Reviews (Washington, D. C.)* **2001**, *101*, 377-90.

(80) Hendewerk, M. L.; Weil, D. A.; Stone, T. L.; Ellenberger, M. R.; Farneth, W. E.; Dixon, D. A. *Journal of the American Chemical Society* **1982**, *104*, 1794-9.

(81) Hopper, S. P.; Tremelling, M. J.; Ginsberg, R. J.; Mendelowitz, P. C. *Journal of Organometallic Chemistry* **1977**, *134*, 173-80.

(82) Groenewold, G. S.; Gross, M. L.; Bursey, M. M.; Jones, P. R. *Journal of Organometallic Chemistry* **1982**, *235*, 165-75.

(83) Tobita, S.; Tajima, S.; Okada, F.; Mori, S.; Tabei, E.; Umemura, M. *Organic Mass Spectrometry* **1990**, *25*, 39-43.

(84) Meyerhoffer, W. J.; Bursey, M. M. *Journal of Organometallic Chemistry* **1989**, *373*, 143-52.

(85) Sharkey, A. G.; Friedel, R. A.; Langer, S. H. *Analytical Chemistry* **1957**, *29*, 770.